NASA TECHNICAL MEMORANDUM

NASA TM X-3391

NASA TM X-3391

STABILITY AND CONTROL CHARACTERISTICS OF AN AIR-BREATHING MISSILE CONFIGURATION HAVING A FORWARD LOCATED INLET

Wallace C. Sawyer and Clyde Hayes

Langley Research Center
Hampton, Va. 23665

NATIONAL AERONAUTICS AND SPACE ADMINISTRATION • WASHINGTON, D. C. • JULY 1976

1. Report No.	2. Government Accession No.	3. Recipient's Catalog No.
NASA TM X-3391		

4. Title and Subtitle	5. Report Date
STABILITY AND CONTROL CHARACTERISTICS OF AN AIR-BREATHING MISSILE CONFIGURATION HAVING A FORWARD LOCATED INLET	July 1976
	6. Performing Organization Code

7. Author(s)	8. Performing Organization Report No.
Wallace C. Sawyer and Clyde Hayes	L-10575
	10. Work Unit No. 505-11-22-01
9. Performing Organization Name and Address	11. Contract or Grant No.
NASA Langley Research Center Hampton, Va. 23665	
	13. Type of Report and Period Covered
12. Sponsoring Agency Name and Address	Technical Memorandum
National Aeronautics and Space Administration Washington, D.C. 20546	14. Sponsoring Agency Code

15. Supplementary Notes

16. Abstract

An investigation has been made to determine the aerodynamic characteristics of an air-breathing missile configuration having a forward located inlet. Control was provided by cruciform tail surfaces. Aerodynamic data were obtained for the body-tail configuration alone and with planar or cruciform wings. At Mach numbers from 2.86 to 4.63, the model had internal flow. At Mach numbers from 1.70 to 2.86, the internal duct was closed and an inlet fairing was installed to simulate boost conditions.

17. Key Words (Suggested by Author(s))	18. Distribution Statement
Air-breathing missile configuration Missile aerodynamics Ramjet propulsion Control-surface hinge moment Forward-located inlet	Unclassified – Unlimited Subject Category 02

19. Security Classif. (of this report)	20. Security Classif. (of this page)	21. No. of Pages	22. Price*
Unclassified	Unclassified	81	$4.75

*For sale by the National Technical Information Service, Springfield, Virginia 22161

STABILITY AND CONTROL CHARACTERISTICS OF AN AIR-BREATHING MISSILE CONFIGURATION HAVING A FORWARD LOCATED INLET

Wallace C. Sawyer and Clyde Hayes
Langley Research Center

SUMMARY

An investigation has been made to determine the aerodynamic characteristics of an air-breathing missile configuration having a forward located inlet. Control was provided by cruciform tail surfaces. Aerodynamic data were obtained for the body-tail configuration alone and with planar or cruciform wings. At Mach numbers from 2.86 to 4.63, the model had internal flow. At Mach numbers from 1.70 to 2.86, the internal duct was closed and an inlet fairing was installed to simulate boost conditions.

The results indicate that the addition of either wing configuration to the body-tail configuration increased longitudinal stability, although the normal-force coefficient available would be insufficient for a highly maneuverable missile, except at very low altitudes. Pitch control provided by the tails was adequate to trim the model at angles of attack to at least 20° with the center of gravity located to provide a margin of longitudinal stability. The tail surfaces were also effective in providing yaw and roll control. The effect of closing the inlet, which simulates boost conditions, was a positive pitching-moment increment and an increase in axial force. The increment was small near a Mach number of 1.70 but increased with increasing Mach number.

INTRODUCTION

Recent trends in missile design have placed increasing emphasis on air-breathing propulsion (ref. 1). Consideration must be given to the effect of type, number, and location of the inlets on the total missile configuration and to the resulting effects on the aerodynamics of the missile. Since the engine is generally located near the aft end of the missile, most design approaches have placed the inlets near the tail. The ramjet powered configuration used in this investigation has a single inlet located below the nose to take advantage of the nose compression field and to avoid adverse effects which may be caused by wings or control surfaces located ahead of an aft inlet or inlets. Thus, the overall performance becomes a compromise between improved inlet performance, increased duct losses, and increased body volume. In this investigation, only the external aerodynamics

(including control effectiveness and hinge moments) of the configuration were investigated. The internal performance was not considered.

The investigation was conducted in the Langley Unitary Plan wind tunnel at Mach numbers from 1.70 to 4.63. The basic body-inlet configuration was an ogive-cylinder with the cylindrical cross section modified to accommodate the duct from the nose inlet to the ramjet combustor. Cruciform tail surfaces were included to provide stability and control in pitch, yaw, and roll. Two winged configurations were tested, one having planar wings and the other having cruciform wings of identical planform.

SYMBOLS

The International System of Units (ref. 2) is used for the physical quantities in this paper. The aerodynamic force and moment coefficients of the model are presented for both the body and stability axes, with the moment reference center located on the center line of the cylindrical portion of the model at model station 49.453 cm.

A cross-sectional area of body, 88.534 cm^2

C_A axial-force coefficient, $\frac{\text{Axial force}}{qA}$

C_D drag coefficient, $\frac{\text{Drag}}{qA}$

C_H control-surface hinge-moment coefficient, $\frac{\text{Hinge moment}}{qAd}$

C_l rolling-moment coefficient (body axes), $\frac{\text{Rolling moment}}{qAd}$

C_{l_β} $= \frac{\Delta C_l}{\Delta \beta}$, per deg

C_L lift coefficient, $\frac{\text{Lift}}{qA}$

C_m pitching-moment coefficient, $\frac{\text{Pitching moment}}{qAd}$

C_n yawing-moment coefficient (body axes), $\frac{\text{Yawing moment}}{qAd}$

C_{n_β} $= \frac{\Delta C_n}{\Delta \beta}$, per deg

C_N normal-force coefficient, $\frac{\text{Normal force}}{qA}$

C_Y side-force coefficient, $\frac{\text{Side force}}{qA}$

C_{Y_β} $= \frac{\Delta C_Y}{\Delta \beta}$, per deg

d body diameter, 10.617 cm

L/D lift-drag ratio

$\frac{m}{m_\infty}$ inlet mass flow ratio (ratio of inlet mass flow to mass flow at free-stream conditions through a stream tube of cross-sectional area equal to inlet projected area)

M Mach number

q free-stream dynamic pressure, Pa

R radius, cm

α angle of attack, deg

β angle of sideslip, deg

δ_p tail deflection in pitch direction, deg (positive deflection creates negative pitching moment)

δ_r tail deflection in roll direction, deg (positive deflection creates positive rolling moment)

δ_y tail deflection in yaw direction, deg (positive deflection creates negative yawing moment)

Subscripts:

1,2,3,4 tail fin designation for hinge-moment coefficients (see fig. 1):
- 1 upper right; positive hinge moment, leading edge down
- 2 lower right; positive hinge moment, leading edge down
- 3 lower left; positive hinge moment, leading edge up
- 4 upper left; positive hinge moment, leading edge up

Model components:

B body

C cruciform wing

P planar wing

T tail

MODEL DESCRIPTION

Details of the model are presented in figure 1, and a photograph of the model is presented in figure 2. The body-inlet configuration was basically an ogive-cylinder with the cylindrical cross section modified to accommodate the duct from the inlet to the ramjet combustor. Configuration variables included internal flow, simulating integral rocket/ramjet propulsion at Mach numbers from 2.86 to 4.63; cruciform wings; low-aspect-ratio planar (horizontal) wings; and aft cruciform control surfaces (fins) to provide stability and control in pitch, yaw, and roll. All four fin surfaces were deflected to provide either pitch, yaw, or roll control. At Mach numbers from 1.70 to 2.86, the internal duct was closed and a fairing covered the inlet to simulate the boost configuration of the missile (no flow to the air-breathing propulsion system).

TESTS AND CORRECTIONS

Tests were conducted in the Langley Unitary Plan wind tunnel, which is a variable-pressure, continuous-flow tunnel. The test section is approximately 1.2 m (4 ft) square and 2.1 m (6.88 ft) long, and the nozzle leading to the test section is of the asymmetric

sliding-block type. The nozzle permits a continuous variation in Mach number from 1.47 to 2.86 (low Mach number section), and 2.29 to-4.63 (high Mach number section). Tunnel operating conditions for this investigation are given in the following table:

Mach number	Stagnation temperature, K	Total pressure, kPa	Reynolds number per meter
1.70	339	56.40	6.56×10^6
2.36	339	75.65	6.56×10^6
2.86	339	98.44	6.56×10^6
3.95	353	184.96	6.56×10^6
4.63	353	252.57	6.56×10^6

The dewpoint was maintained below 240 K to insure negligible condensation effects. The tests were made with fixed transition consisting of a 0.16-cm-wide band located 3.05 cm aft of the model nose and 1.02 cm aft, in a streamwise direction, of the leading edges of the fins, wings, and inlet. At Mach numbers of 1.70, 2.36, and 2.86 No. 50 grit was used, and at Mach numbers of 3.95 and 4.63 No. 35 grit was used. Single-spaced No. 35 grit was used inside the inlet at all Mach numbers.

The data have been corrected for deflection of the sting and balance due to aerodynamic loads and for tunnel flow angularity. Model-cavity and base pressures were measured in the vicinity of the strain-gage balance and/or the model base. The axial-force and drag data were adjusted to a condition of free-stream static pressure acting over the base of the model. For the inlet-closed runs with no internal flow, the duct exit area was considered part of the base area. Internal flow measurements were made using a rake at the model base during runs separate from the force-measurement runs. An adjustment has been made to the data for the configurations having internal flow to remove the internal drag. The internal drag is that drag associated with the buoyancy and change in momentum of the internal flow from free-stream to exit conditions. The internal-flow rake data have also been used to compute the inlet mass-flow ratio, which is presented in figure 3.

PRESENTATION OF RESULTS

The results of the investigation are presented in the following figures:

DISCUSSION OF RESULTS

The longitudinal aerodynamic characteristics of three missile configurations are presented for various control deflections and Mach numbers in figures 4, 5, and 6. In figure 7, the characteristics of all three configurations are presented for 0^{o} pitch control deflection at $M = 2.86$. Both the planar-wing and cruciform-wing configurations showed greater longitudinal stability than the body-tail configuration. Although all three configurations were unstable or near neutral stability about the assumed moment center, the data indicate that the center of gravity could be located so that with a margin of longitudinal stability, the pitch control would be sufficient to trim the model at an angle of attack of at least 20^{o}. Addition of either wing configuration caused an increase in normal force, which resulted in a small increase in maximum L/D. For all three configurations, the normal force available was insufficient for a highly maneuverable missile, except at very low altitudes.

The lateral-directional data of figure 9 show that the body-tail configuration was unstable up to about 7^{o} angle of attack and became somewhat stable at higher angles of attack. The addition of cruciform wings increased the directional stability at angles of attack above 5^{o}. The addition of planar wings, however, decreased the directional stability, and the configuration was unstable throughout the angle-of-attack range of the tests. All these configurations had nearly neutral lateral stability throughout the angle-of-attack range, with the exception of the cruciform-wing configuration, which was stable at angles of attack above 10^{o}.

The effect of yaw control on the longitudinal and lateral-directional characteristics is shown in figures 10, 11, and 12. At $M = 2.86$, the body-tail configuration (fig. 10) had effective yaw control throughout the angle-of-attack range. The resulting negative yawing moment was accompanied by a rolling moment of about zero near 0^{o} angle of attack. The rolling moment became negative as the angle of attack was increased. The addition of either the planar or cruciform wings had essentially no effect on yaw control effectiveness.

Roll control, which was applied only to the planar-wing configuration (fig. 11), was generally effective. Positive rolling moment was accompanied by zero yawing moment at angles of attack near zero. Yawing moment increased in the positive direction above angles of attack of approximately 7^{o}.

In general, the effect of Mach number on the control effectiveness was to reduce the moment coefficients as the Mach number was increased. The data presented in figures 13, 14, and 15 were taken at the lower Mach numbers. These Mach numbers represent the boost condition, where the internal duct is closed and the inlet fairing cover is installed. At a Mach number of 1.70, the pitching moment near 0^{o} angle of attack was small, but as the Mach number increased, the configurations tended to pitch up. The magnitude of the

pitching moment due to the inlet cover at $M = 2.86$ can be seen in figure 16, which is a comparison of the data of figures 5 and 14. With internal flow, the pitching moment near 0° angle of attack was about -0.2 compared with 0.5 without internal flow and with the inlet cover installed. A similar comparison of axial-force coefficient shows an increase from about 0.25 to 0.32.

The lateral-directional stability of the planar-wing configuration with the inlet closed is presented in figure 15. Generally, the configuration was stable at $M = 1.70$ but became directionally unstable as the Mach number was increased. The model retained lateral stability throughout the Mach number range at positive angles of attack. A comparison of the data of figures 15 and 9 (fig. 17) shows little effect of the inlet cover on the lateral-directional stability at $M = 2.86$.

Control-surface hinge-moment data are presented in figures 18 to 20 for the body-tail, planar-wing configuration with the inlet both open and closed. The data show little effect of inlet configuration or Mach number on the hinge-moment coefficients.

CONCLUDING REMARKS

An investigation has been made to determine the aerodynamic characteristics of an air-breathing missile configuration having a forward located inlet, planar or cruciform wings, and cruciform tails for control. The tests were made at Mach numbers from 2.86 to 4.63 with internal flow and from 1.70 to 2.86 without internal flow, to simulate boost conditions. The results indicate that the addition of either wing configuration to the body-tail configuration increased longitudinal stability. The normal-force coefficient available would be insufficient for a highly maneuverable missile, except at very low altitudes. Pitch control provided by the tails was adequate to trim the model at angles of attack to at least 20° when the center of gravity was moved to provide a margin of longitudinal stability. The tail surfaces were also effective in providing yaw and roll control. The effect of closing the inlet, to simulate boost conditions, was a positive pitching-moment increment and an increase in axial force. The pitch-up was small at a Mach number of 1.70 but increased with increasing Mach number.

Langley Research Center
National Aeronautics and Space Administration
Hampton, Va. 23665
June 21, 1976

REFERENCES

1. Hayes, Clyde; and Monta, William J.: Aerodynamic Characteristics of a 1/4-Scale Model of MORASS Missile Configurations at Supersonic Speeds. NASA TM X-3354, 1976.

2. Mechtly, E. A.: The International System of Units – Physical Constants and Conversion Factors (Second Revision). NASA SP-7012, 1973.

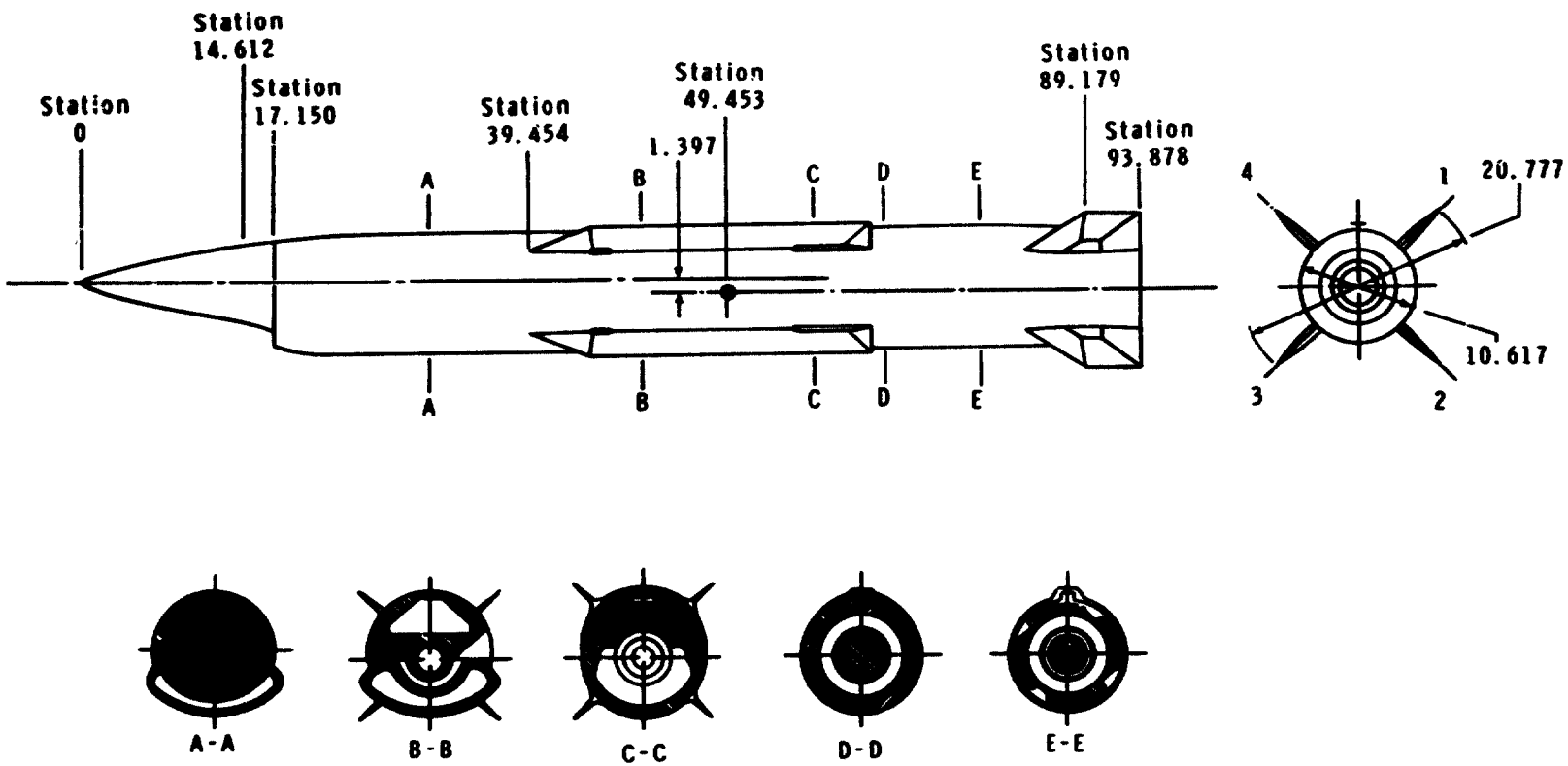

(a) Body-tail, cruciform-wing configuration.

Figure 1.- Wind-tunnel model of forward-inlet missile. (Model dimensions are in centimeters.)

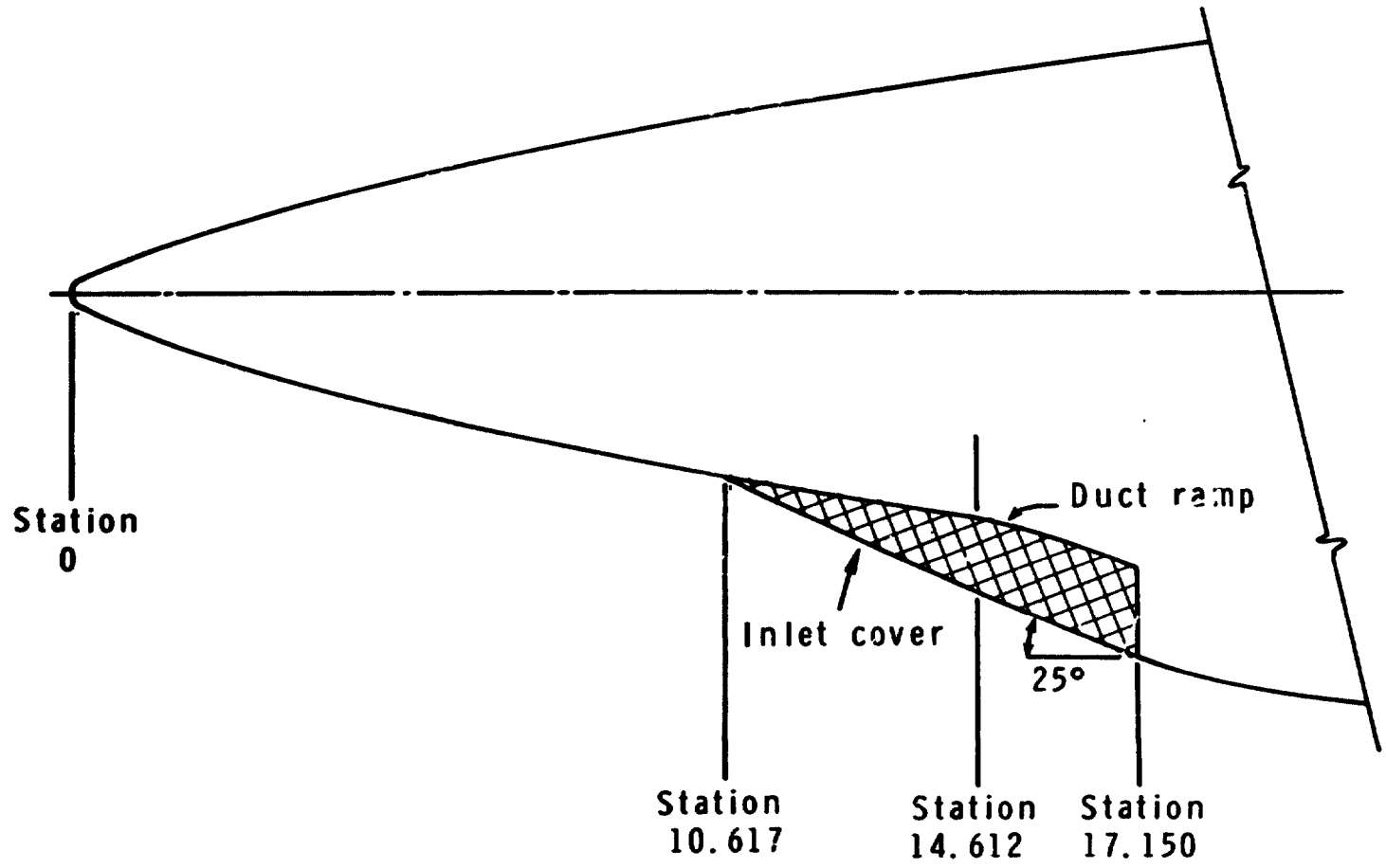

(b) Inlet cover.

Figure 1.- Continued.

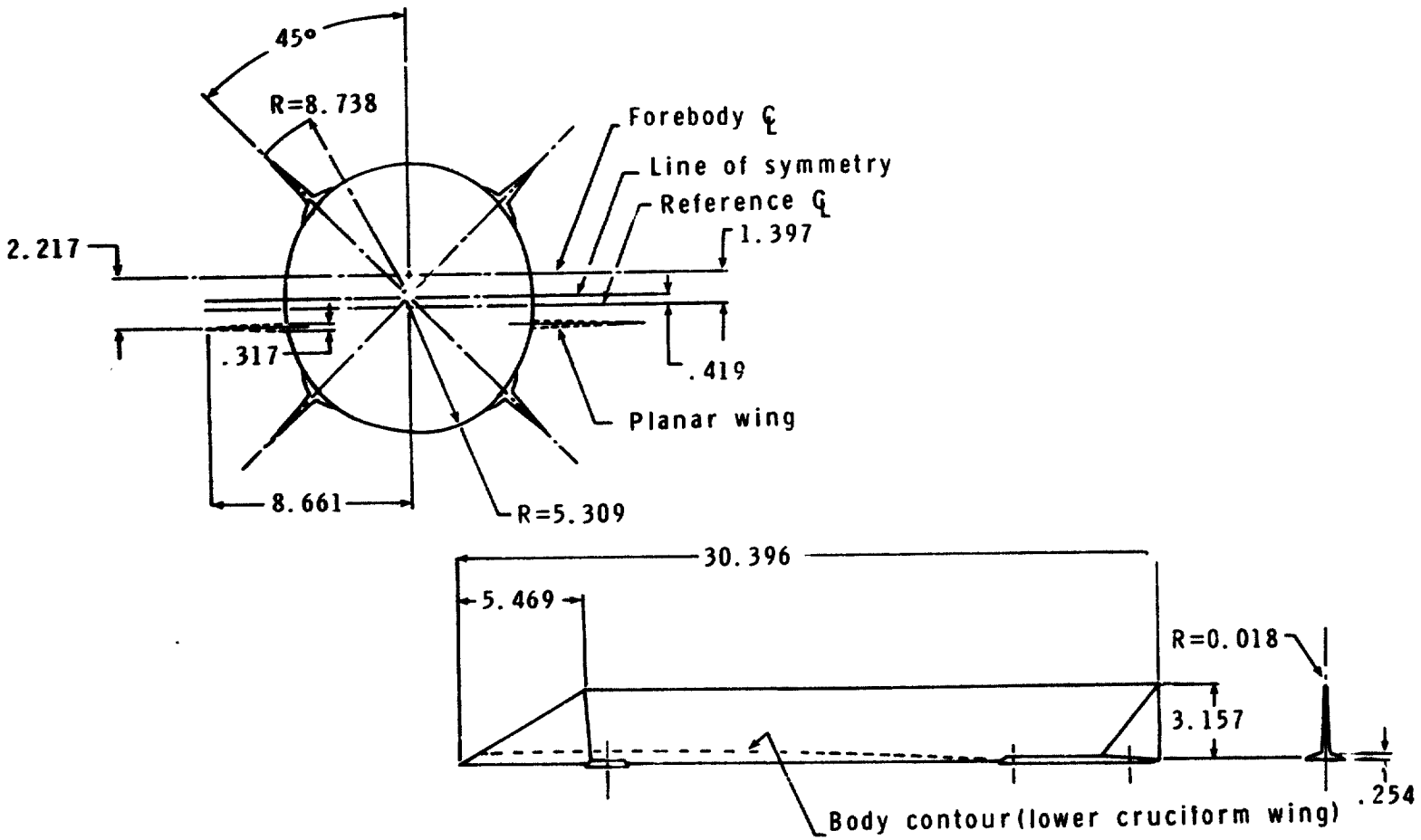

(c) Wing geometry.

Figure 1.- Continued.

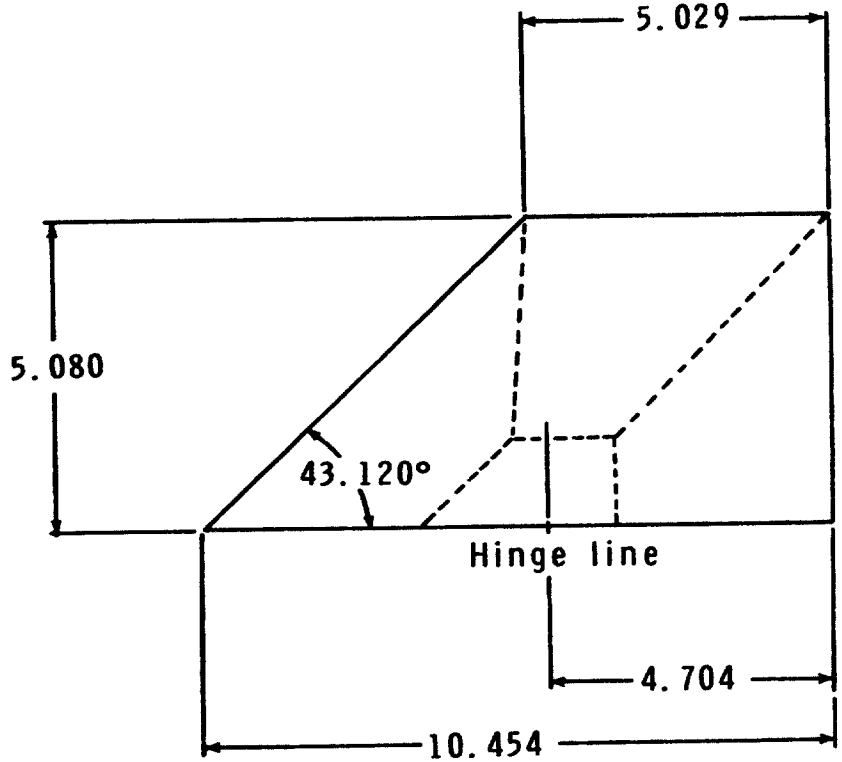

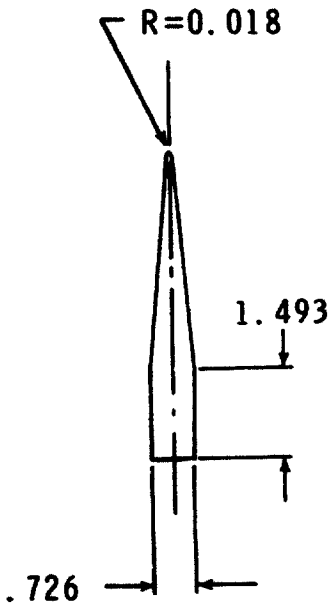

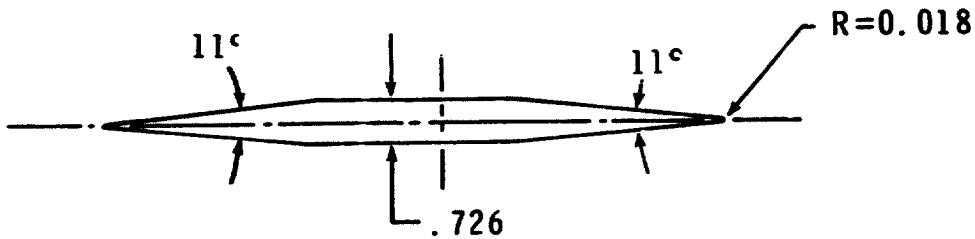

(d) Tail dimensions.

Figure 1.- Concluded.

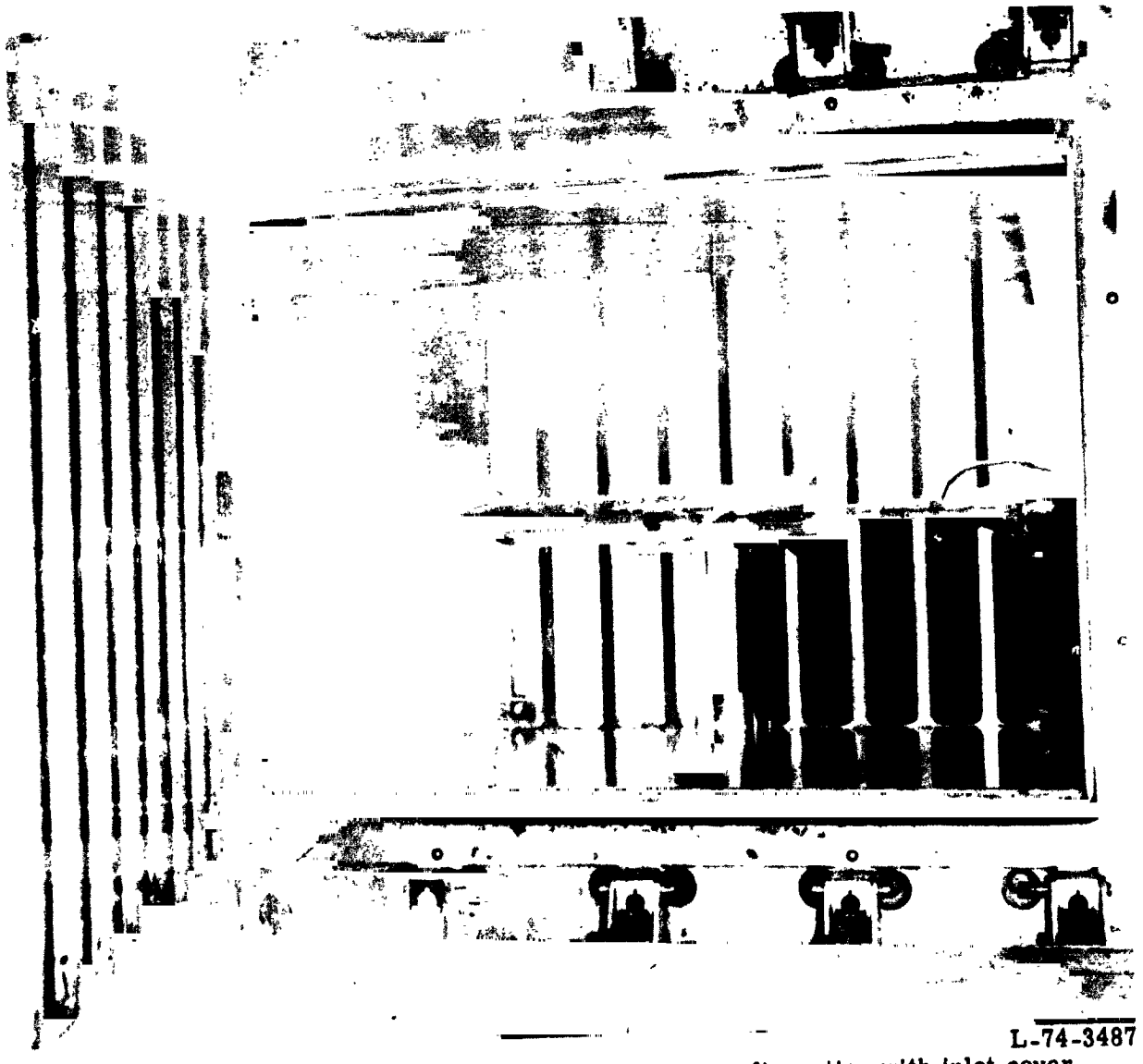

L-74-3487

Figure 2.- Wind-tunnel model of cruciform-wing configuration with inlet cover.

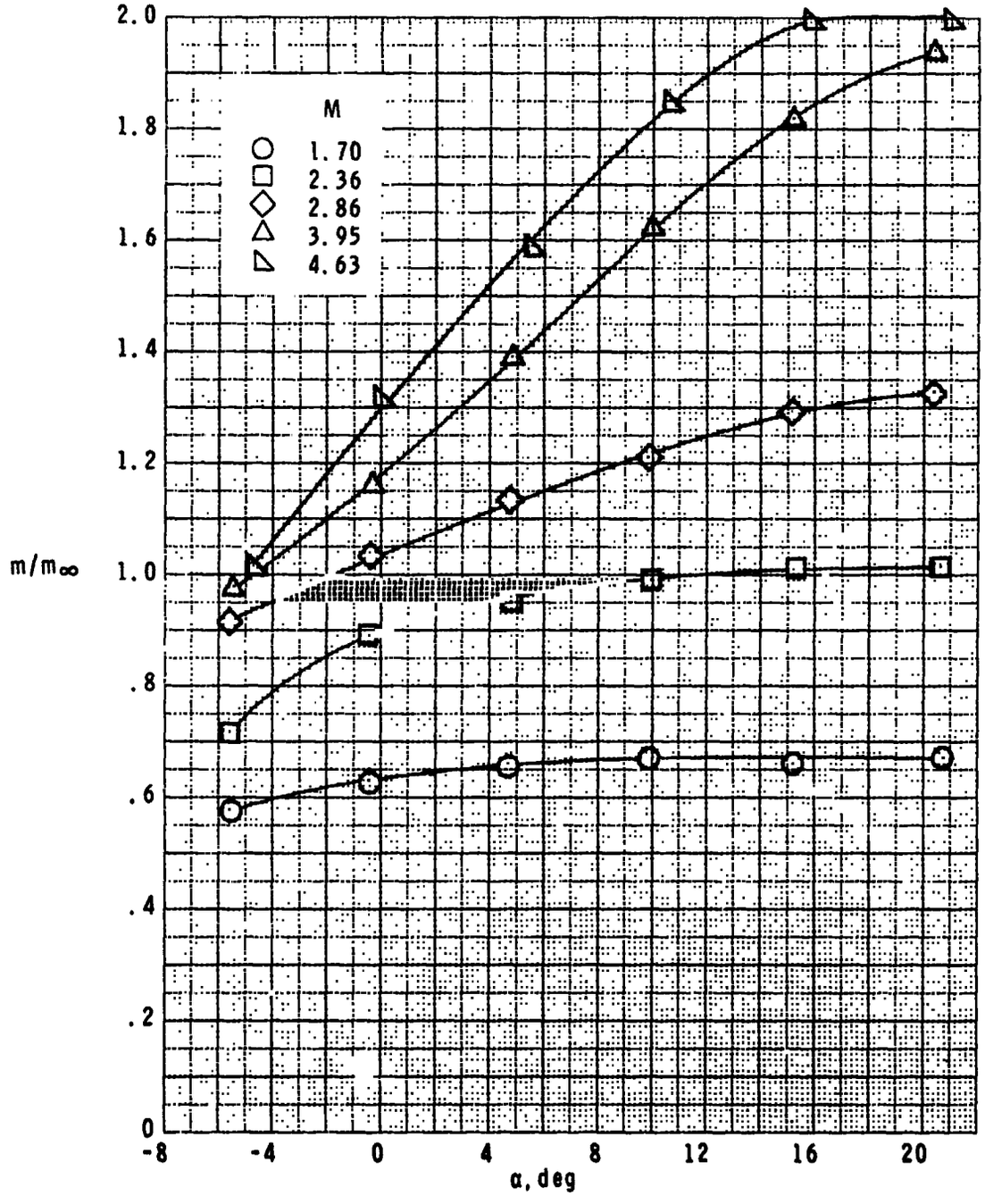

Figure 3.- Inlet mass-flow ratio.

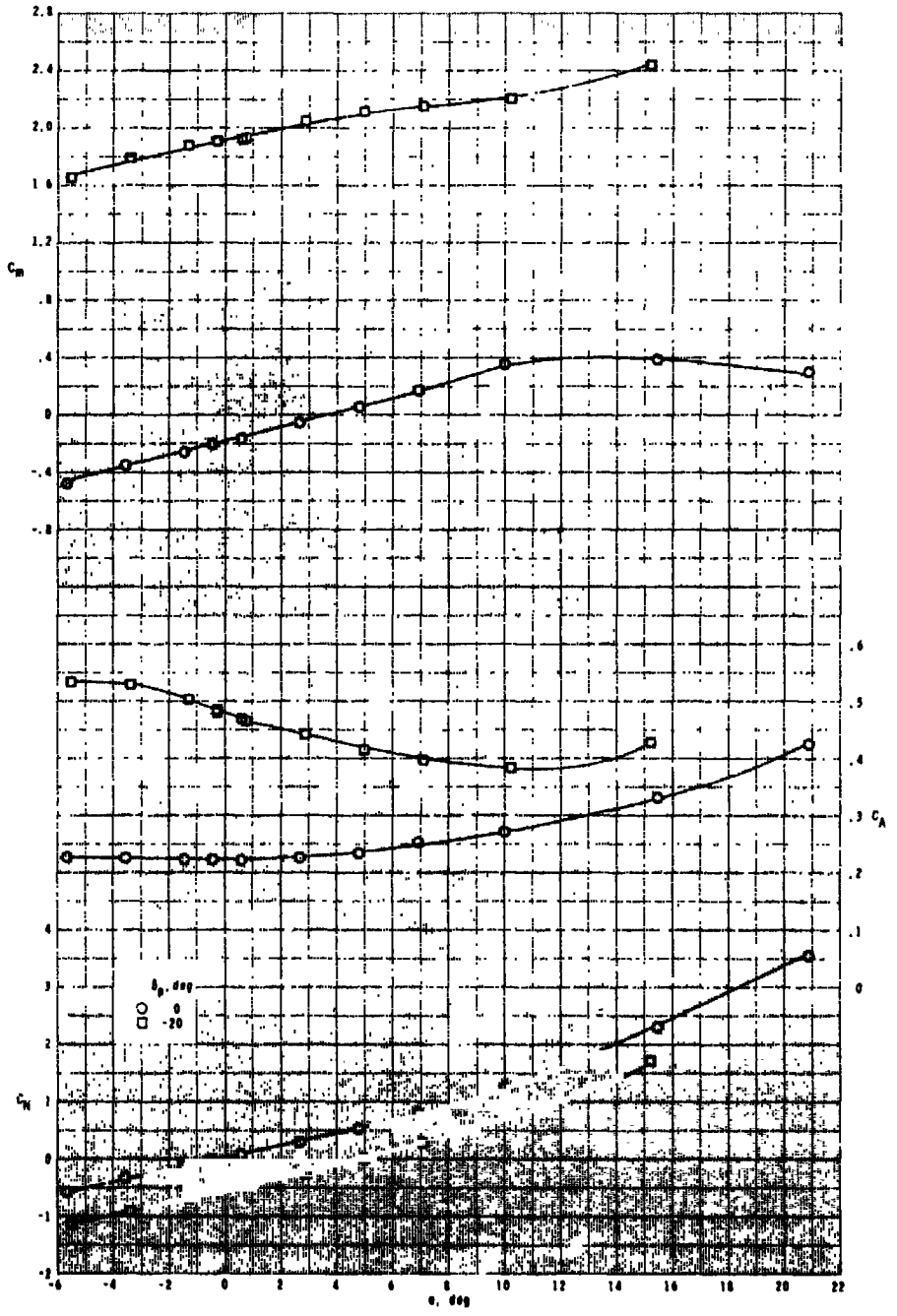

(a) M = 2.86.

Figure 4.- Longitudinal aerodynamic characteristics of body-tail configuration with pitch control.

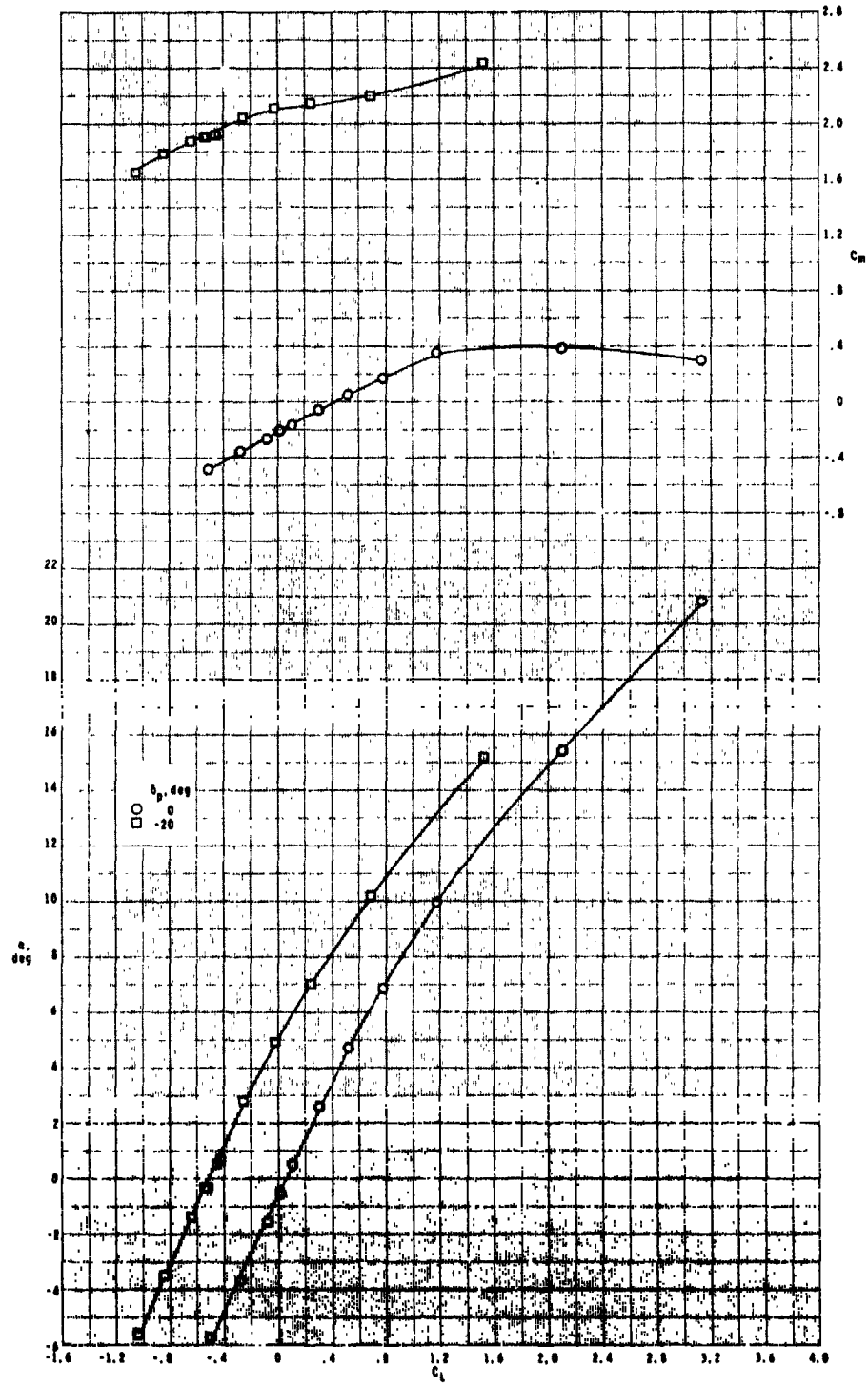

(a) Continued.

Figure 4.- Continued.

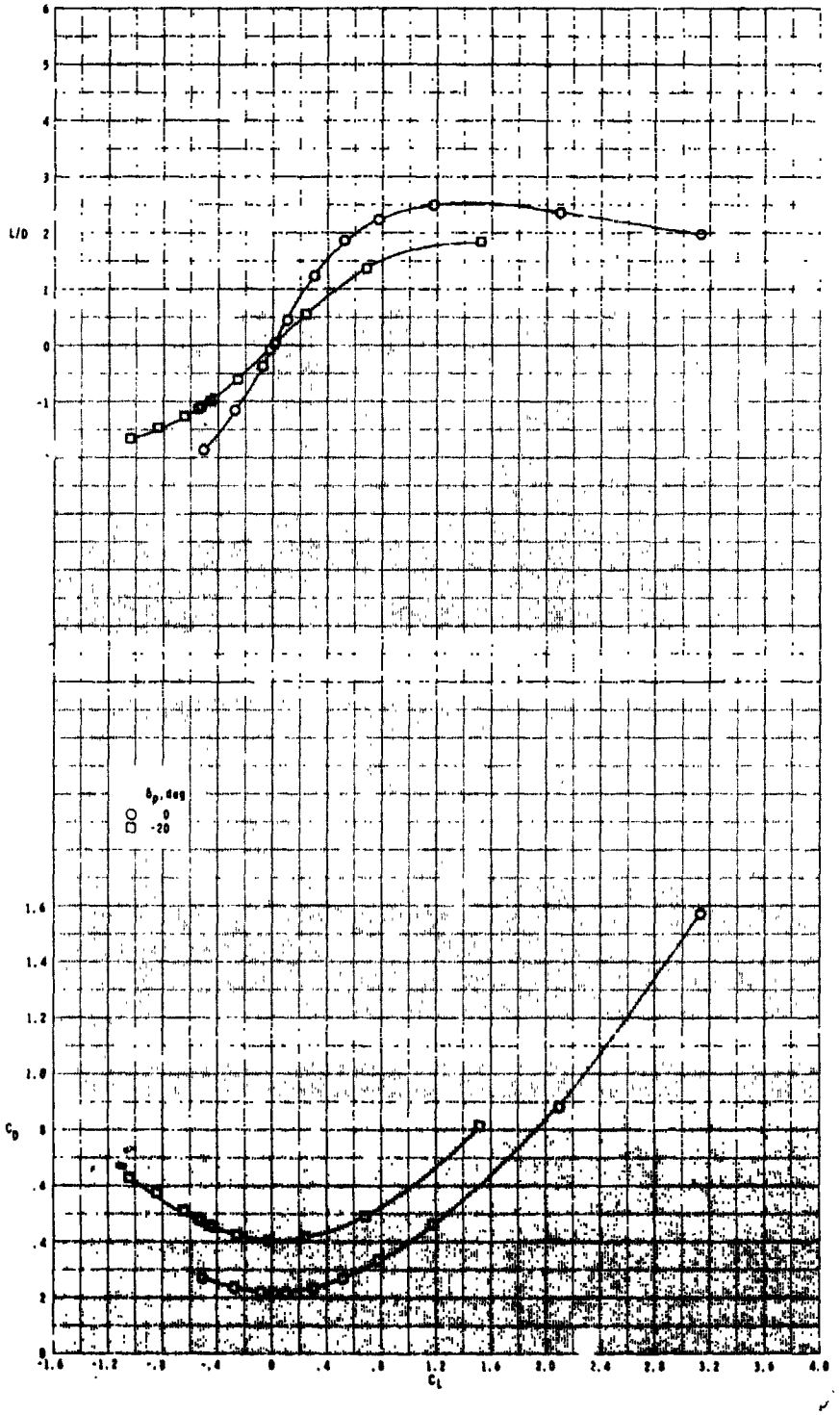

(a) Concluded.

Figure 4.- Continued.

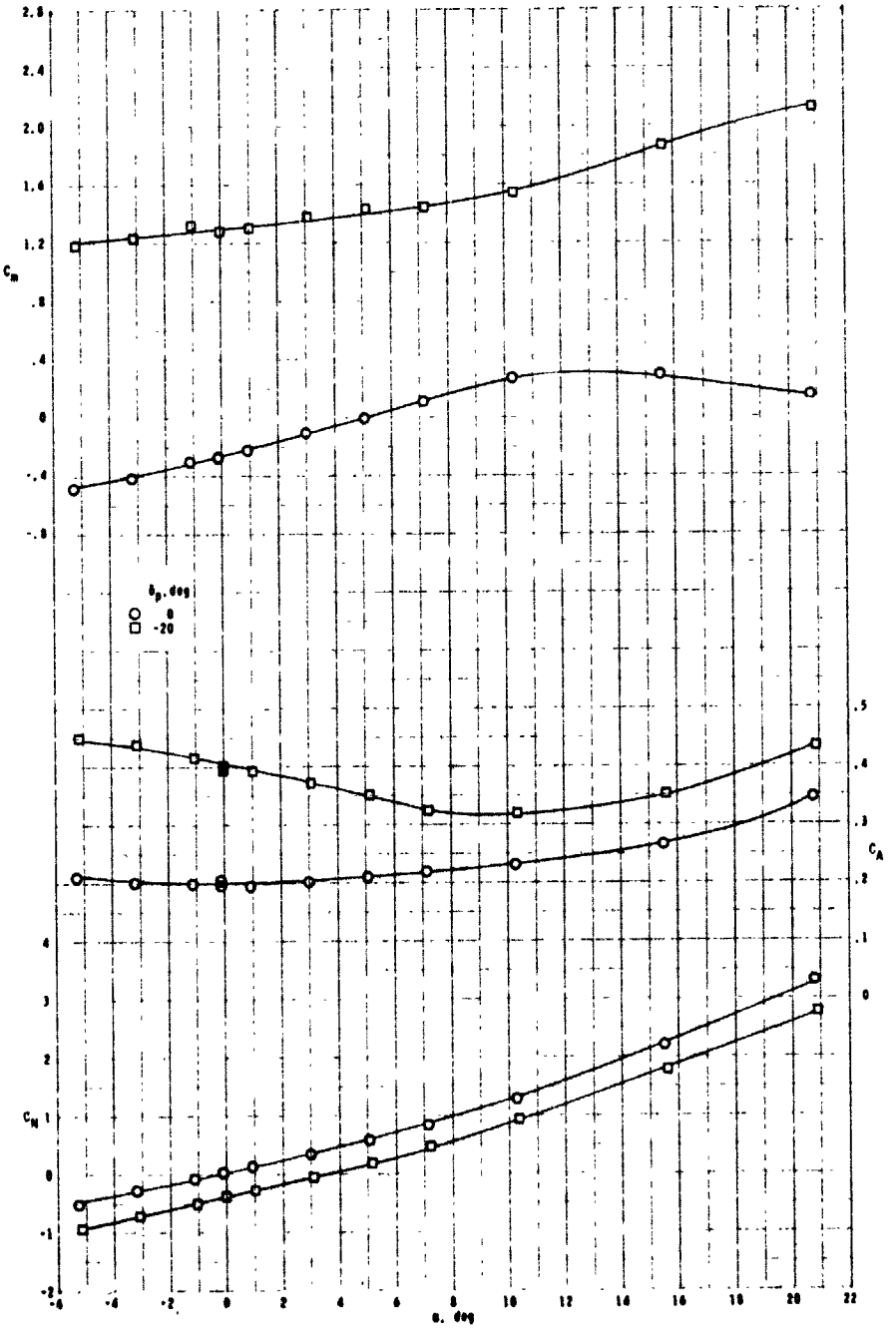

(b) M = 3.95.

Figure 4.- Continued.

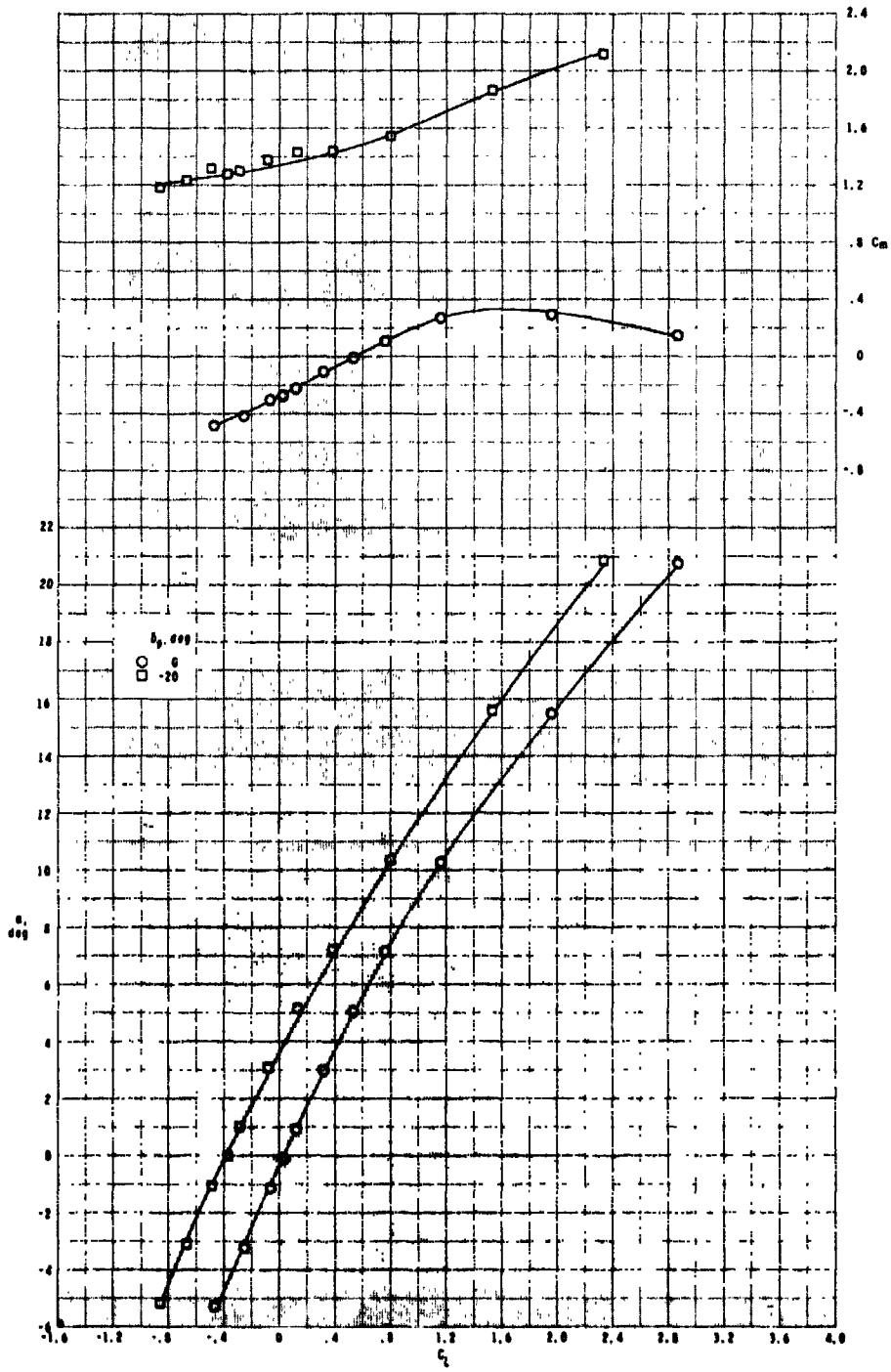

(b) Continued.

Figure 4.- Continued.

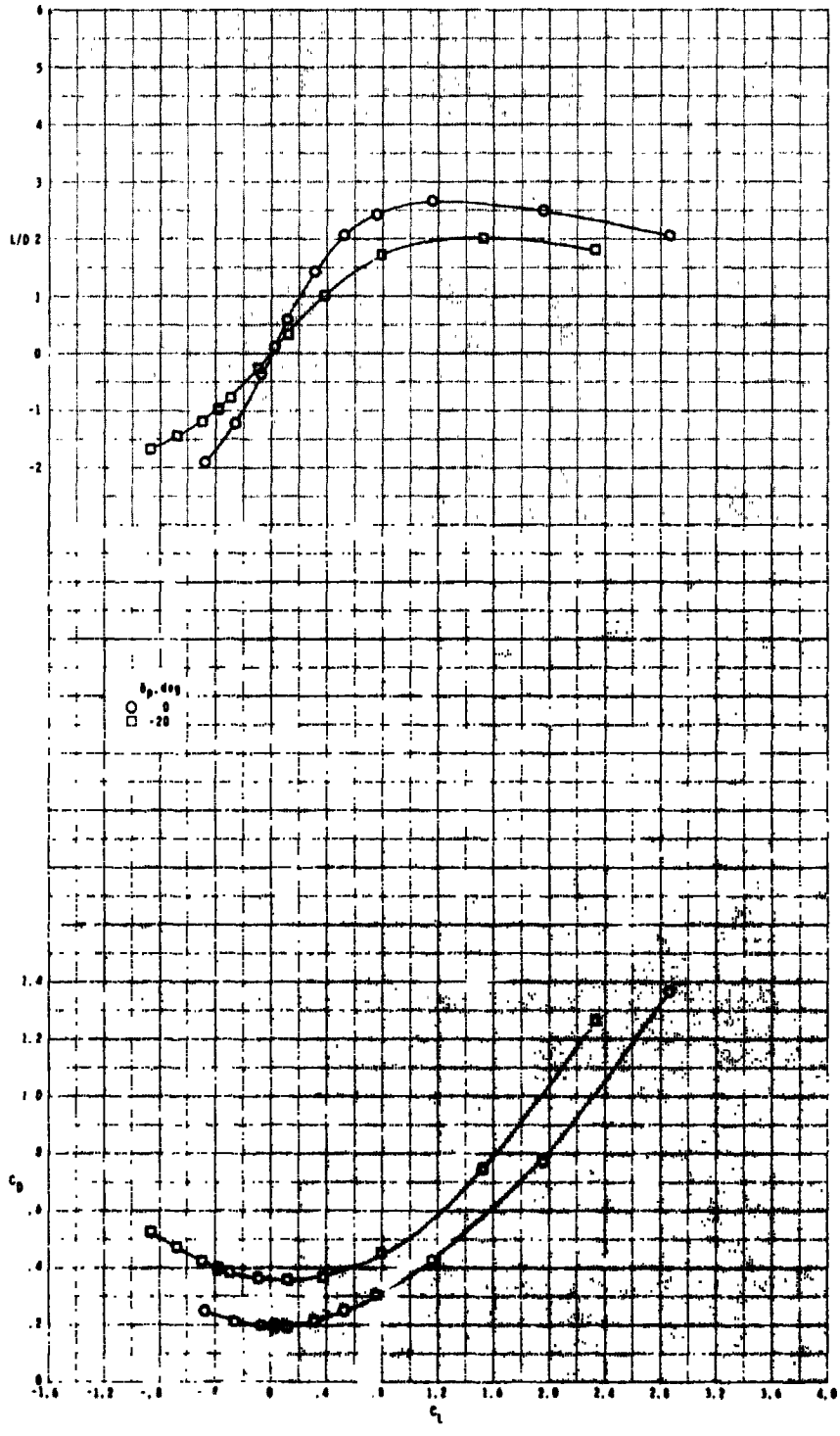

(b) Concluded.

Figure 4.- Continued.

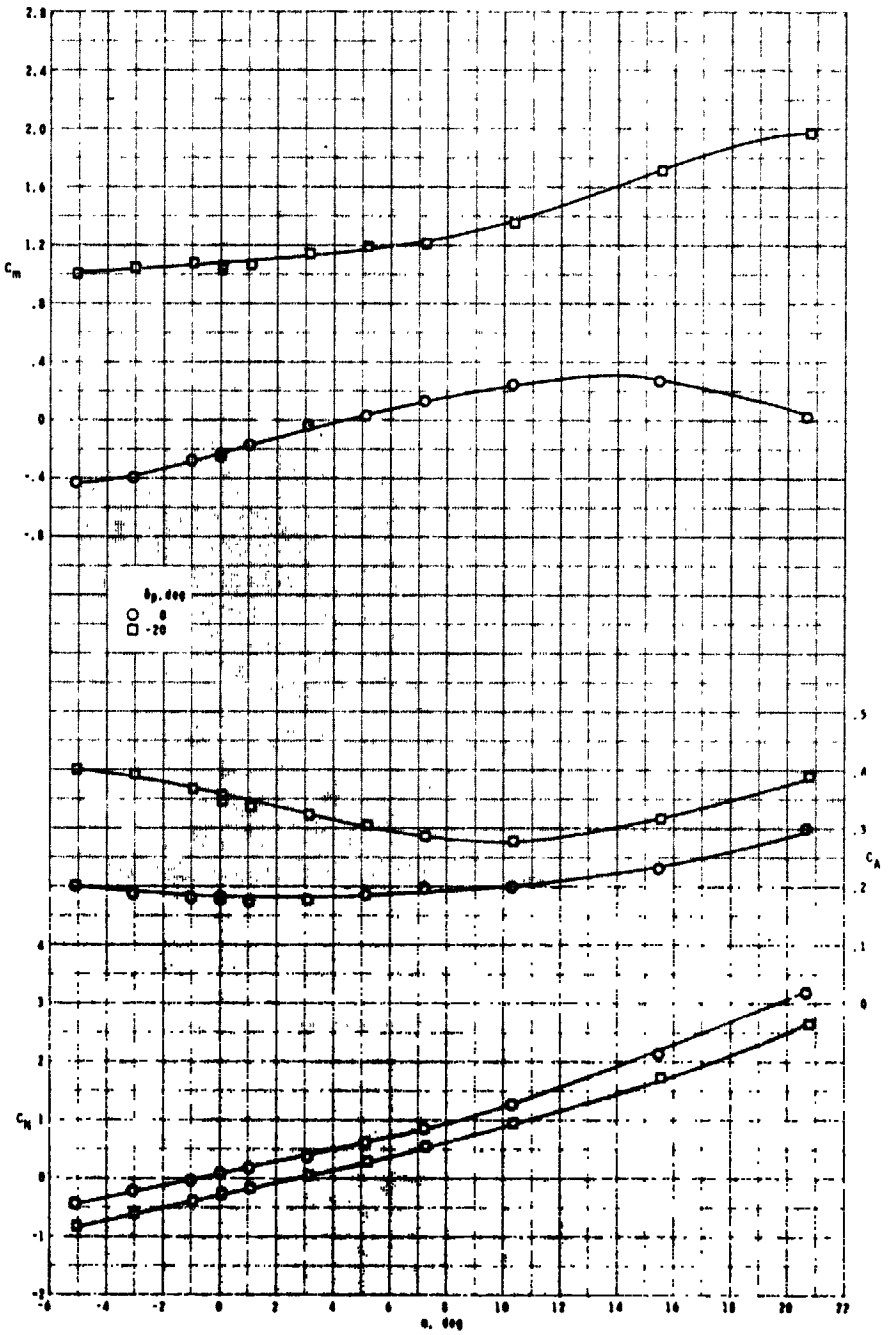

(c) M = 4.63.

Figure 4.- Continued.

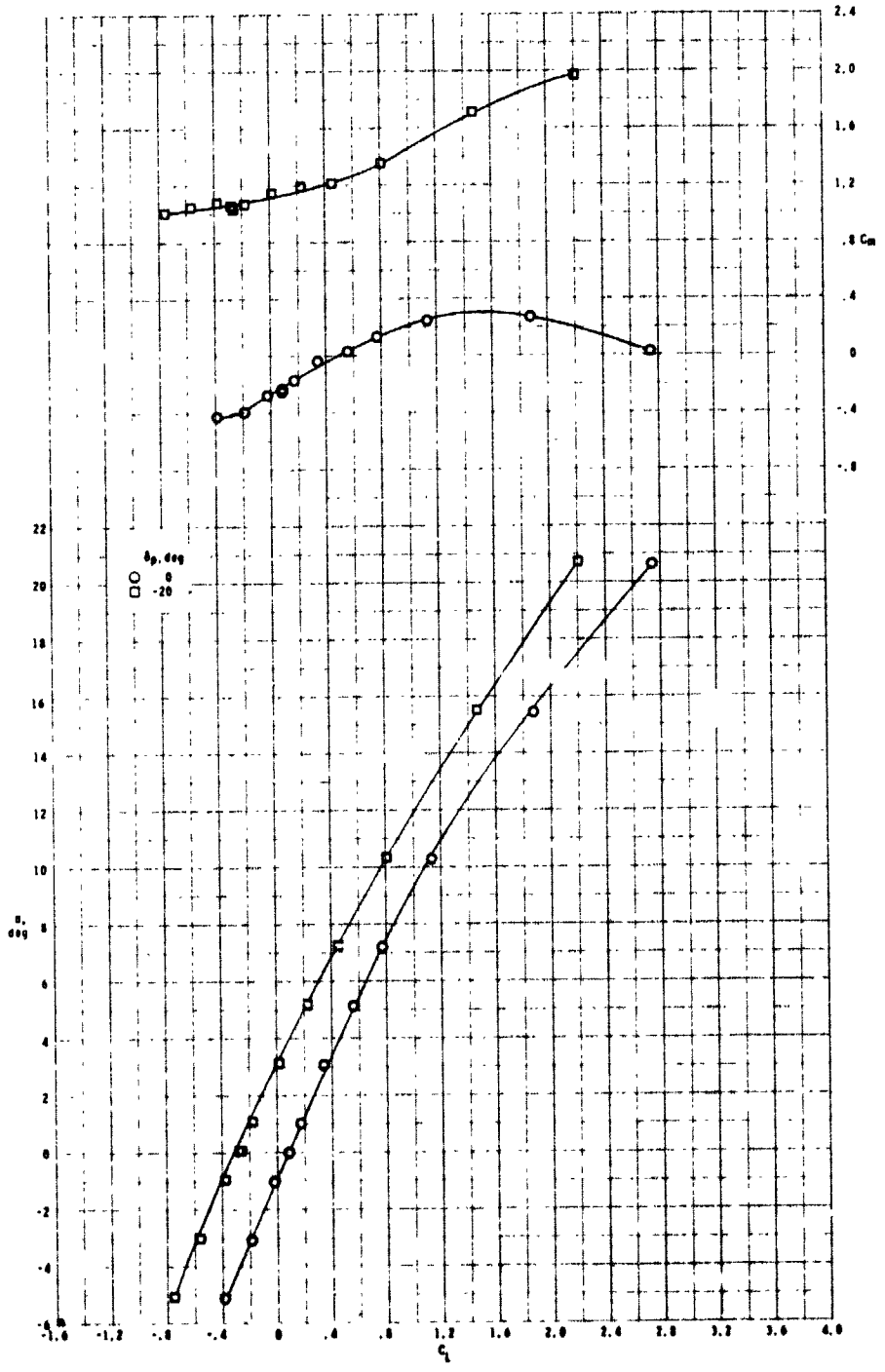

(c) Continued.

Figure 4.- Continued.

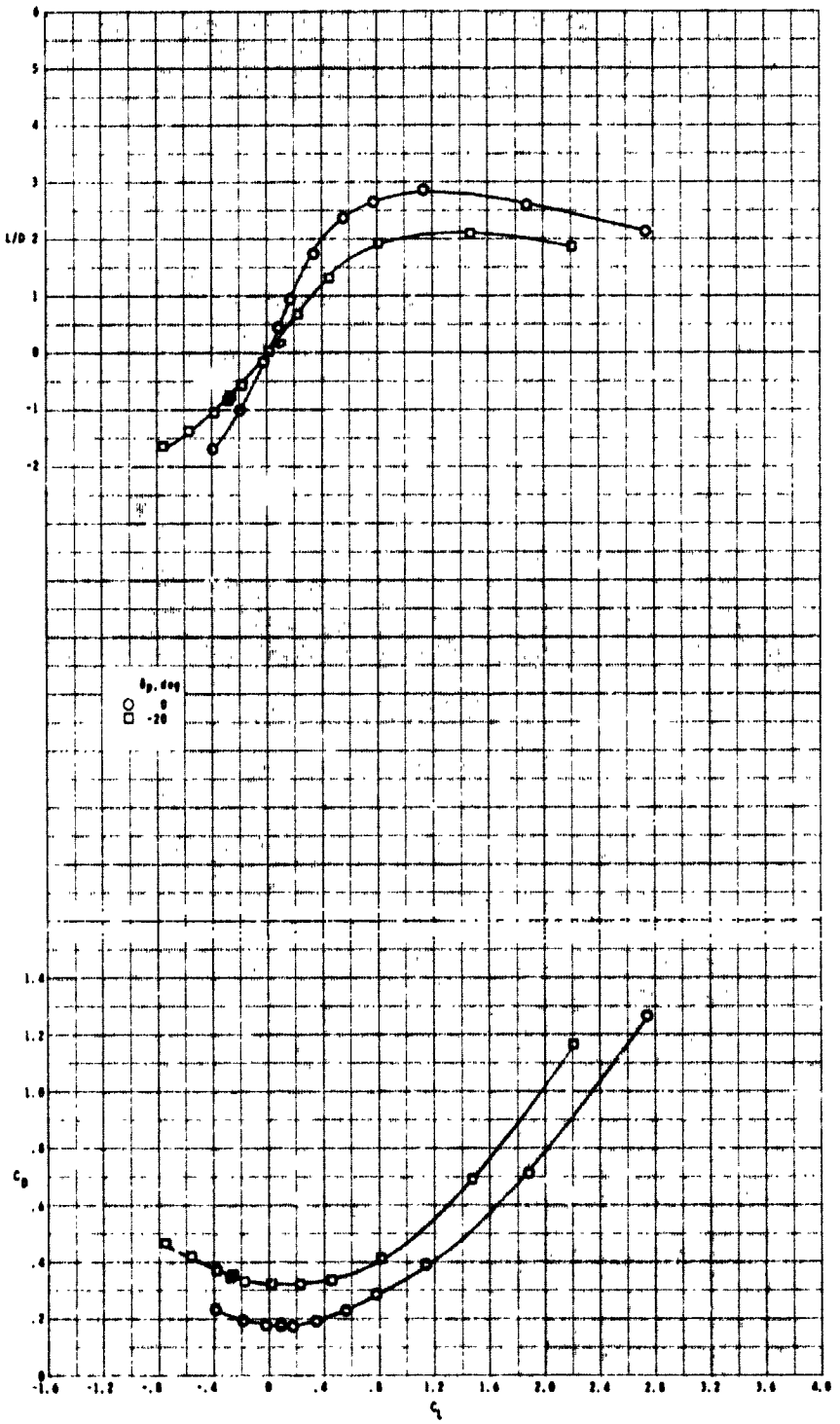

(c) Concluded.

Figure 4.- Concluded.

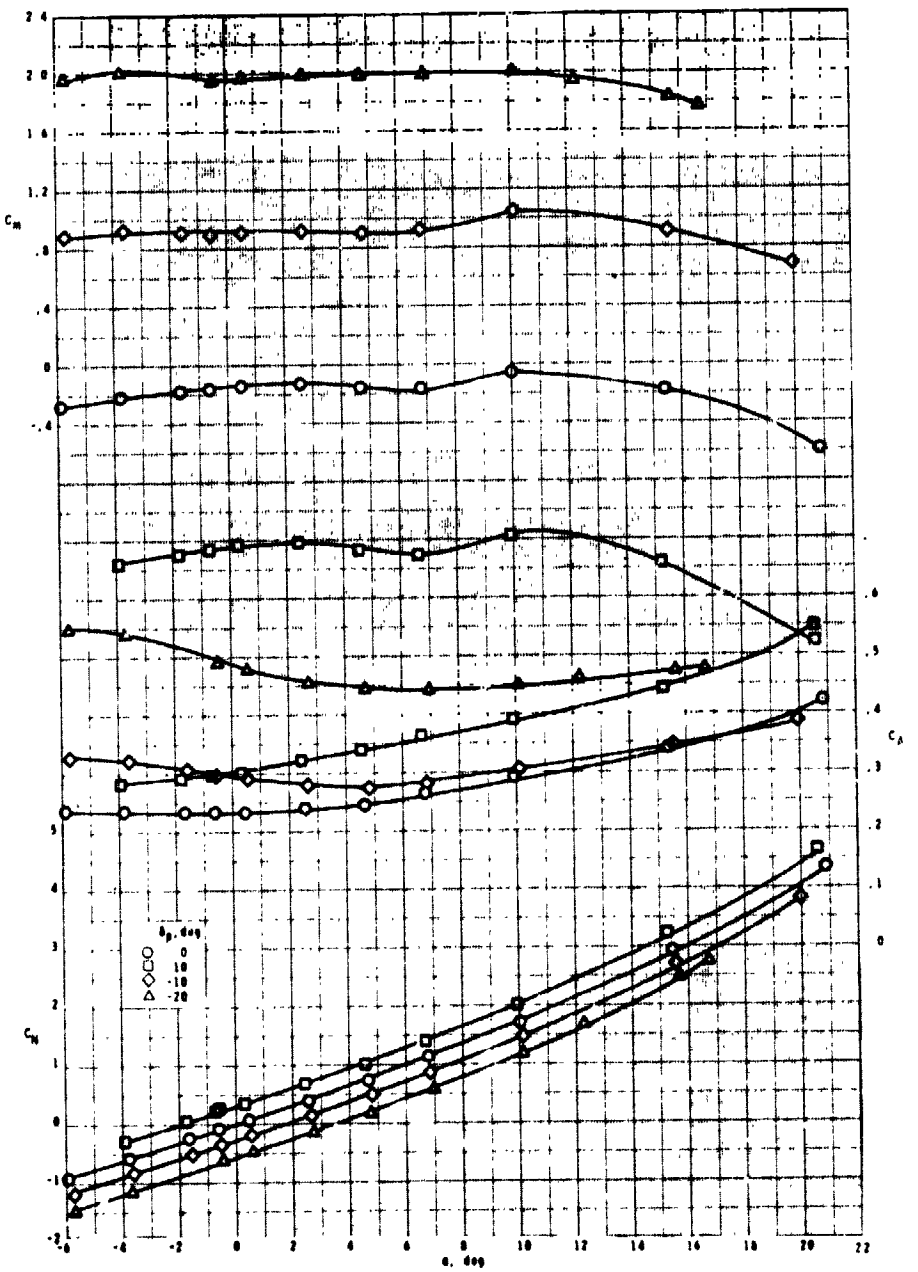

(a) M = 2.86.

Figure 5.- Longitudinal aerodynamic characteristics of body-tail, planar-wing configuration with pitch control.

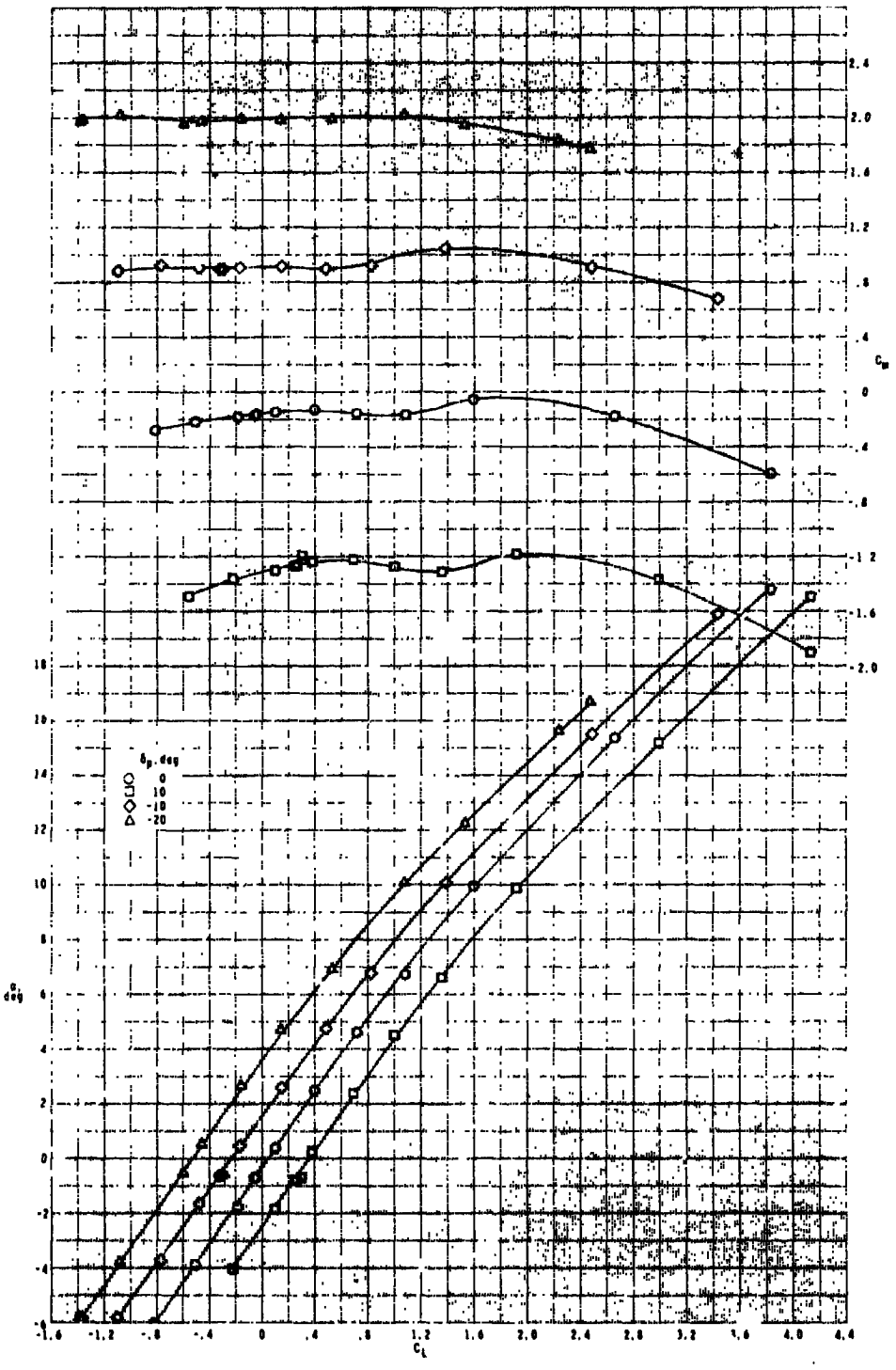

(a) Continued.

Figure 5.- Continued.

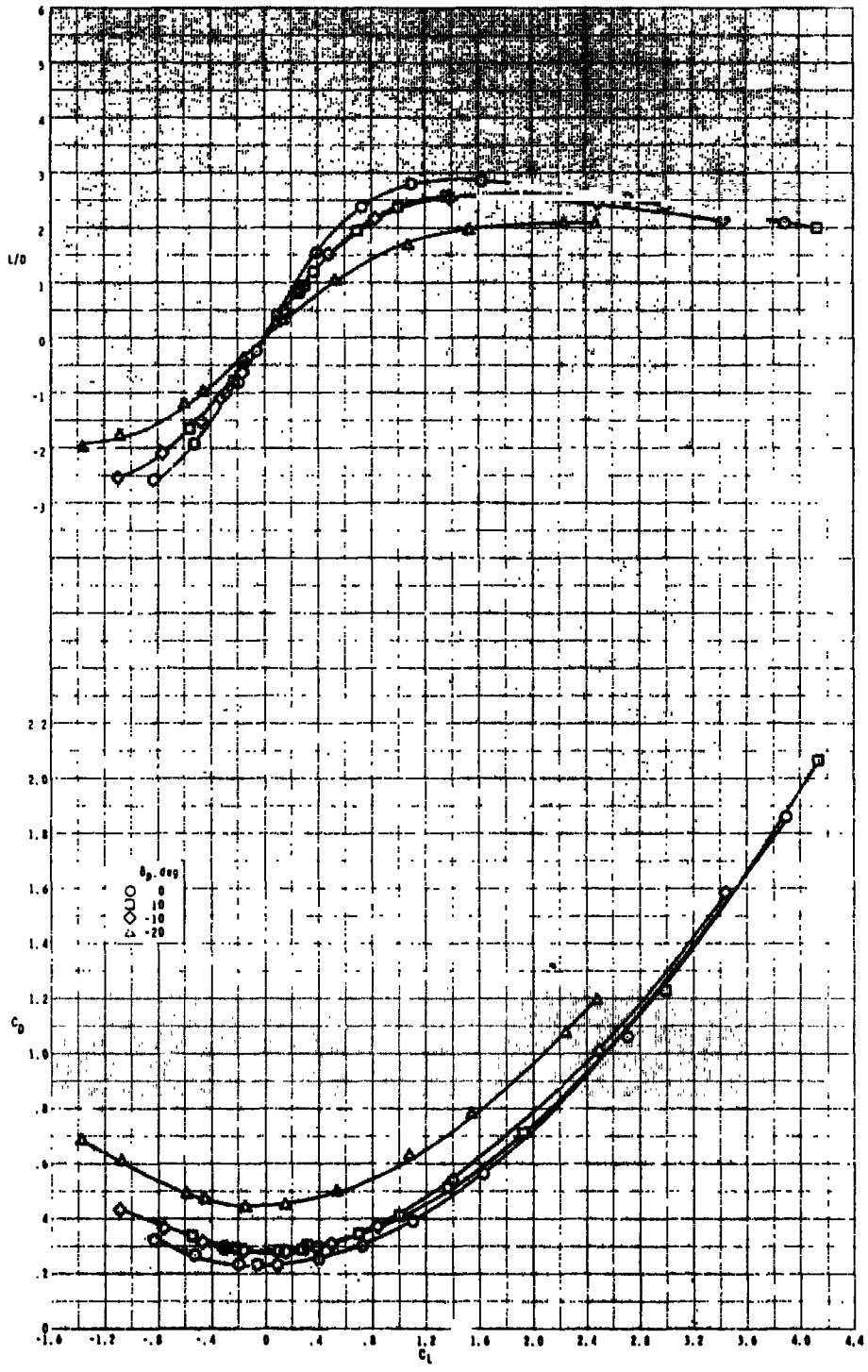

(a) Concluded.

Figure 5.- Continued.

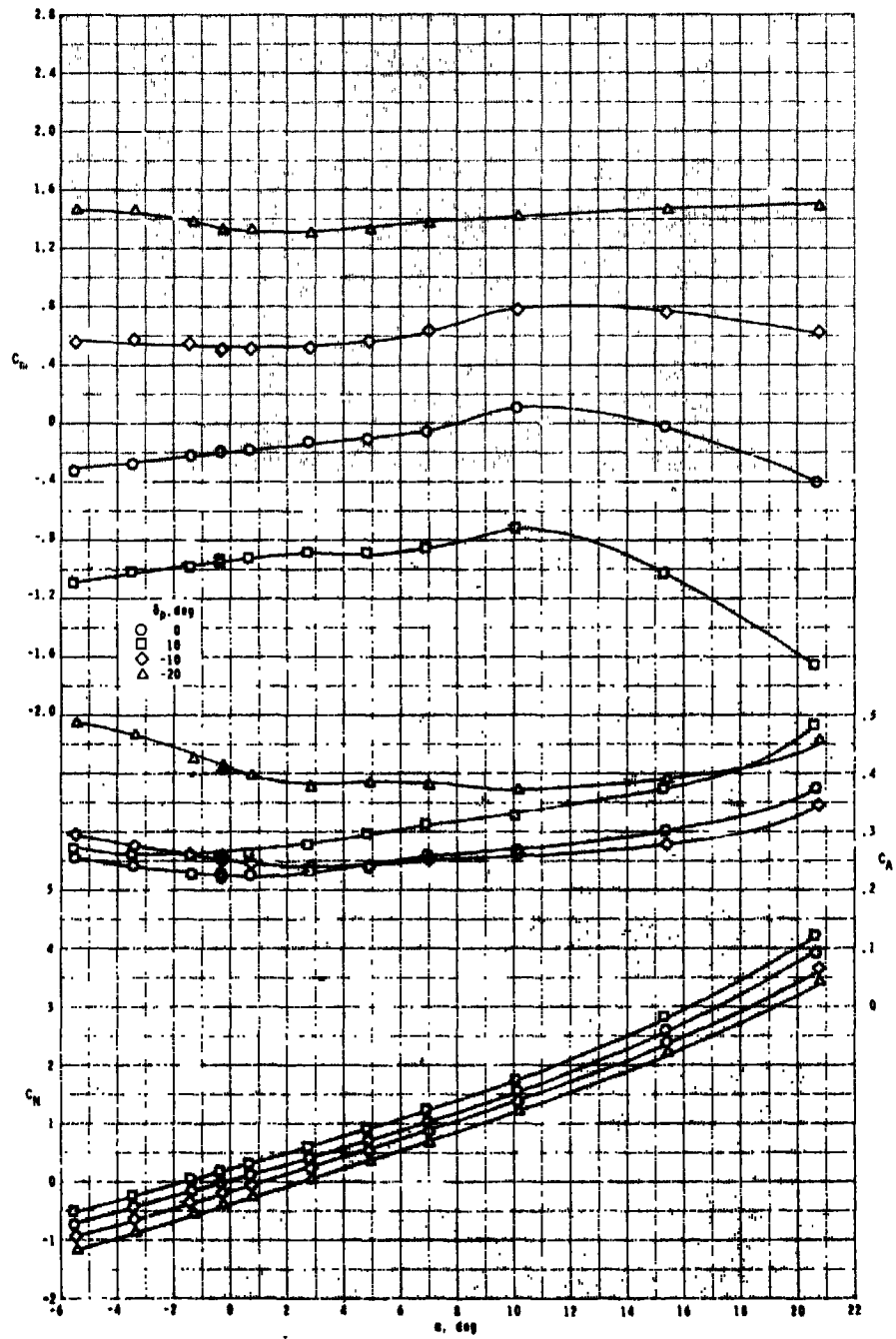

(b) M = 3.95.

Figure 5.- Continued.

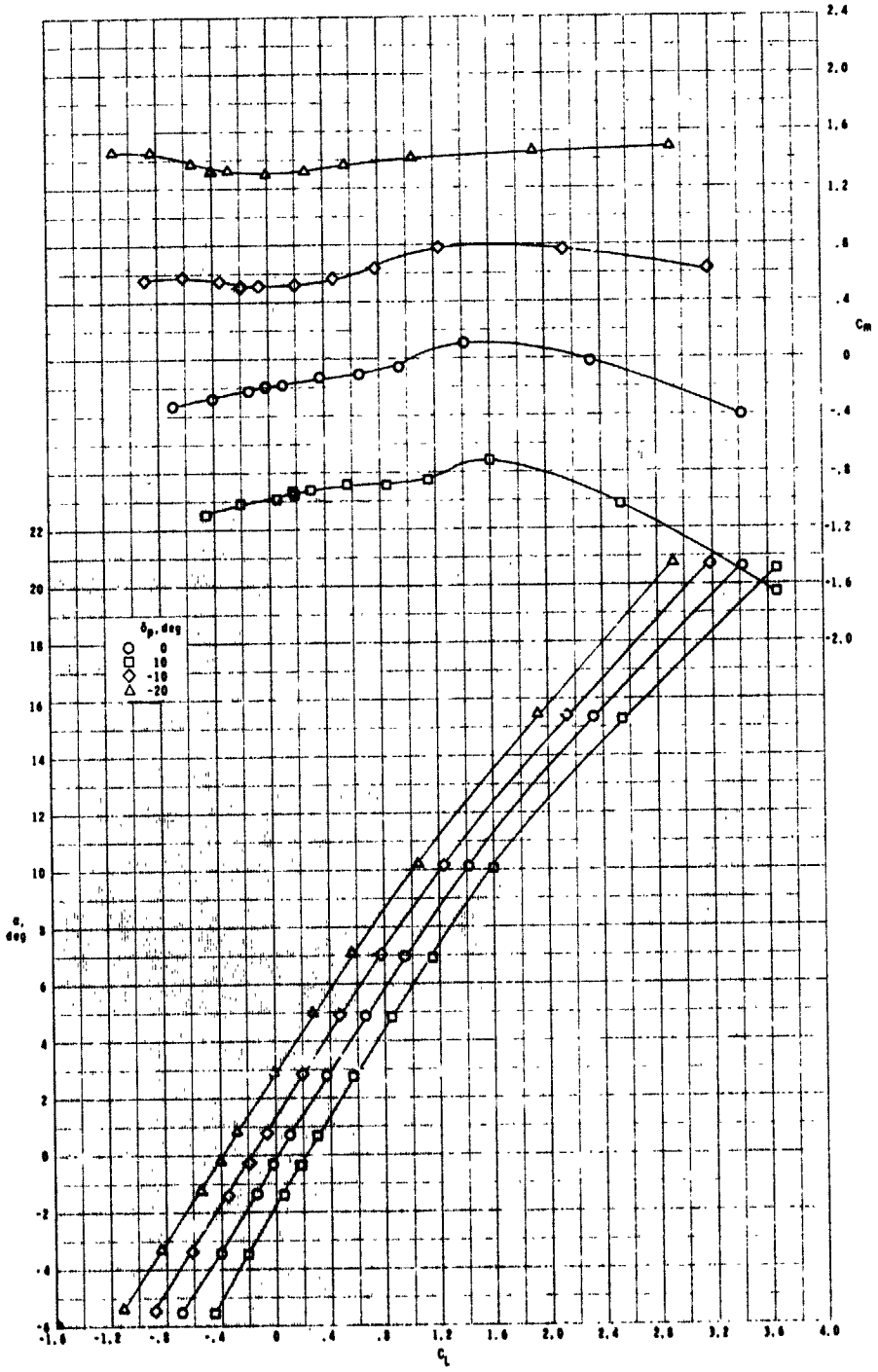

(b) Continued.

Figure 5.- Continued.

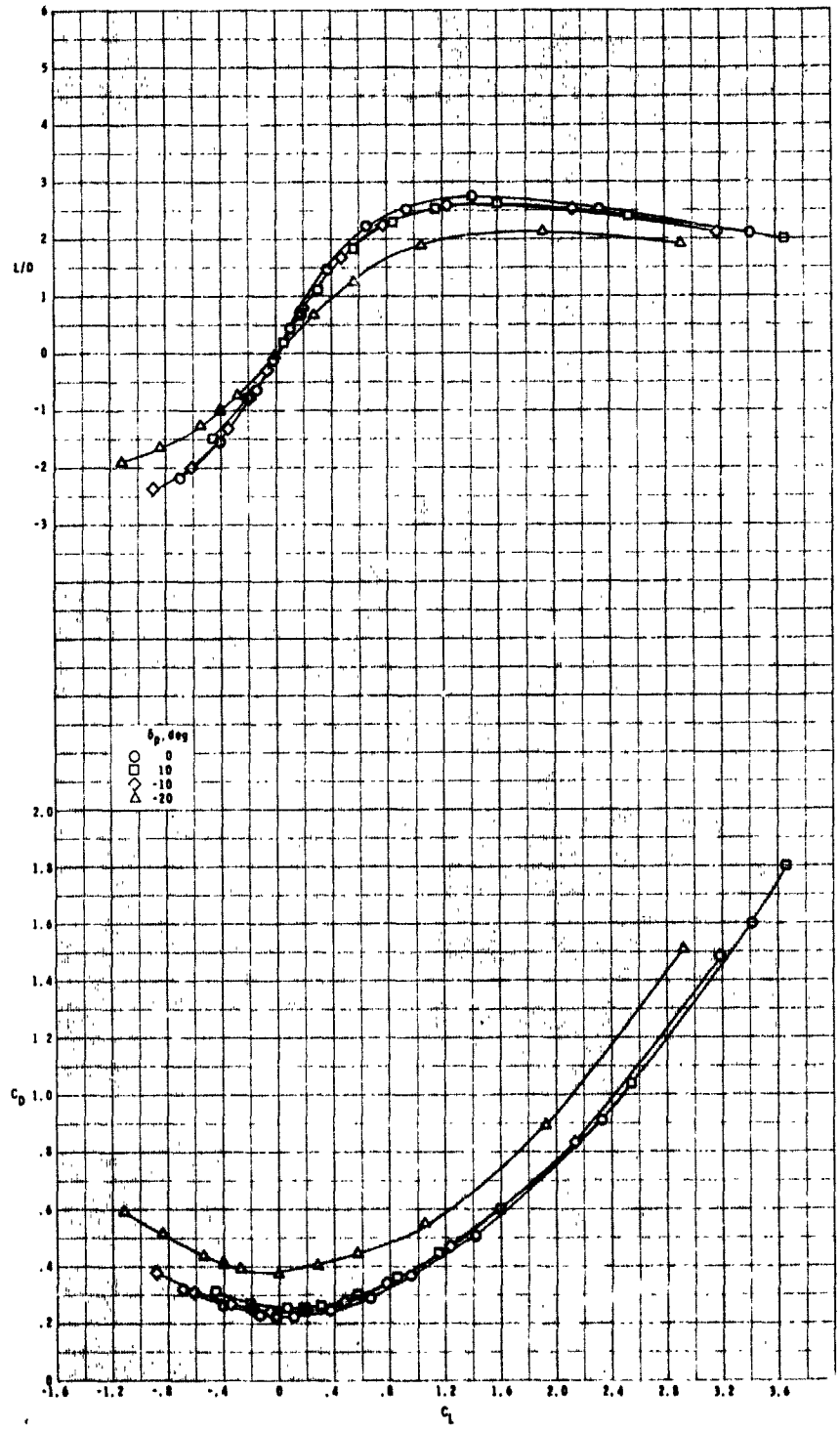

(b) Concluded.

Figure 5.- Continued.

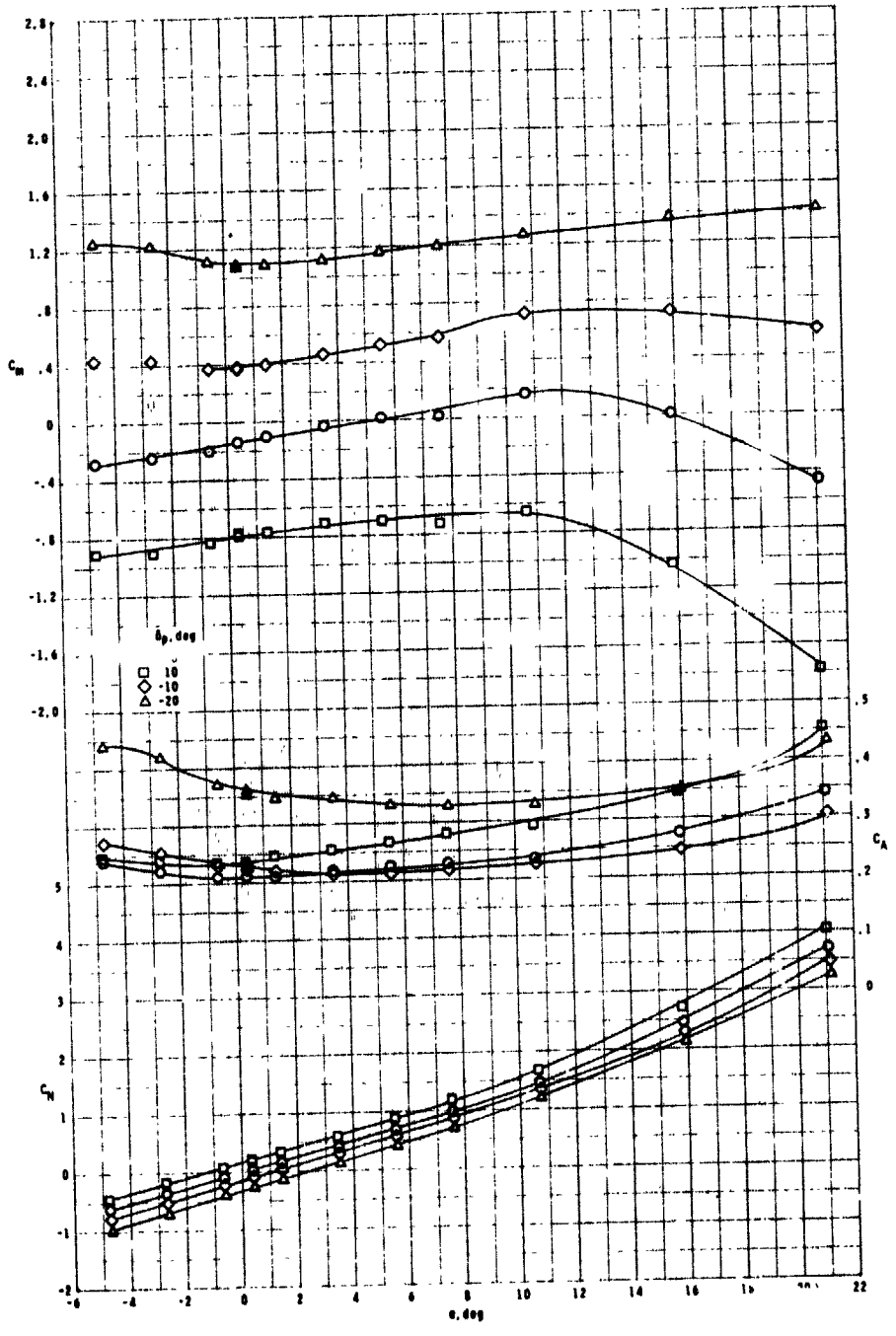

(c) M = 4.63.

Figure 5.- Continued.

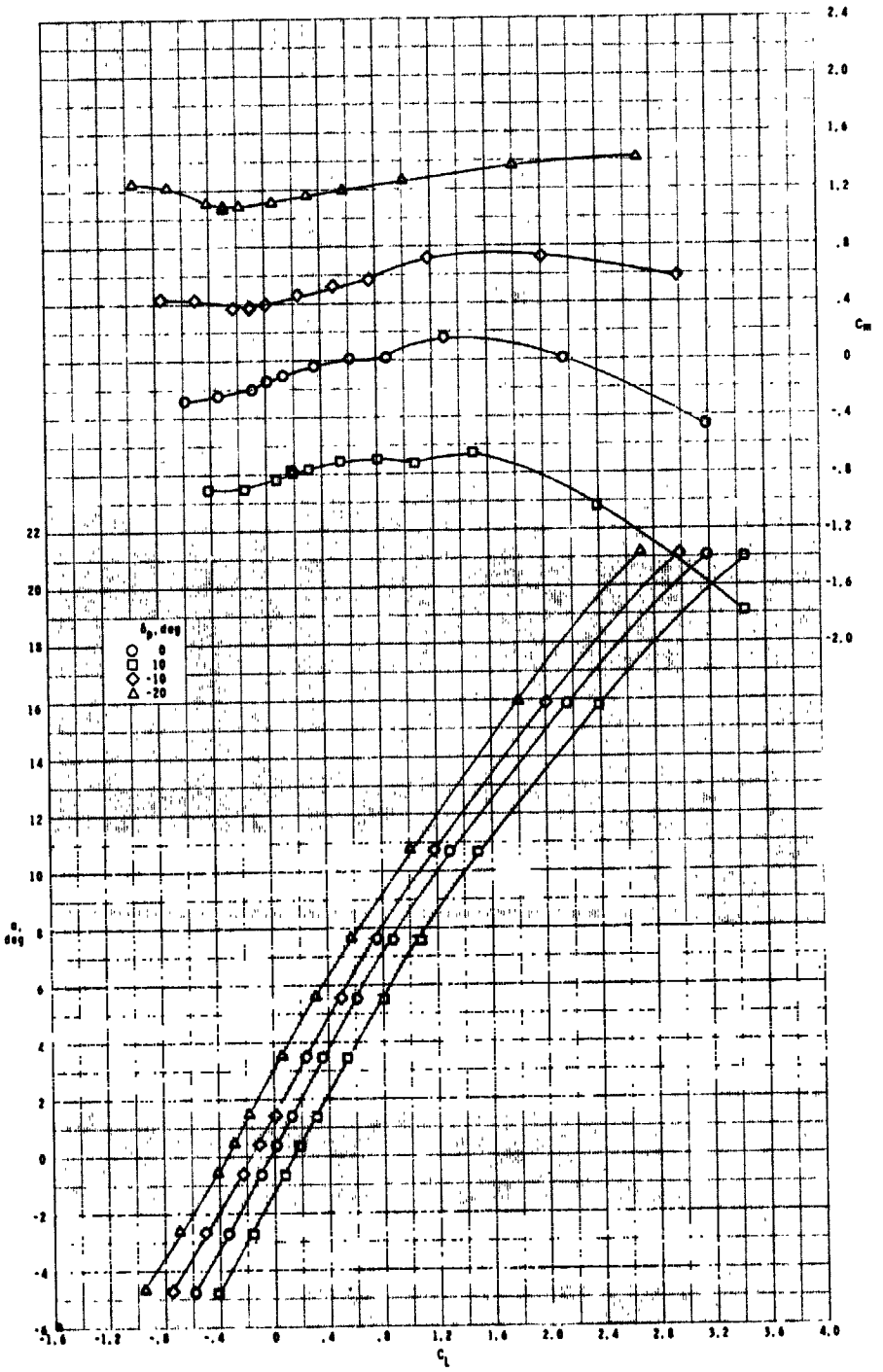

(c) Continued.

Figure 5.- Continued.

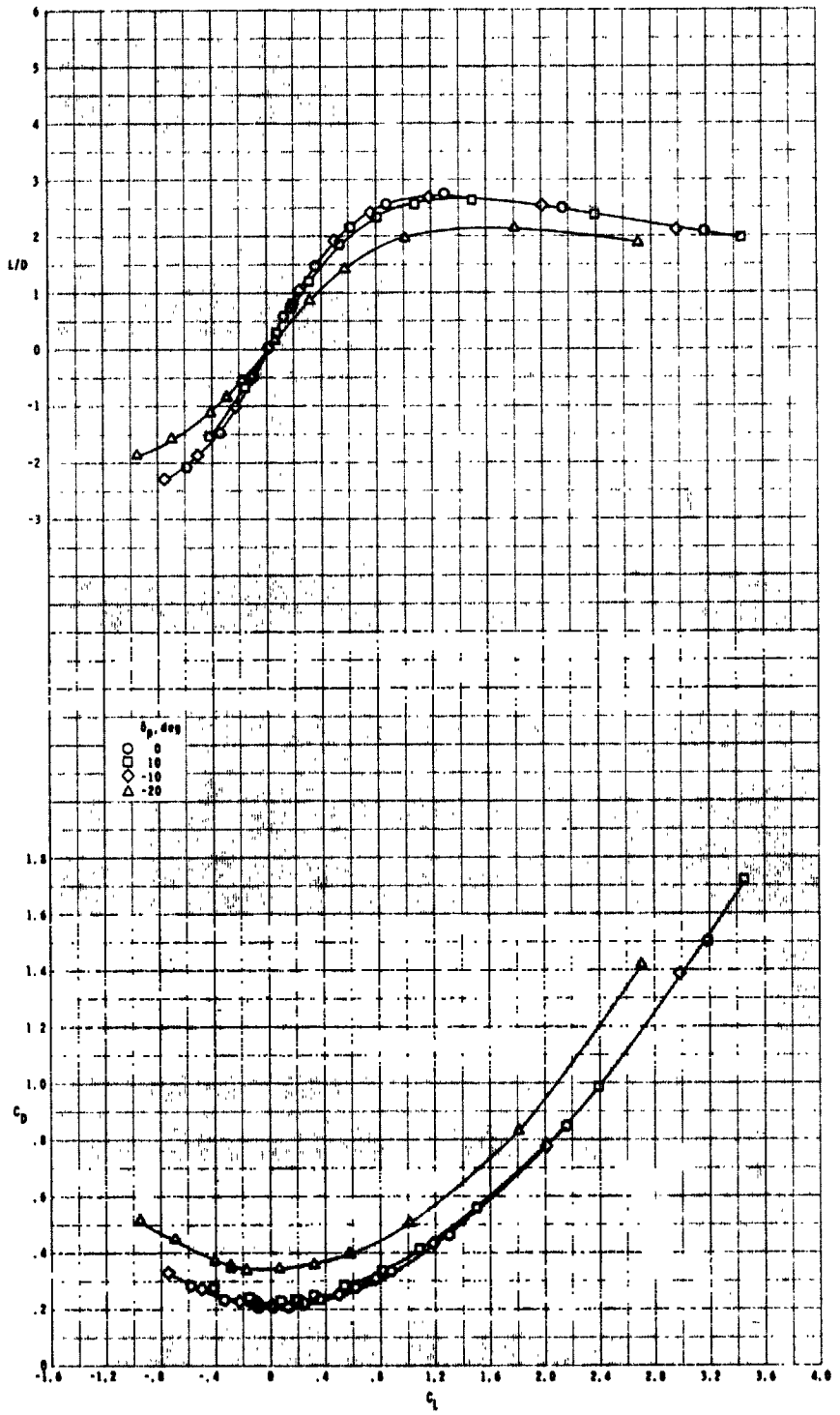

(c) Concluded.

Figure 5.- Concluded.

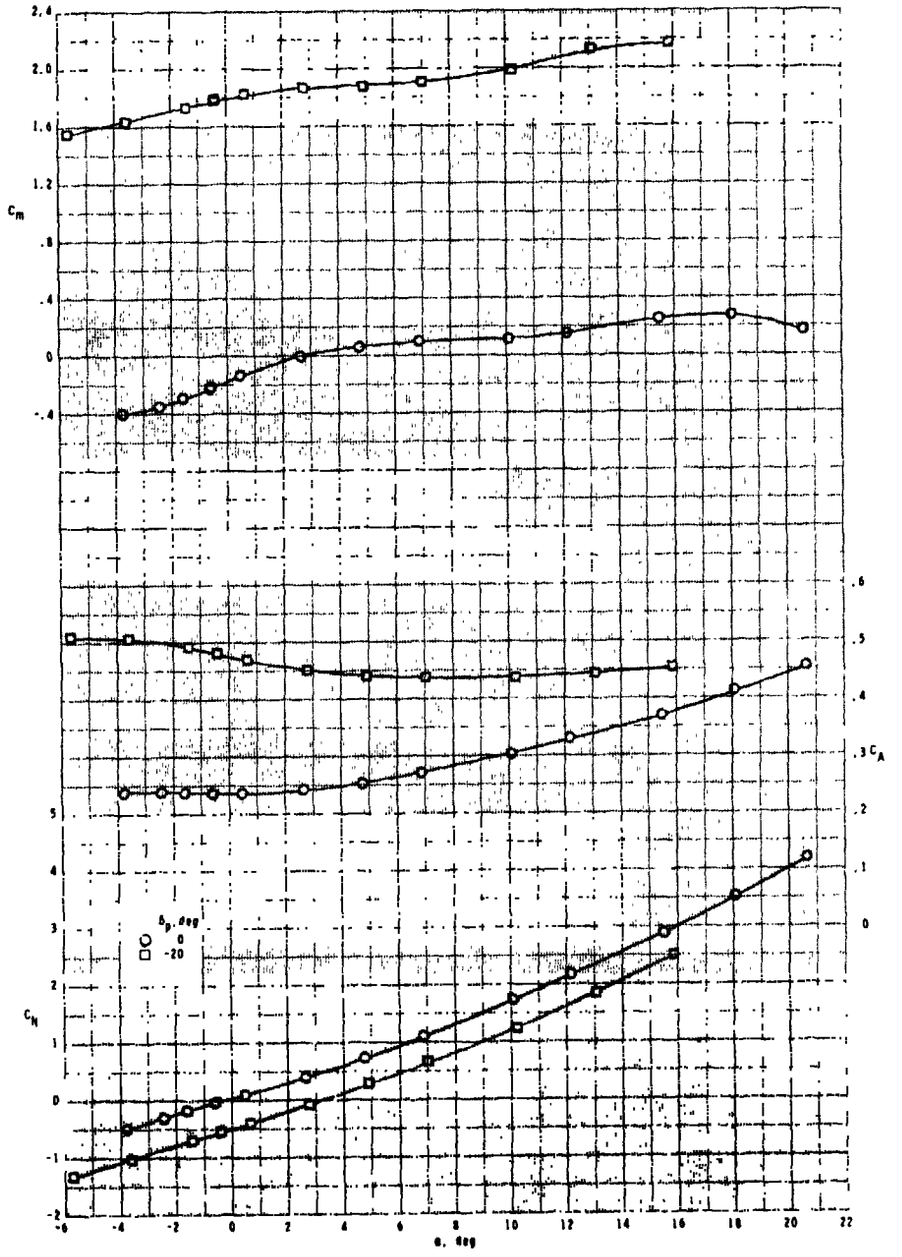

(a) M = 2.86.

Figure 6.- Longitudinal aerodynamic characteristics of body-tail, cruciform-wing configuration with pitch control.

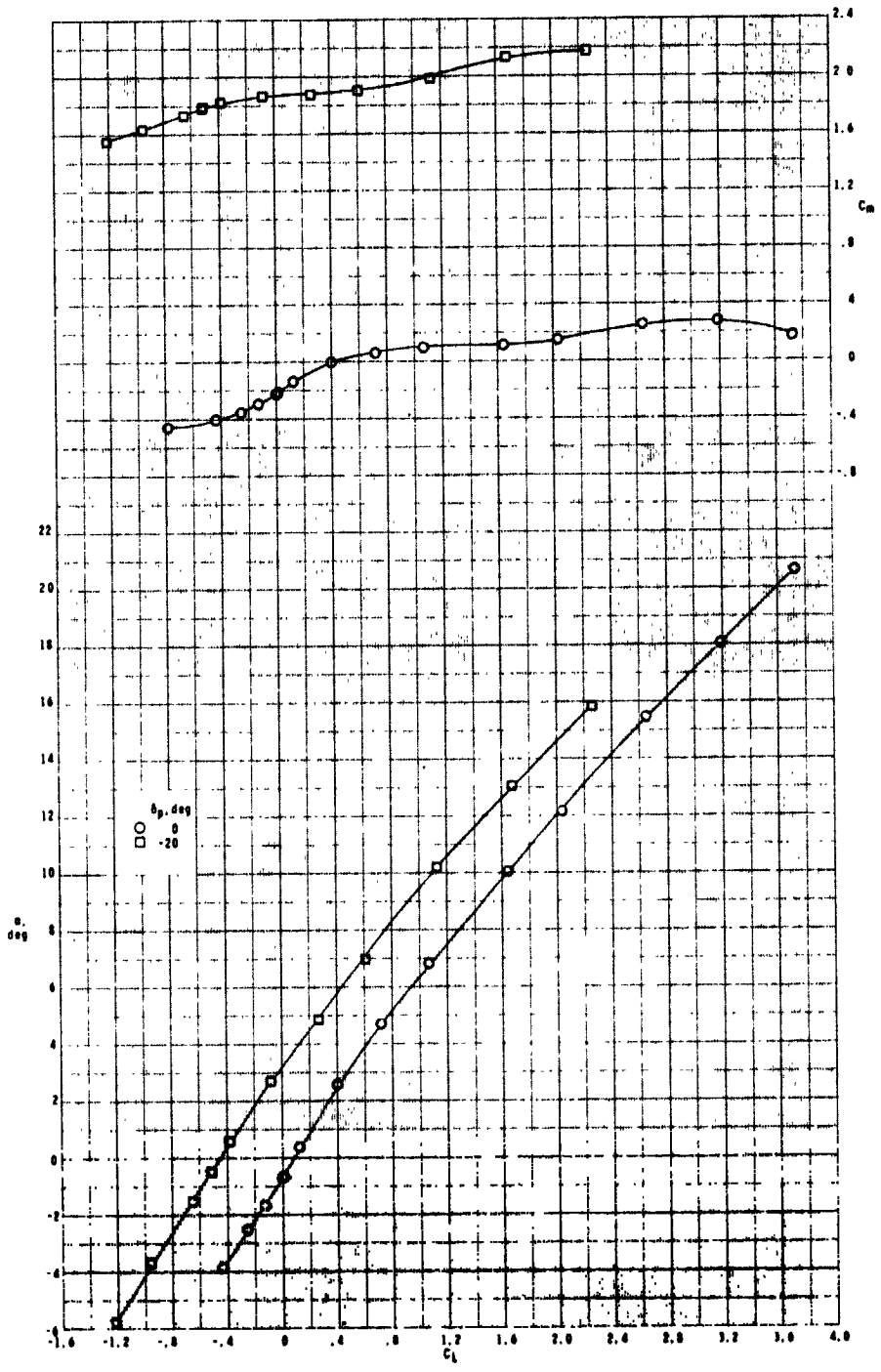

(a) Continued.

Figure 6.- Continued.

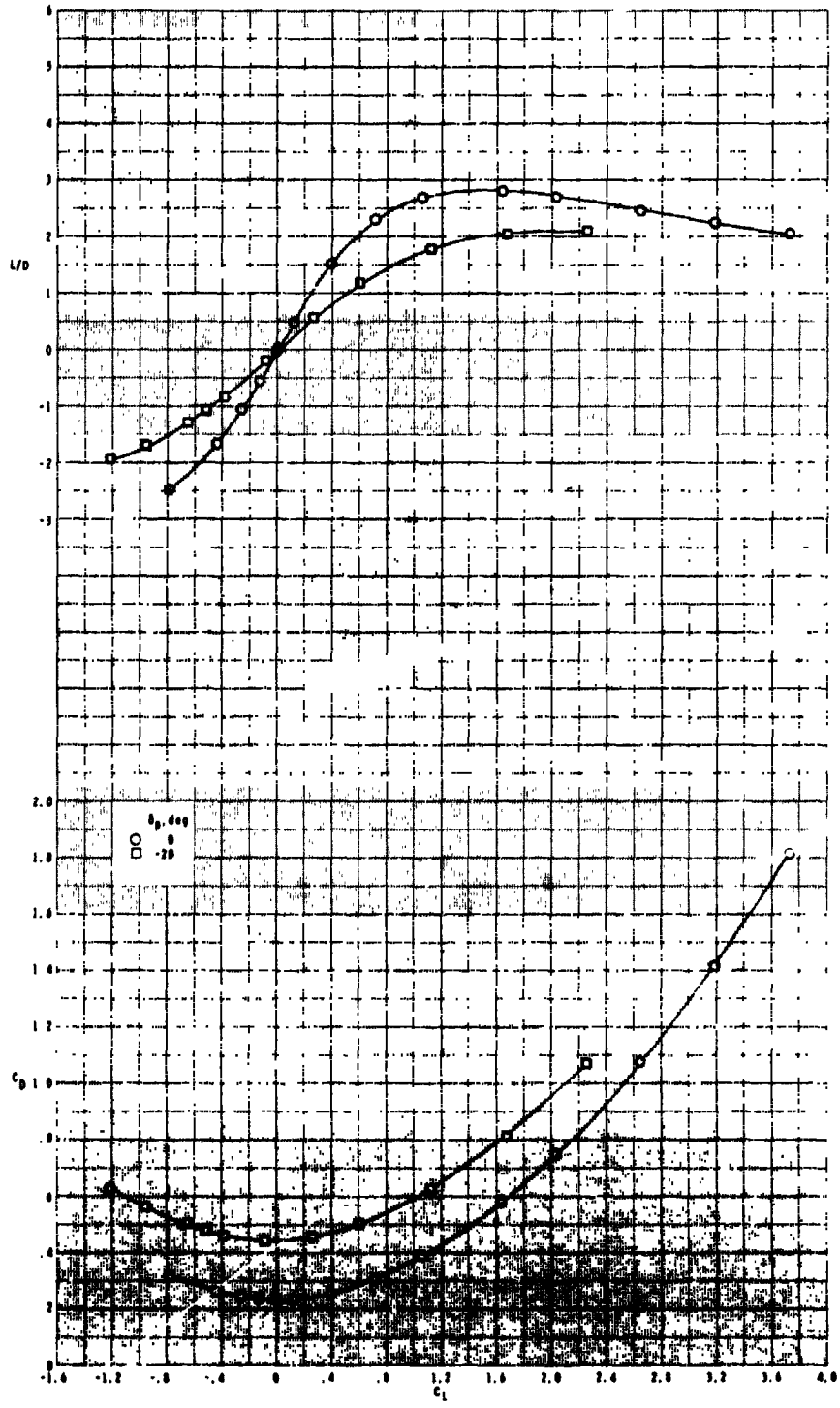

(a) Concluded.

Figure 6.- Continued.

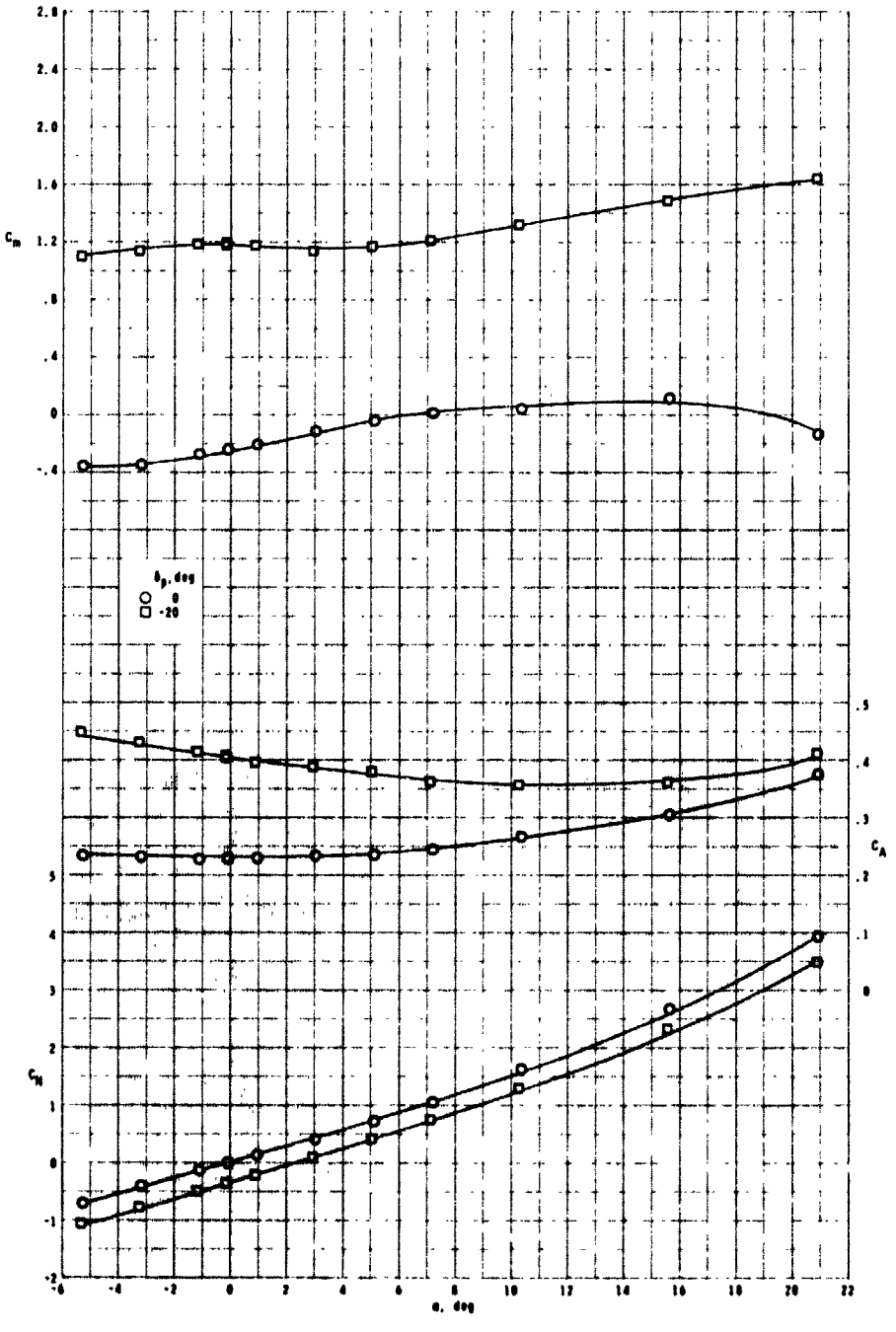

(b) M = 3.95.

Figure 6.- Continued.

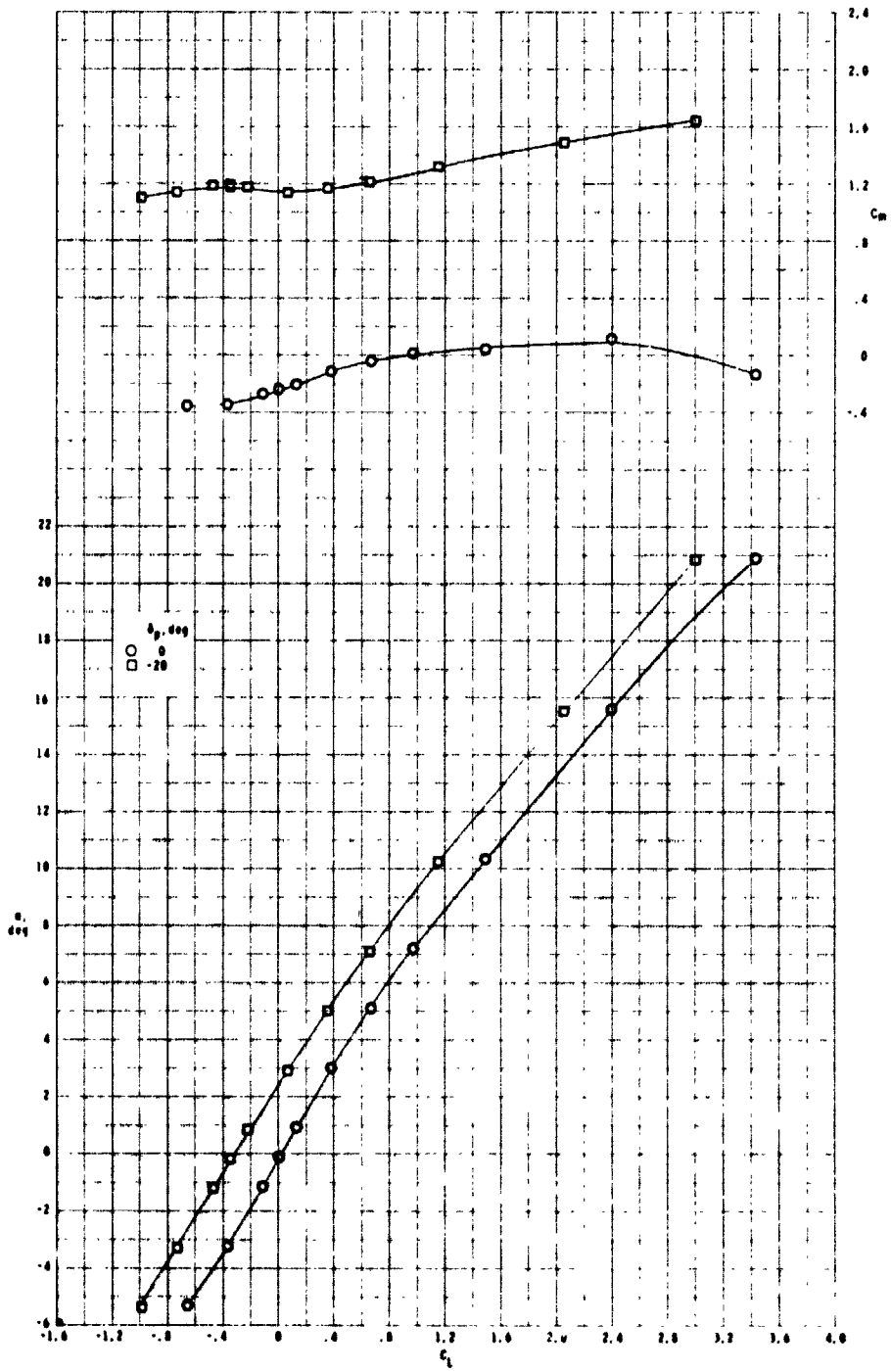

(b) Continued.

Figure 6.- Continued.

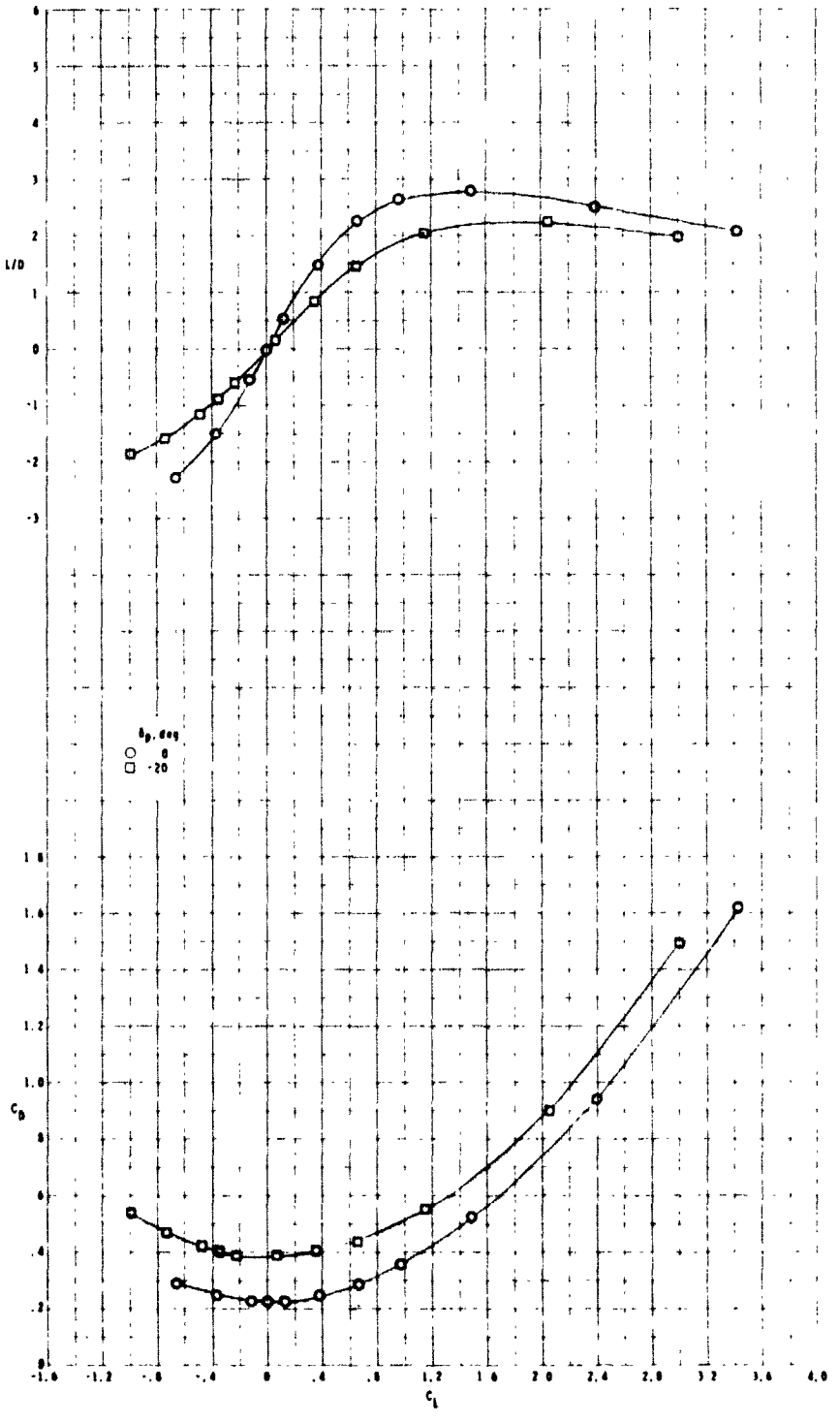

(b) Concluded.

Figure 6.- Continued.

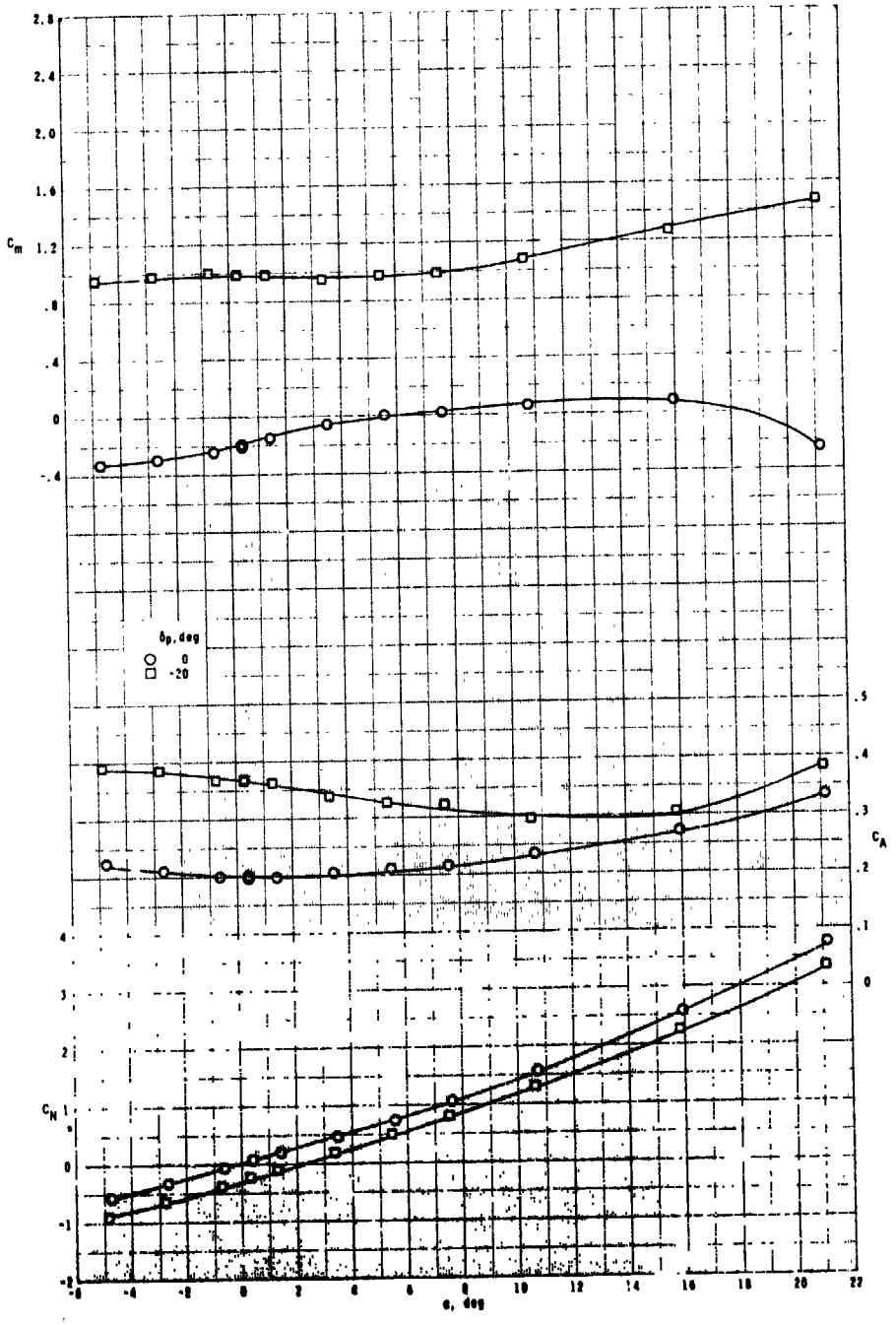

(c) M = 4.63.

Figure 6.- Continued.

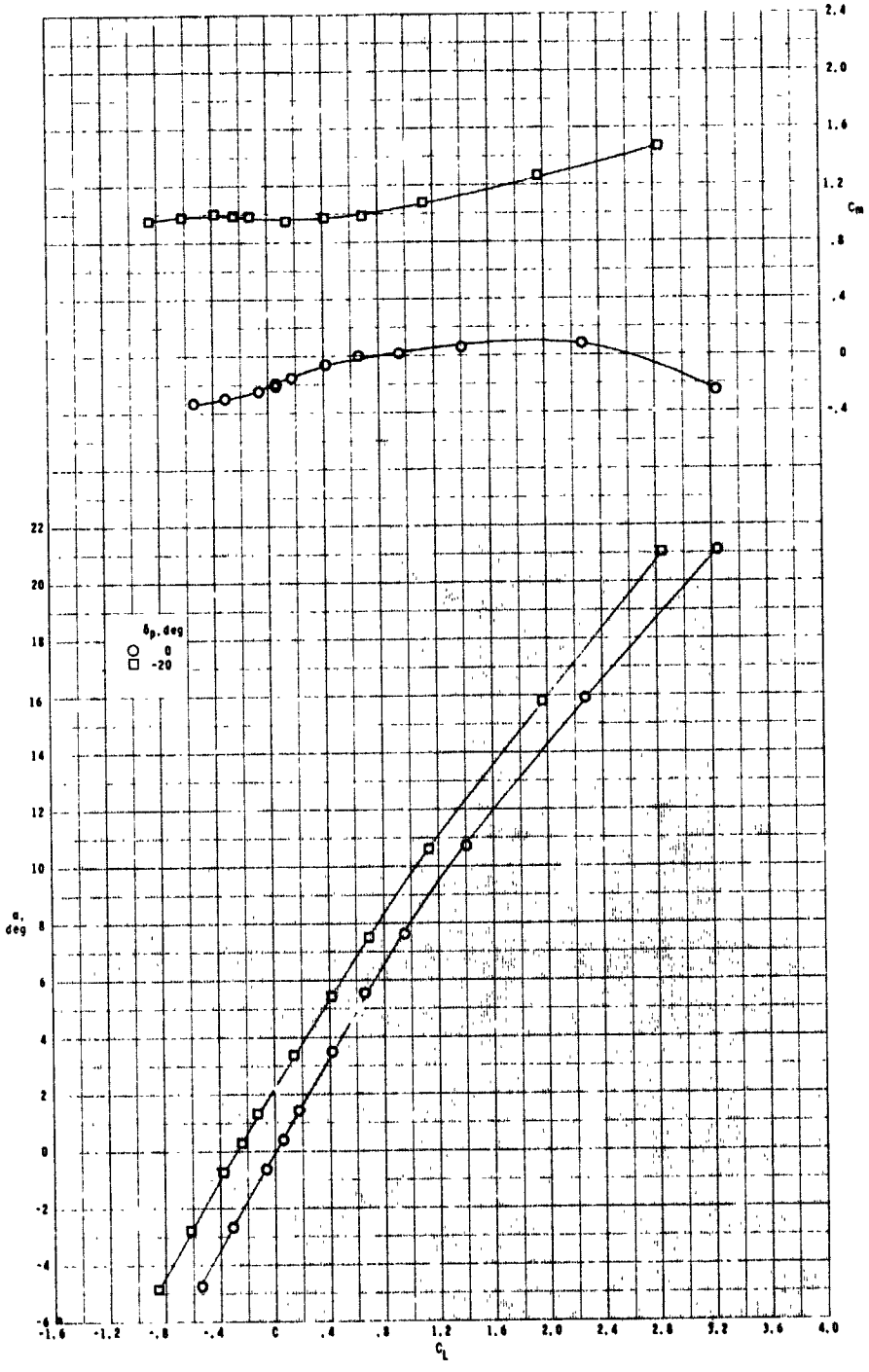

(c) Continued.

Figure 6.- Continued.

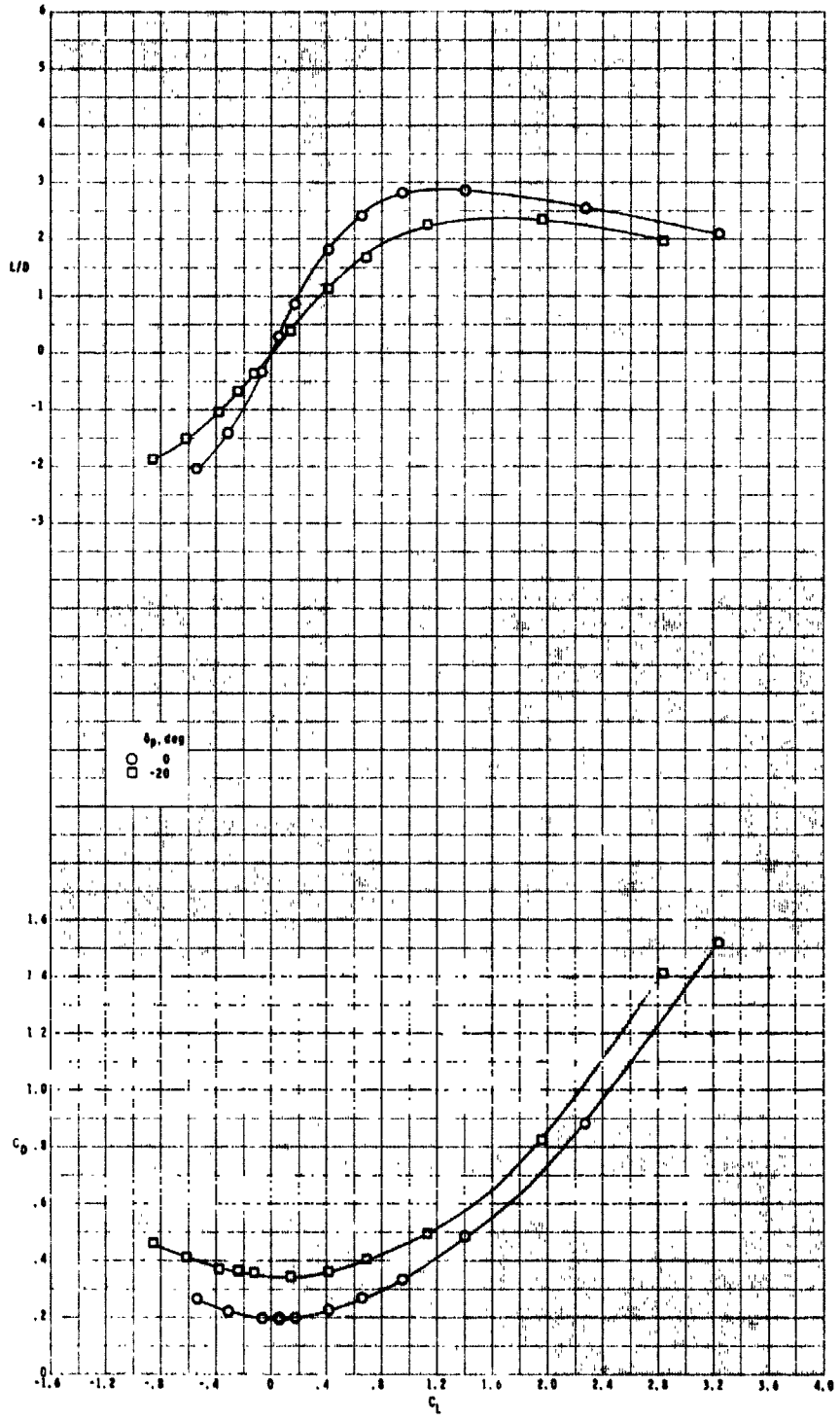

(c) Concluded.

Figure 6.- Concluded.

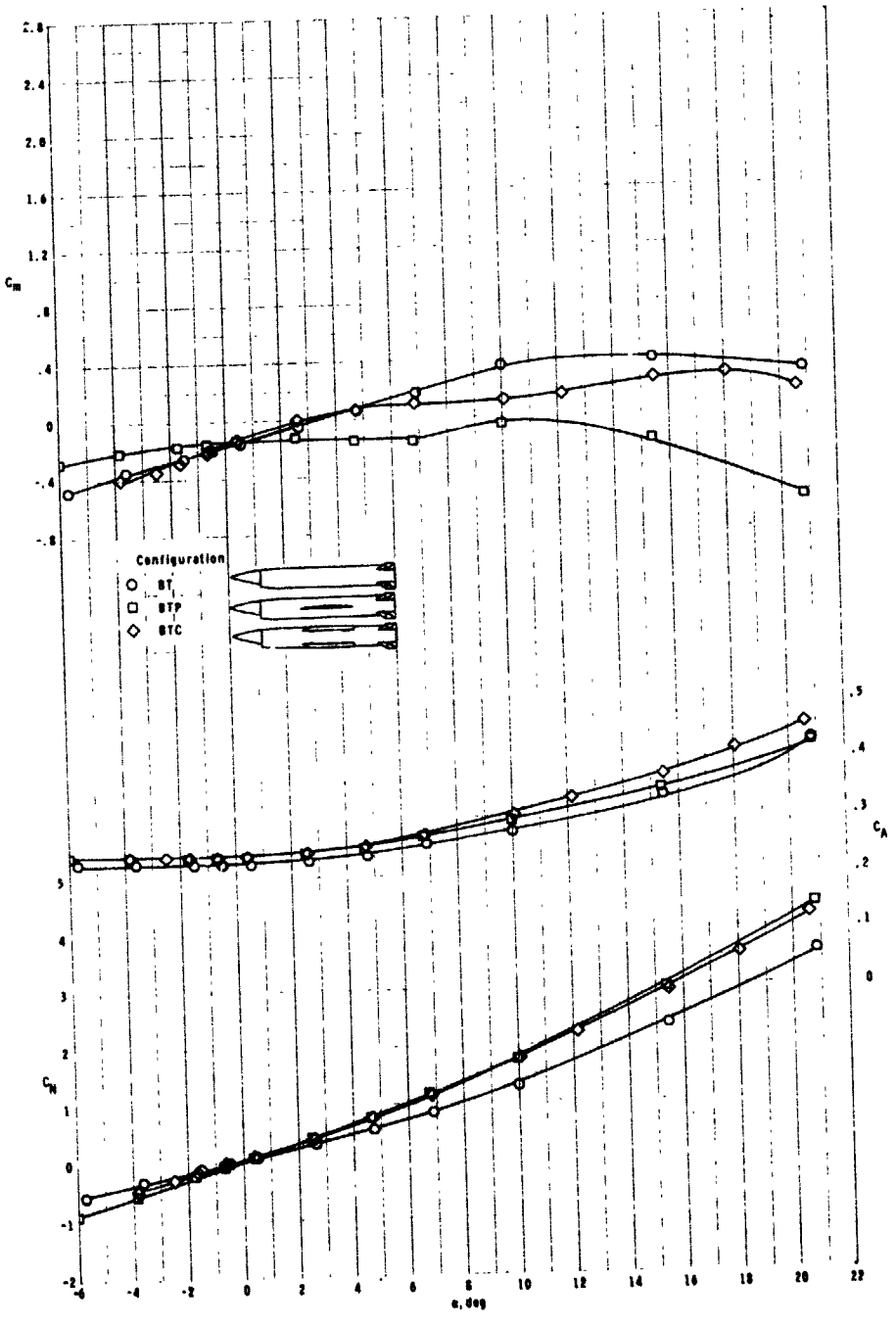

(a) Body axes.

Figure 7.- Comparison of longitudinal aerodynamic characteristics of three configurations at M = 2.86.

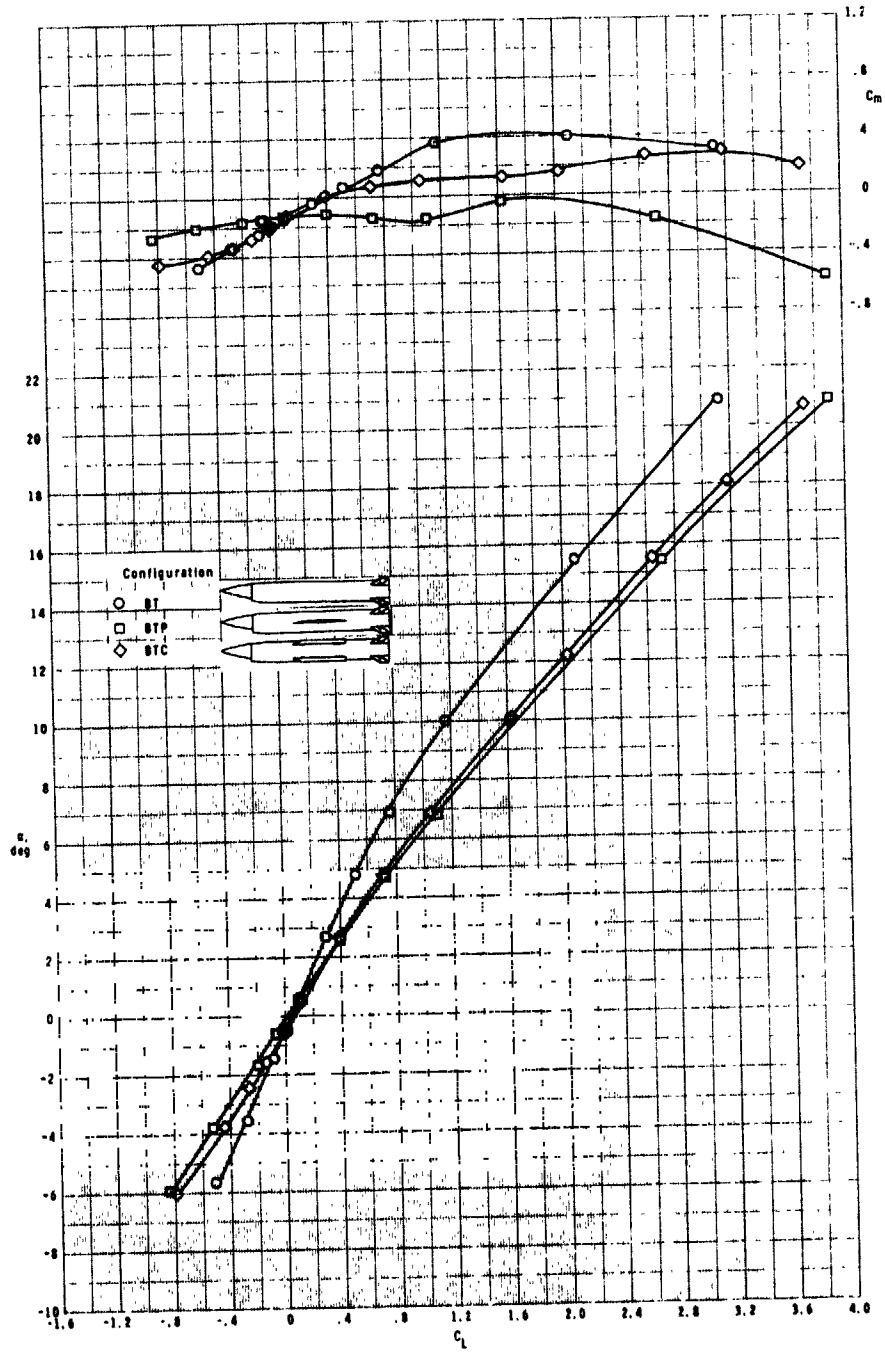

(b) Stability axes.

Figure 7.- Continued.

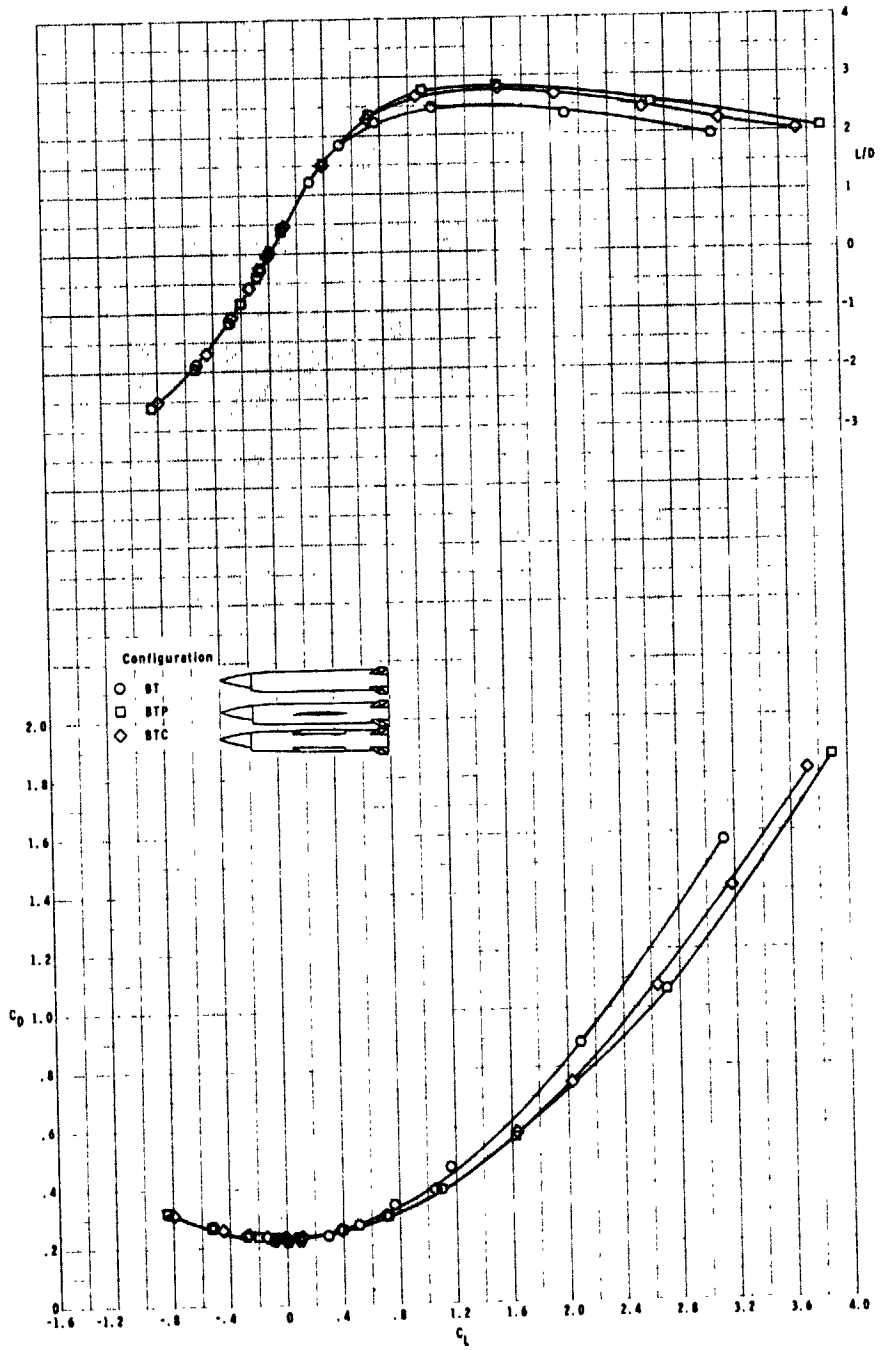

(b) Concluded.

Figure 7.- Concluded.

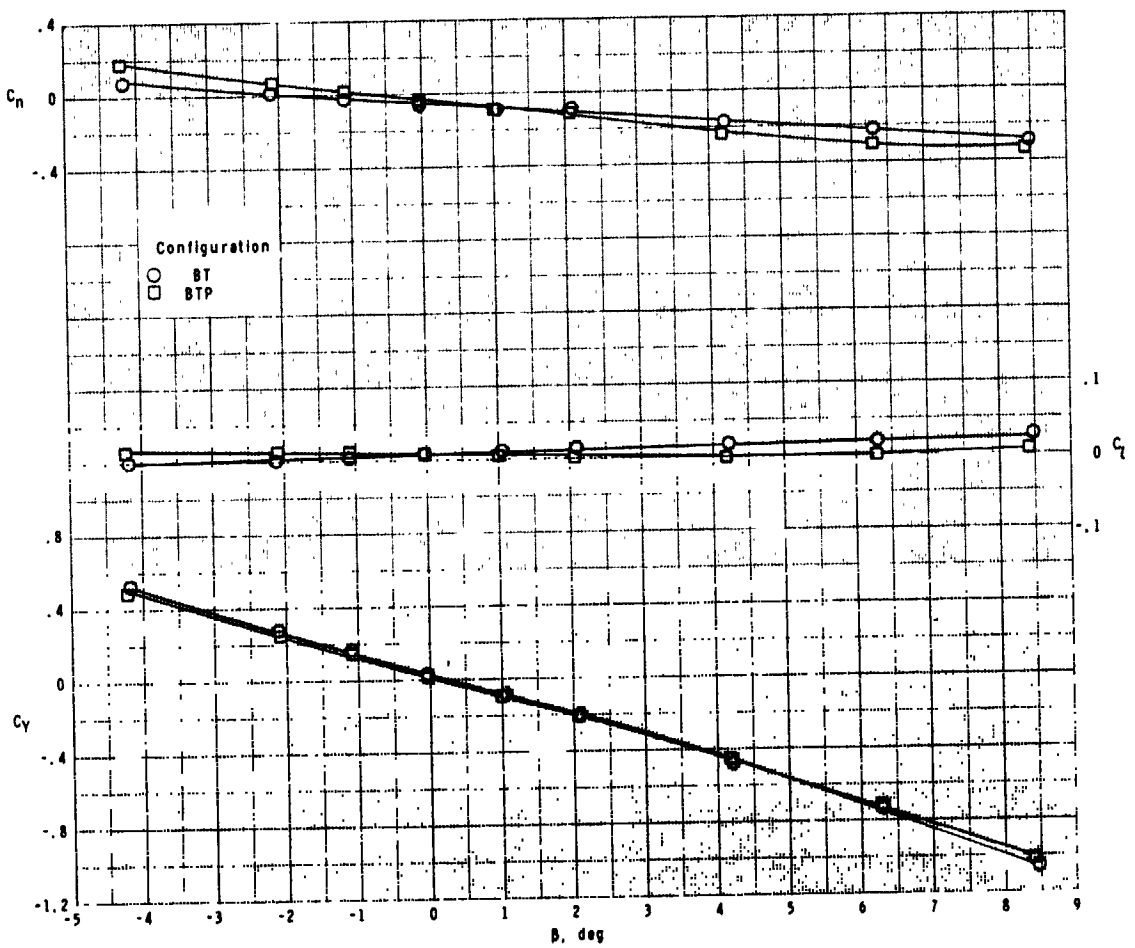

Figure 8.- Effect of sideslip on lateral-directional aerodynamic characteristics of body-tail configuration, with and without a planar wing. M = 2.86; α = 5°.

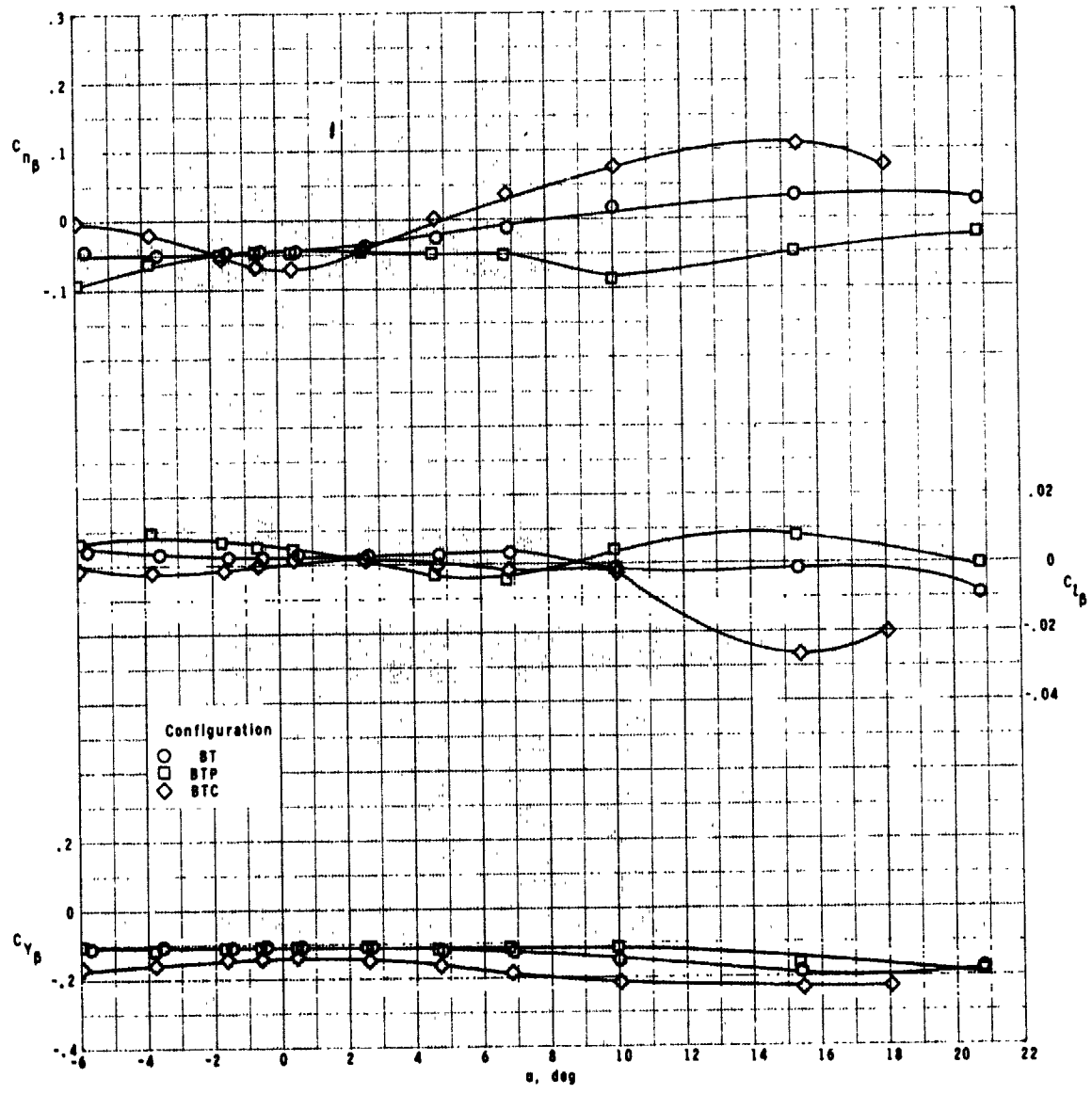

(a) M = 2.86.

Figure 9.- Effect of wing configuration on lateral-directional stability.

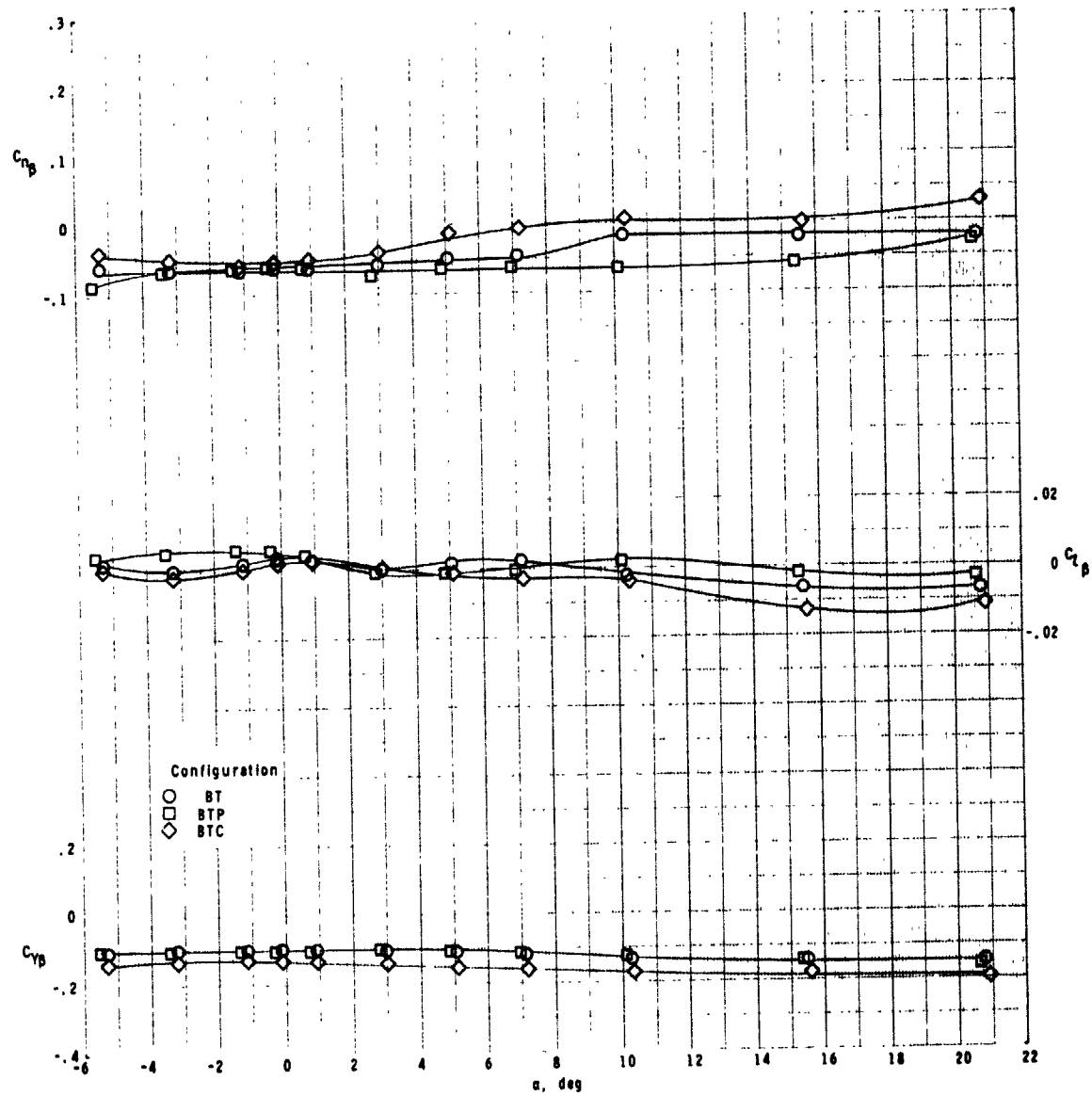

(b) M = 3.95.

Figure 9.- Continued.

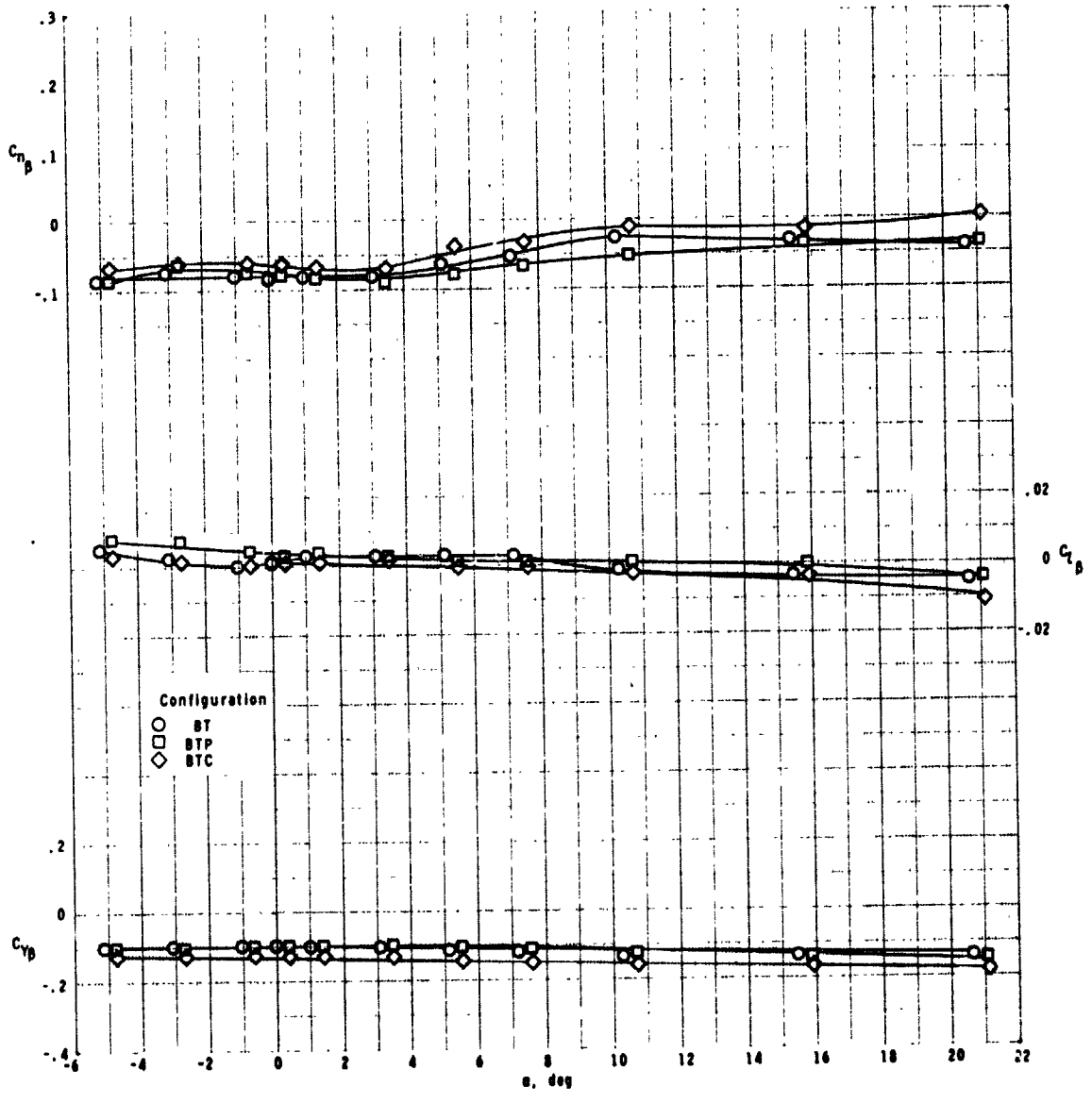

(c) M = 4.63.

Figure 9.- Concluded.

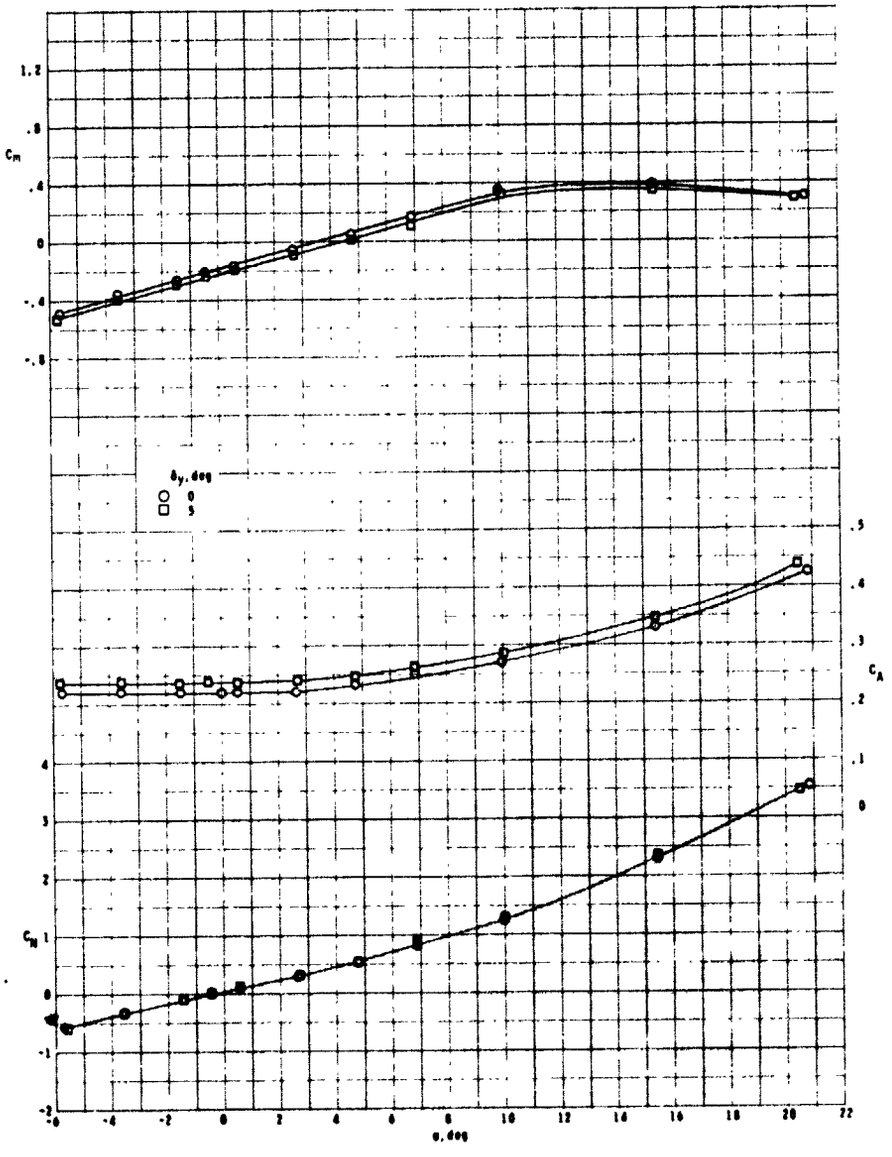

(a) Longitudinal aerodynamic characteristics.

Figure 10.- Effect of yaw control on longitudinal and lateral-directional aerodynamic characteristics of body-tail configuration. M = 2.86.

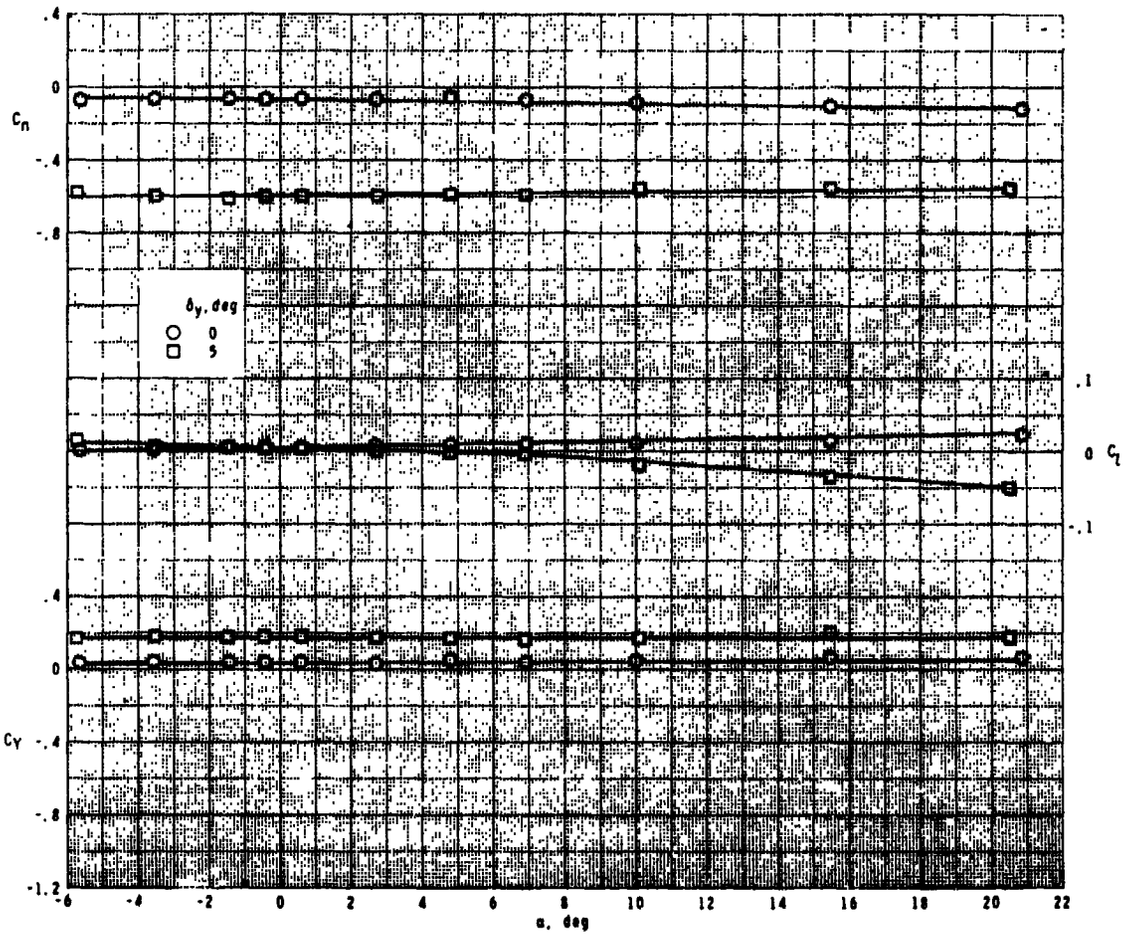

(b) Lateral-directional aerodynamic characteristics.

Figure 10.- Concluded.

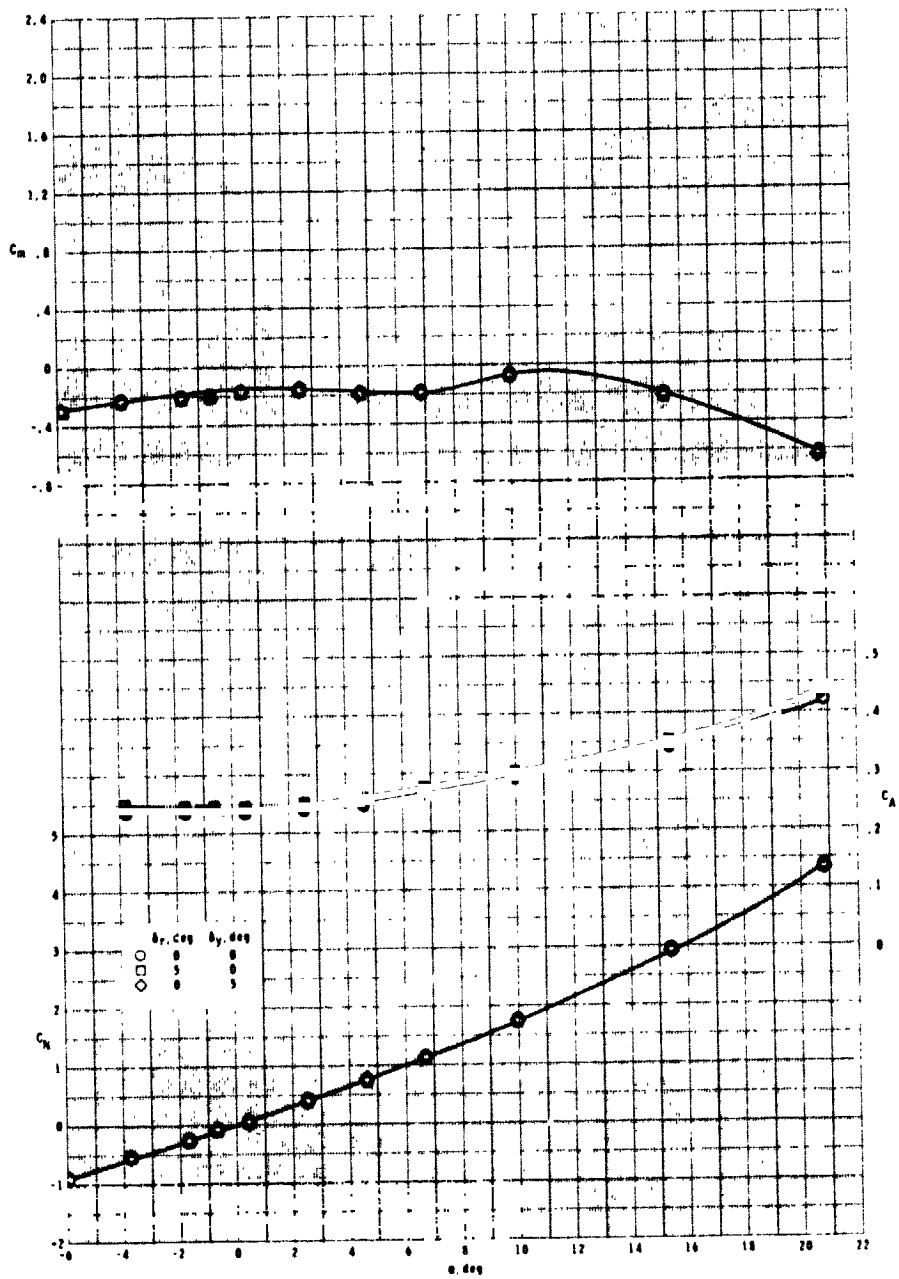

(a) M = 2.86.

Figure 11.- Effect of roll and yaw control on longitudinal and lateral-directional aerodynamic characteristics of body-tail, planar-wing configuration.

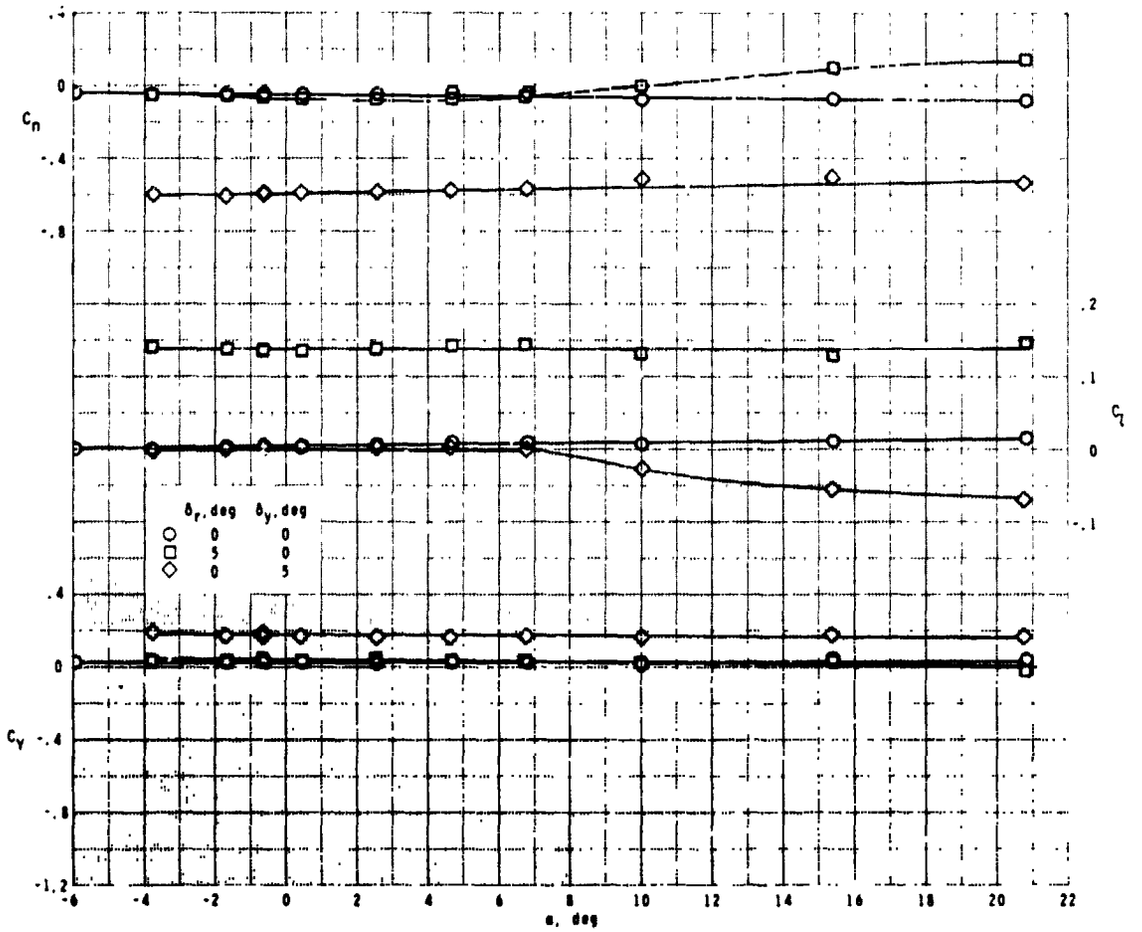

(a) Concluded.

Figure 11.- Continued.

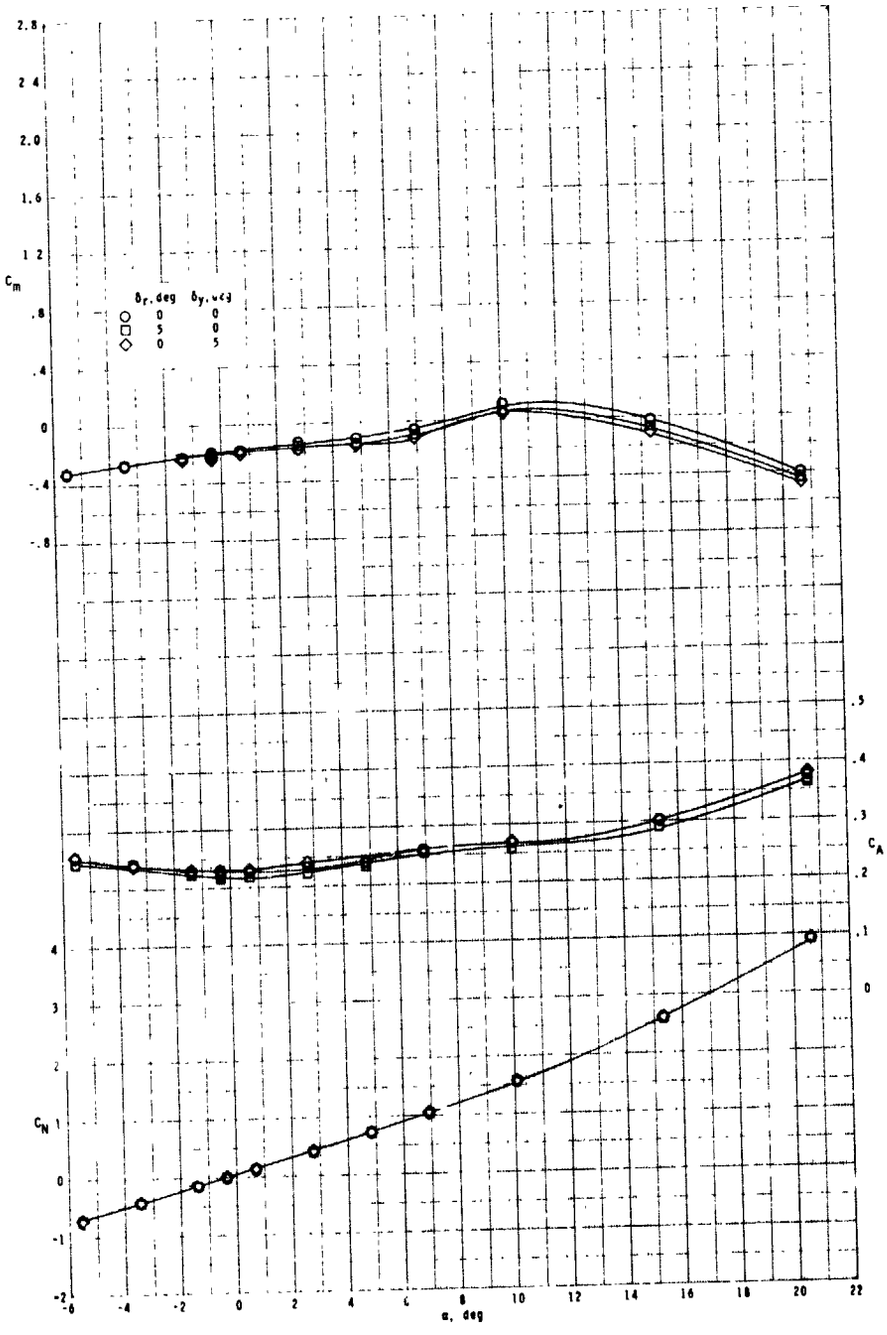

(b) M = 3.95.

Figure 11.- Continued.

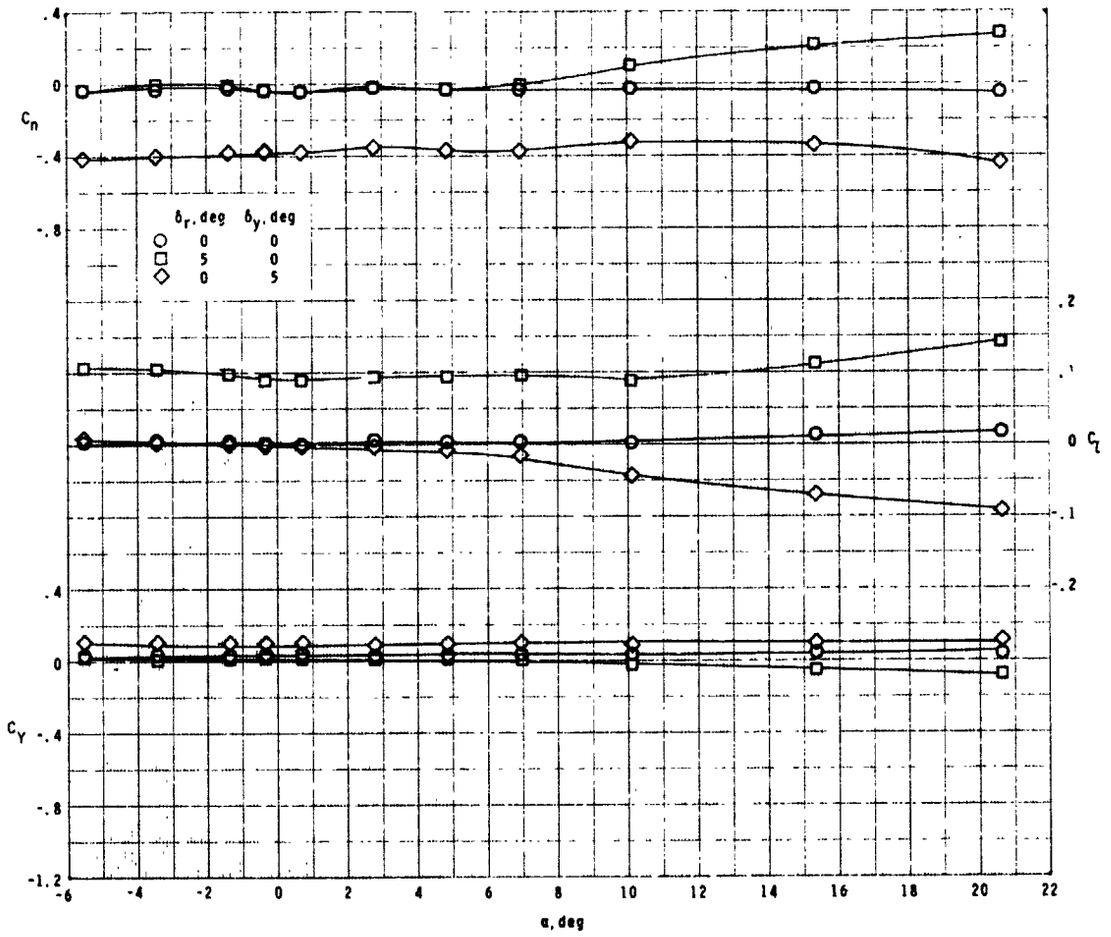

(b) Concluded.

Figure 11.- Continued.

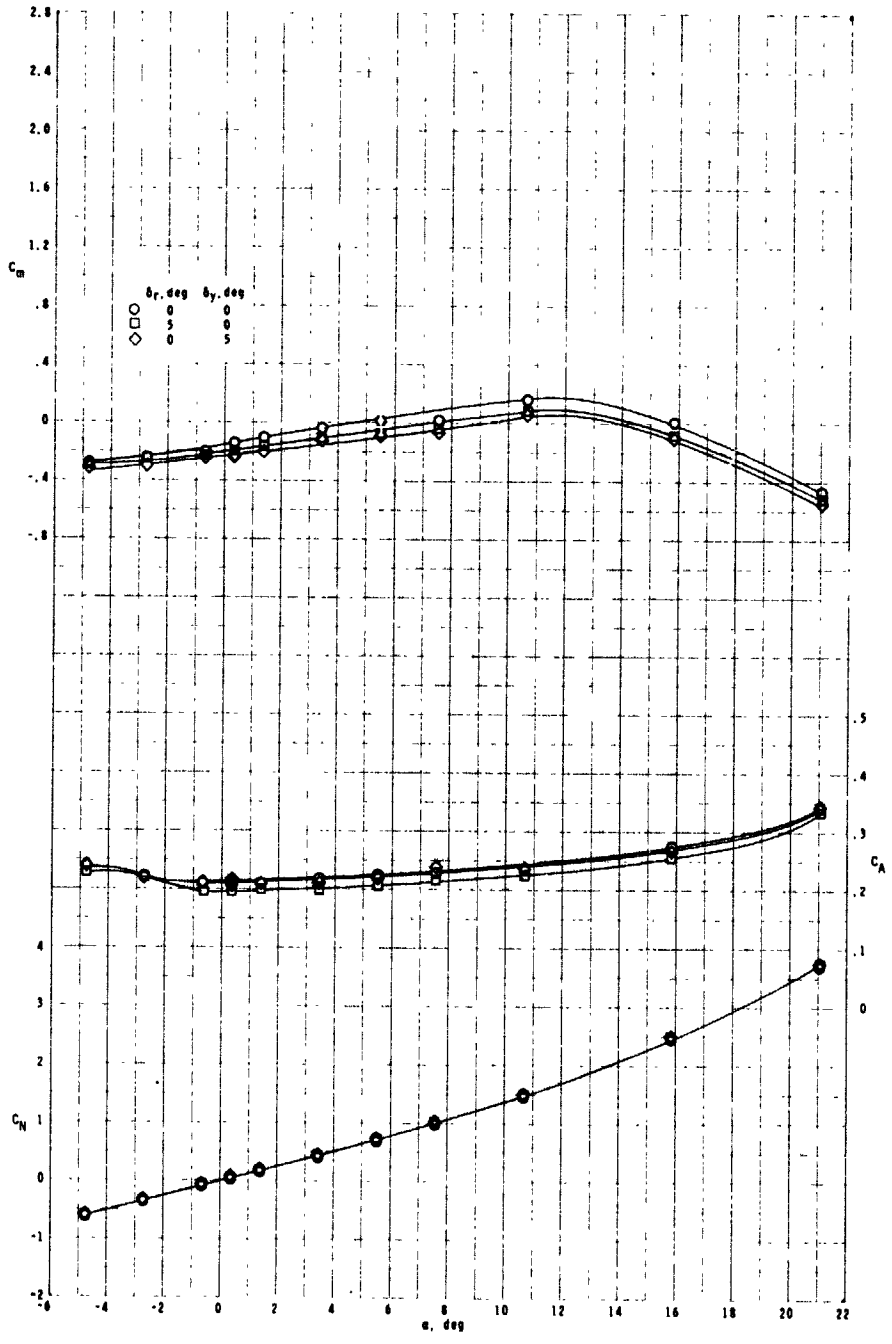

(c) M = 4.63.

Figure 11.- Continued.

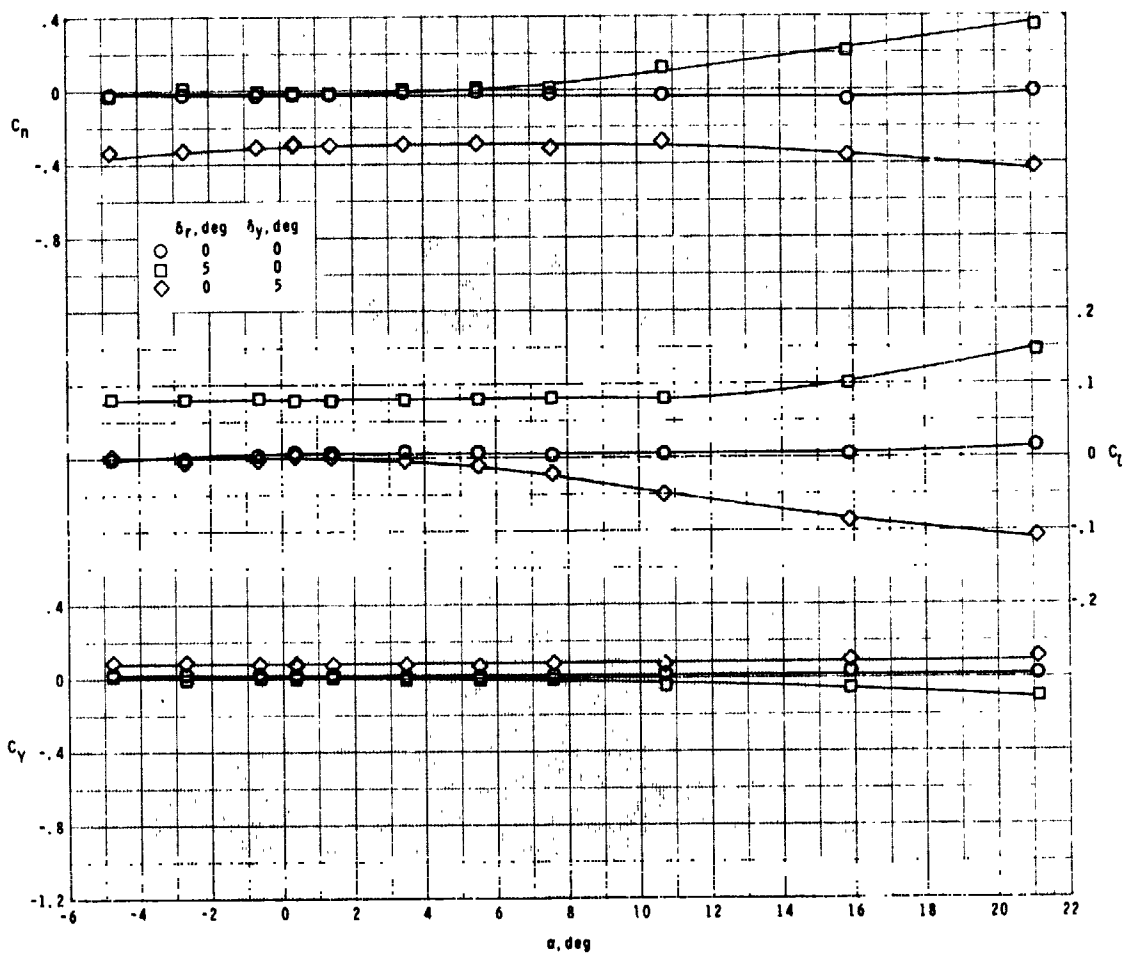

(c) Concluded.

Figure 11.- Concluded.

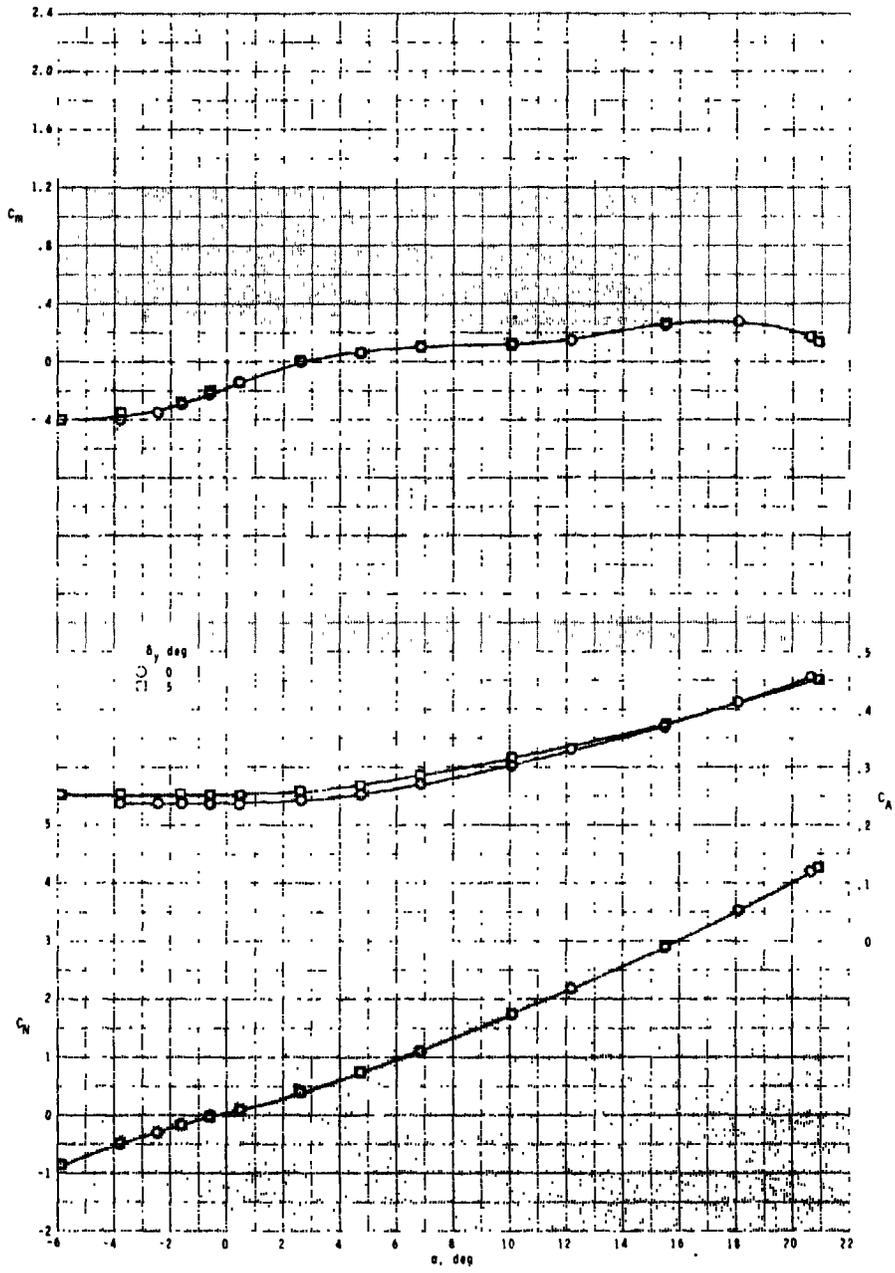

(a) Longitudinal aerodynamic characteristics.

Figure 12.- Effect of yaw control on longitudinal and lateral-directional aerodynamic characteristics of body-tail, cruciform-wing configuration. M = 2.86.

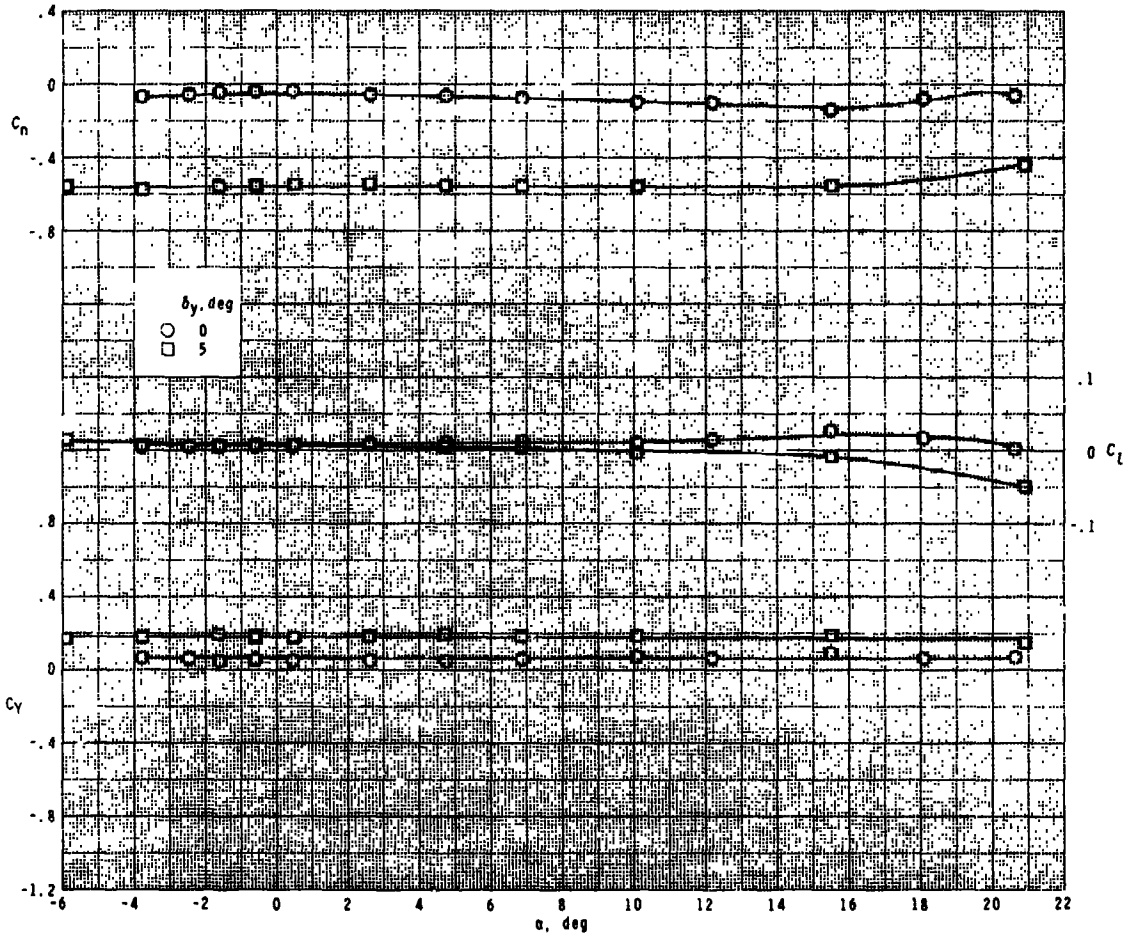

(b) Lateral-directional aerodynamic characteristics.

Figure 12.- Concluded.

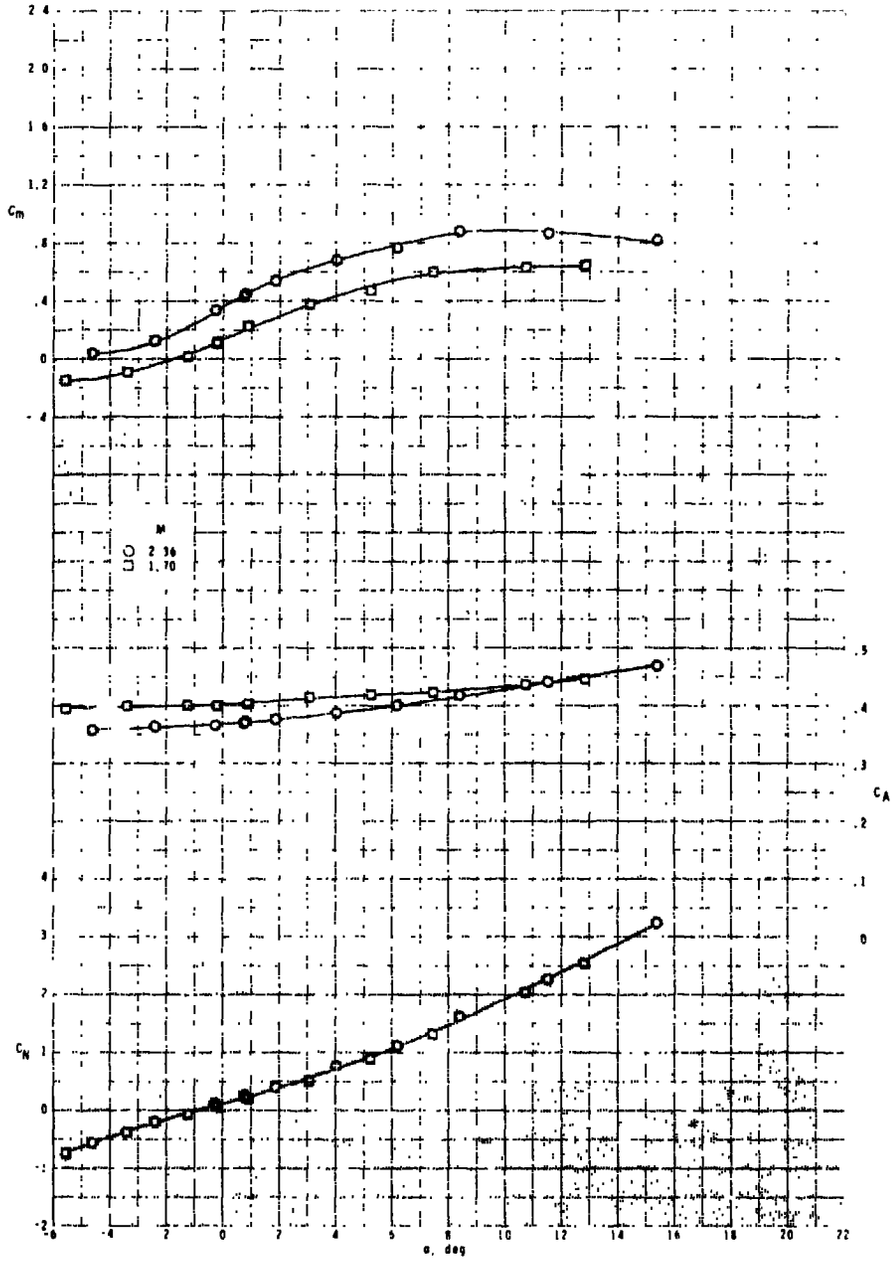

(a) Body axes.

Figure 13.- Longitudinal aerodynamic characteristics of body-tail, cruciform-wing, inlet-closed configuration.

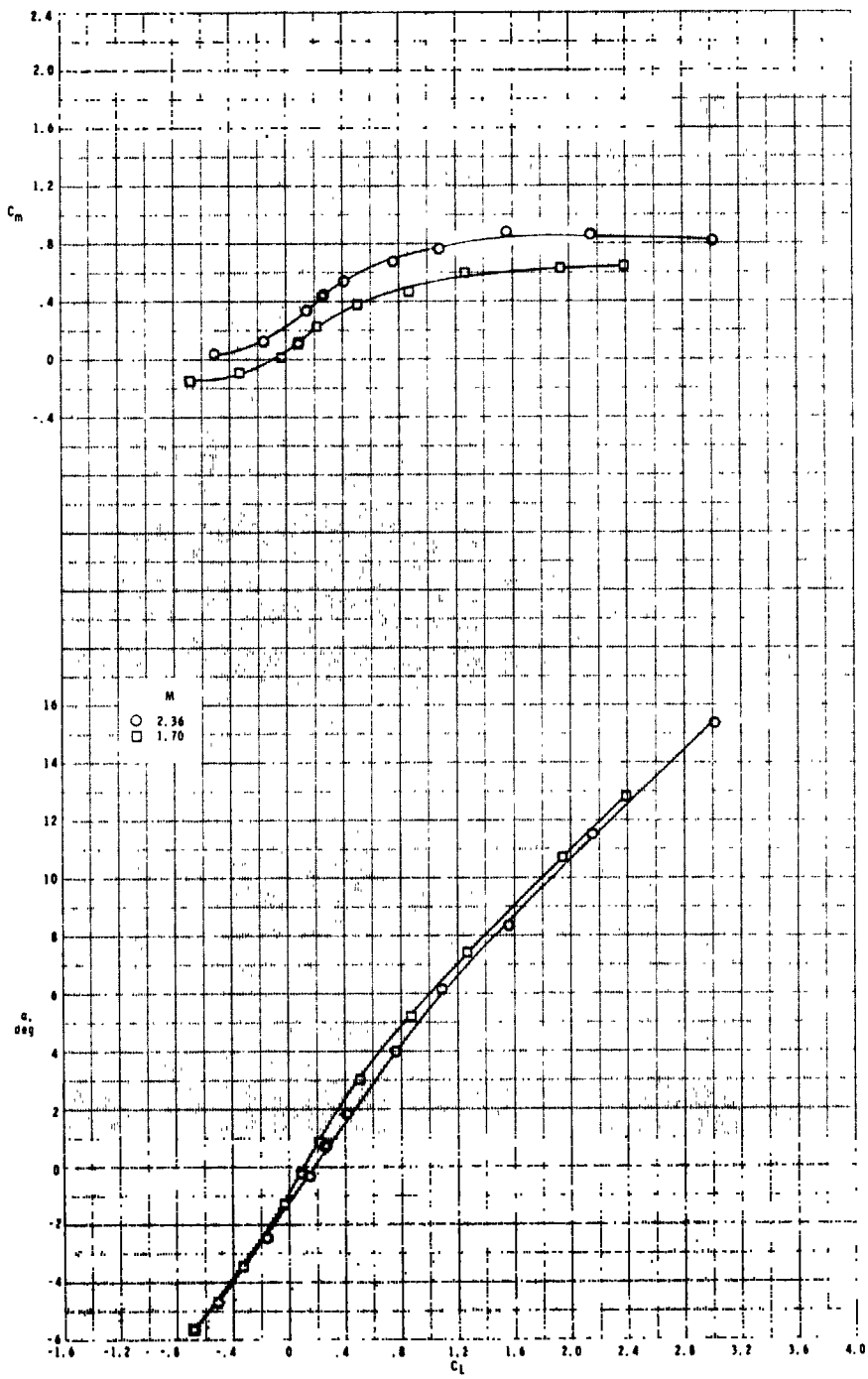

(b) Stability axes.

Figure 13.- Continued.

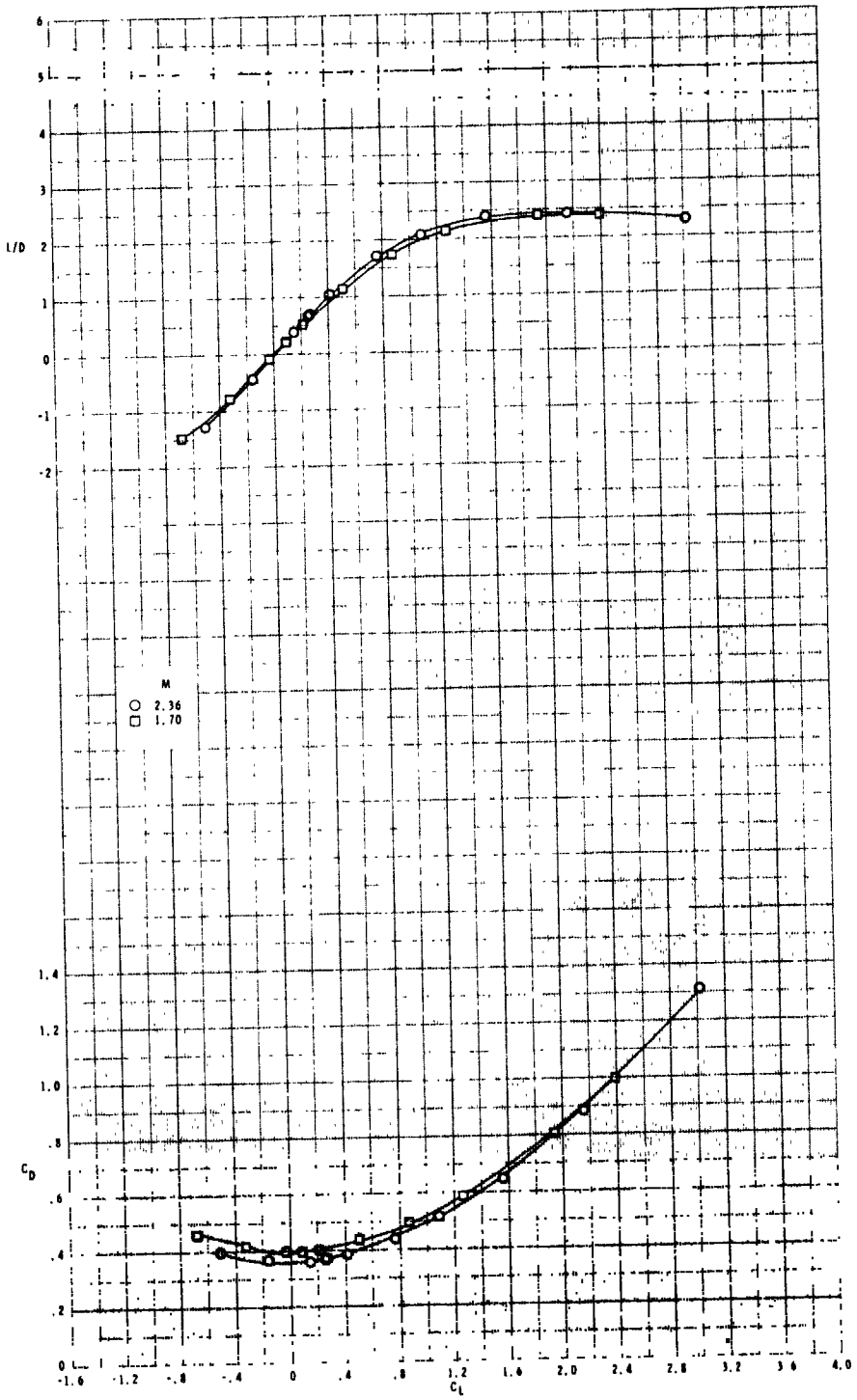

(b) Concluded.

Figure 13.- Concluded.

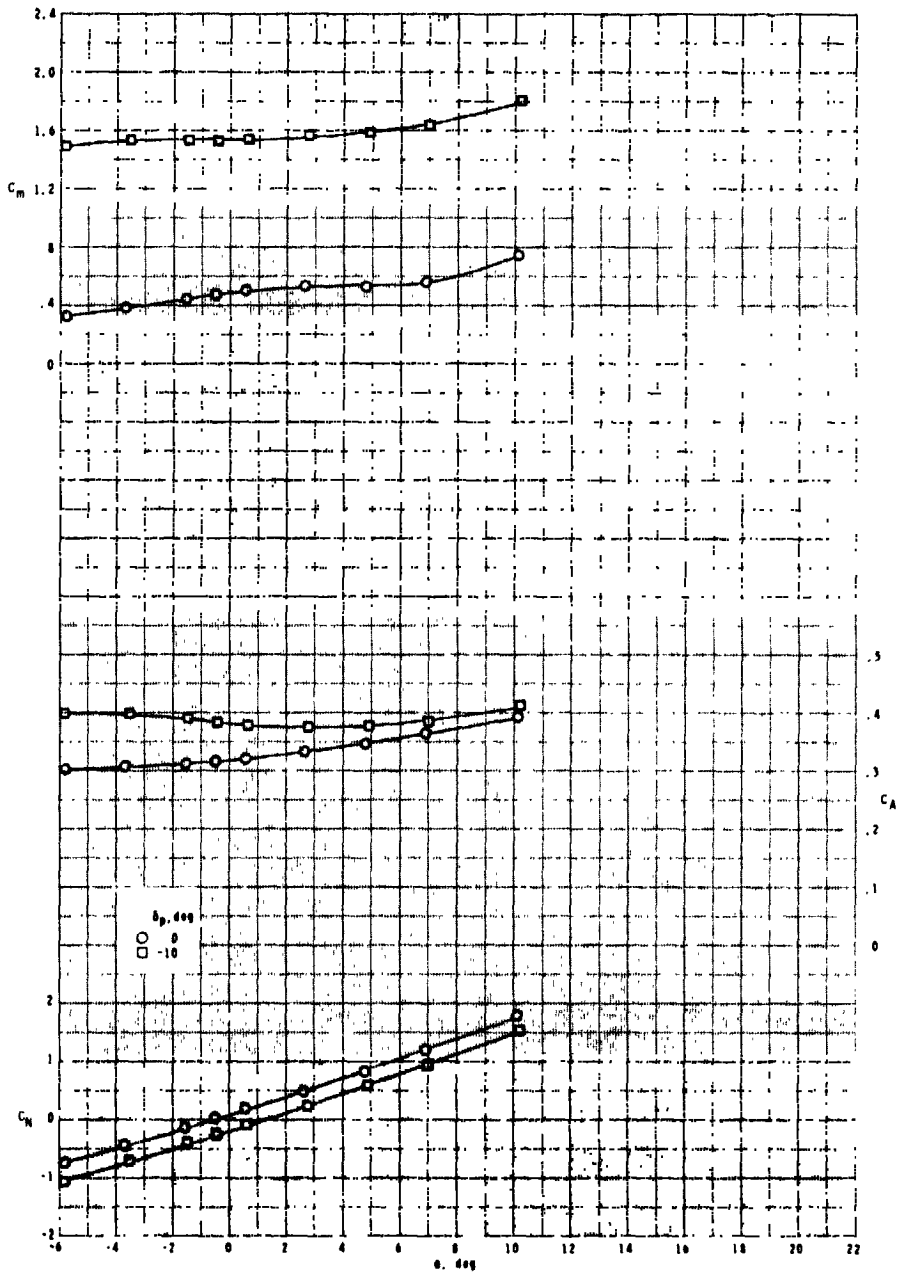

(a) M = 2.86.

Figure 14.- Longitudinal aerodynamic characteristics of body-tail, planar-wing, inlet-closed configuration with pitch control.

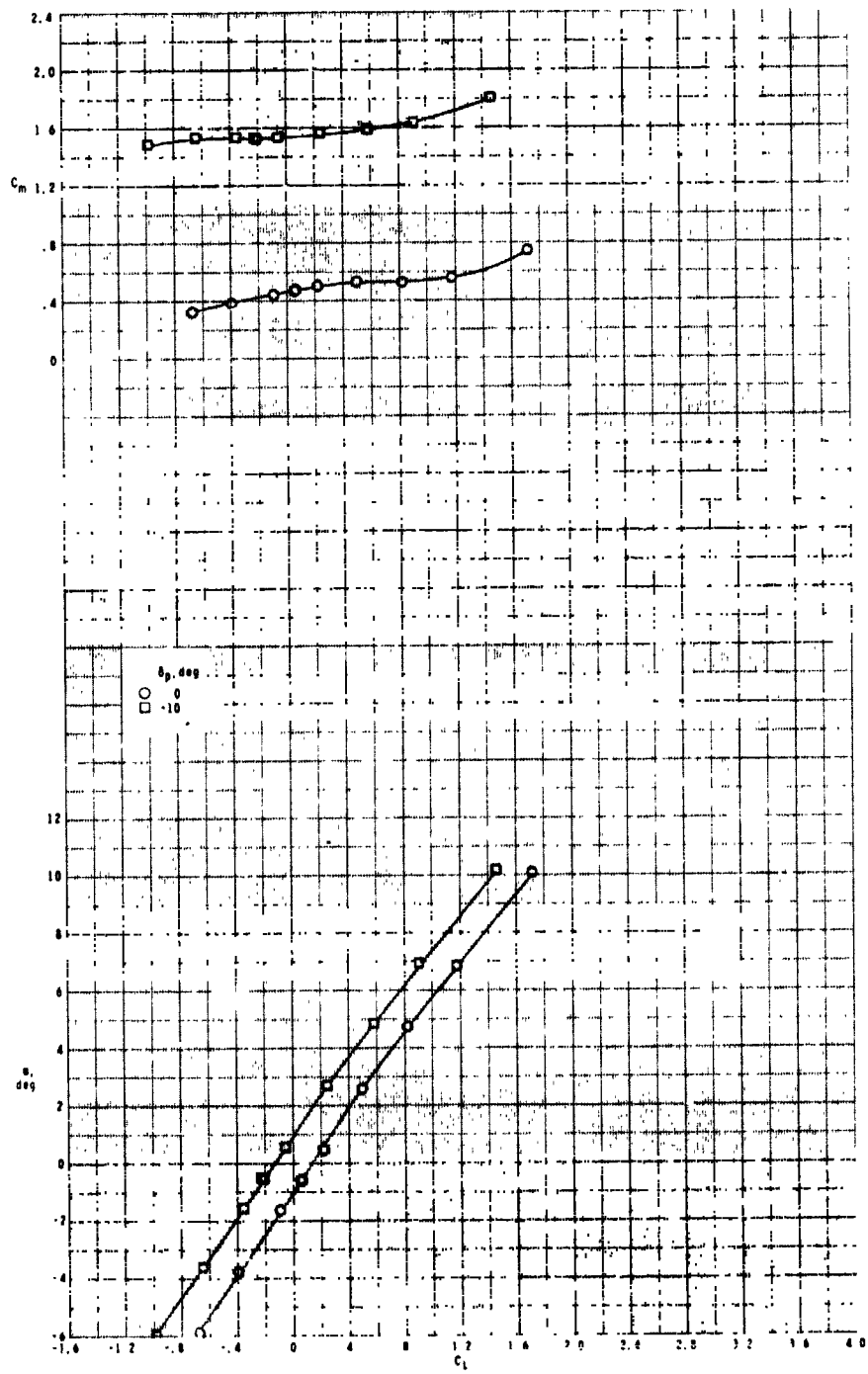

(a) Continued.

Figure 14.- Continued.

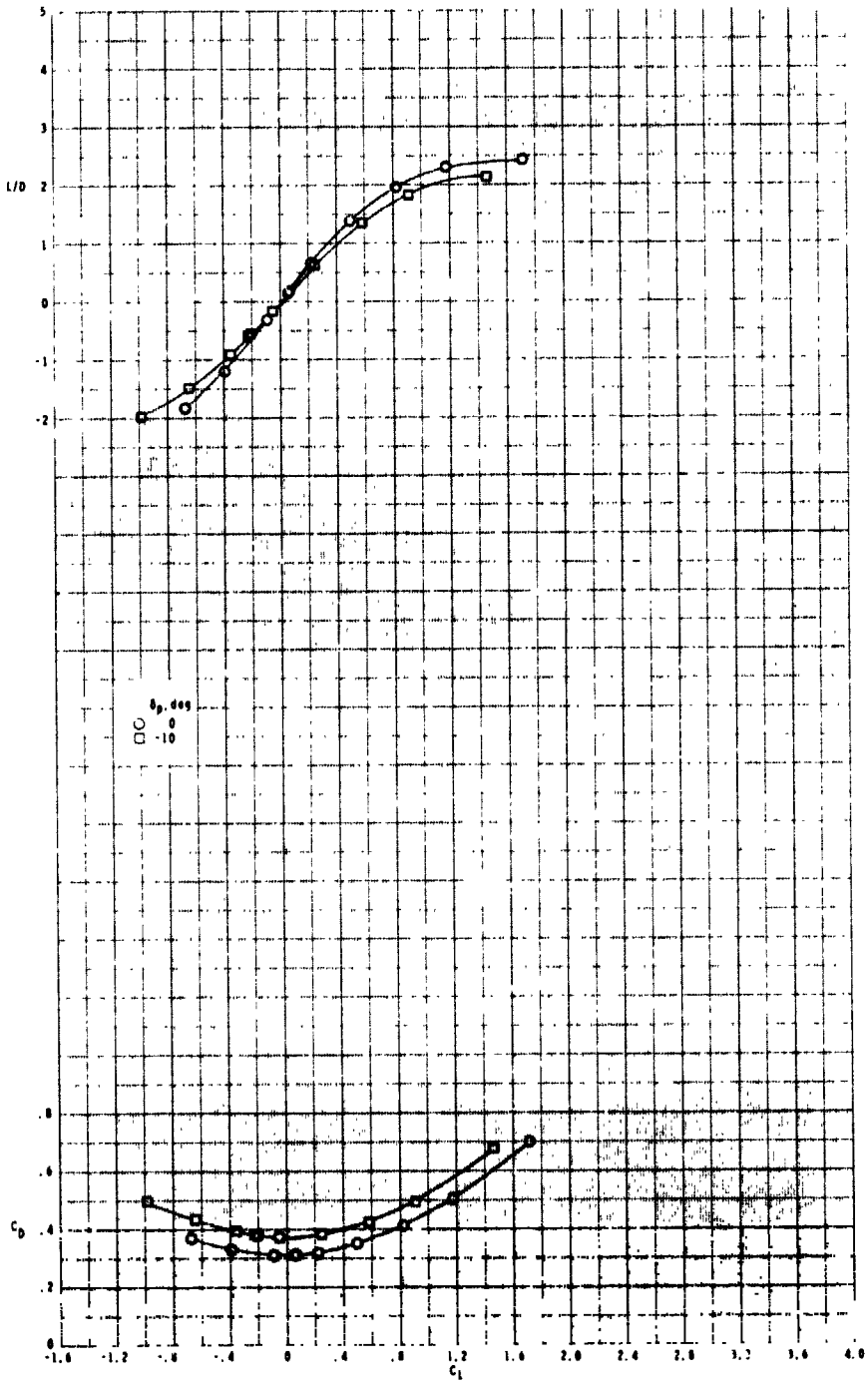

(a) Concluded.

Figure 14.- Continued.

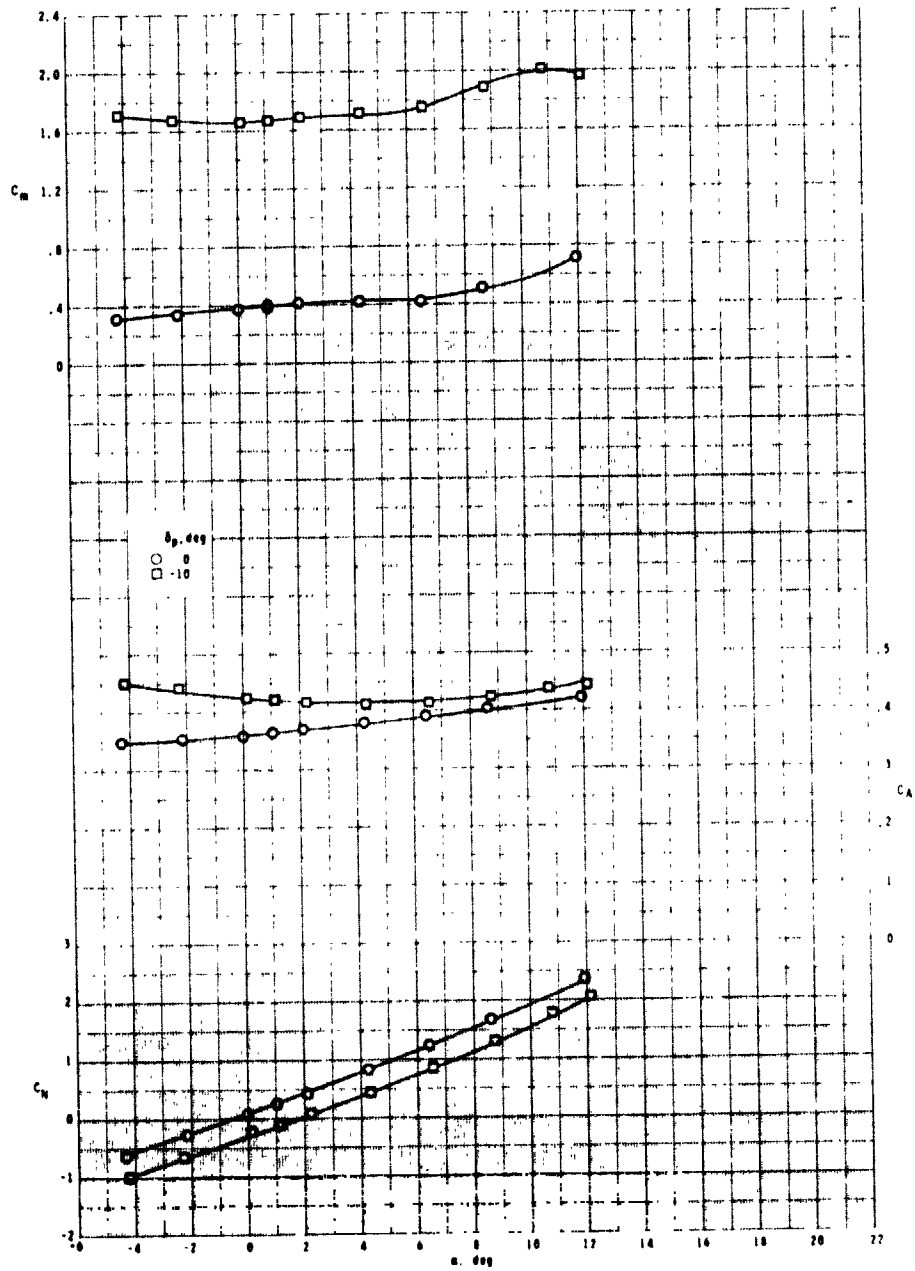

(b) M = 2.36.

Figure 14.- Continued.

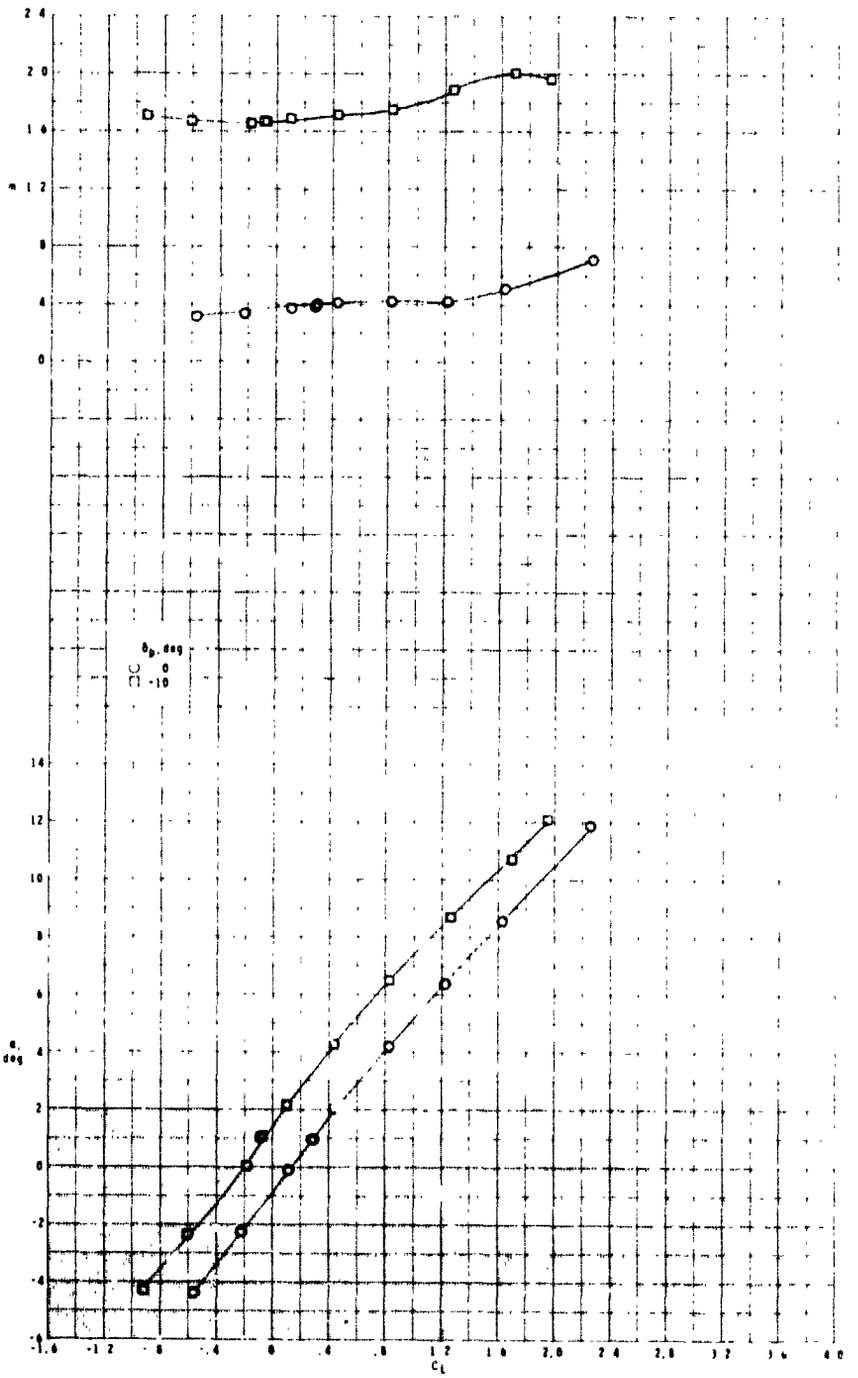

(b) Continued.

Figure 14.- Continued.

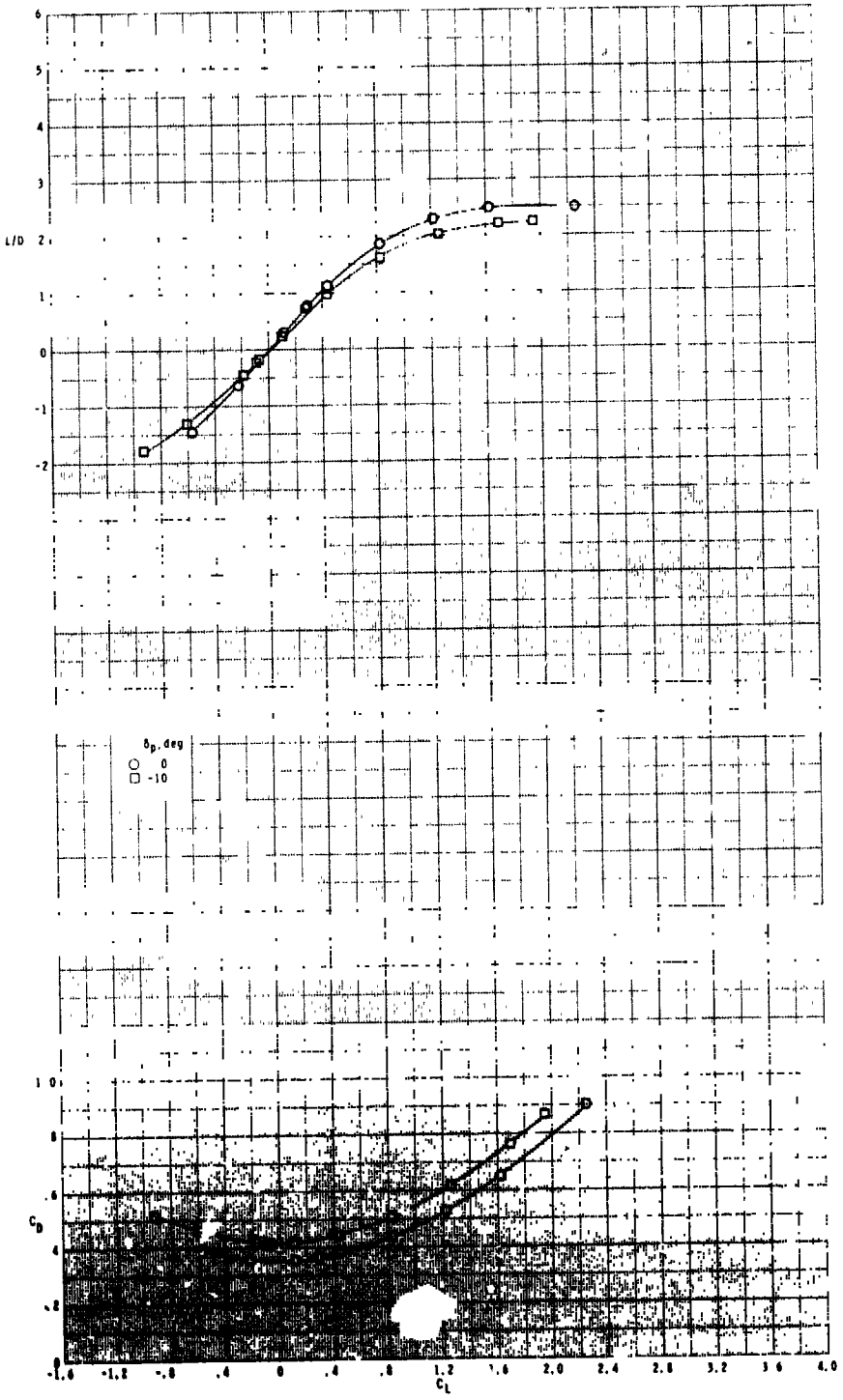

(b) Concluded.

Figure 14. - Continued.

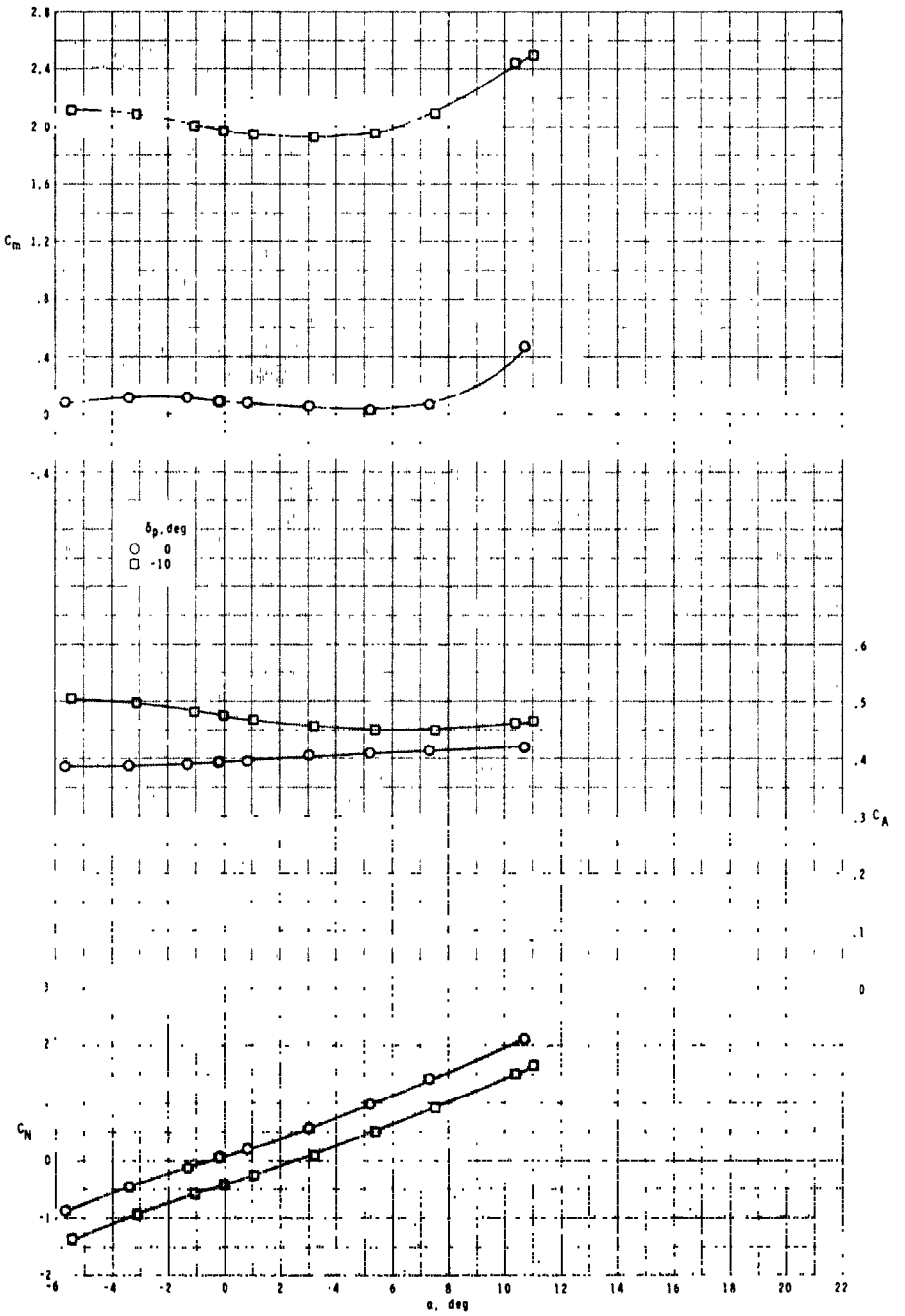

(c) M = 1.70.

Figure 14.- Continued.

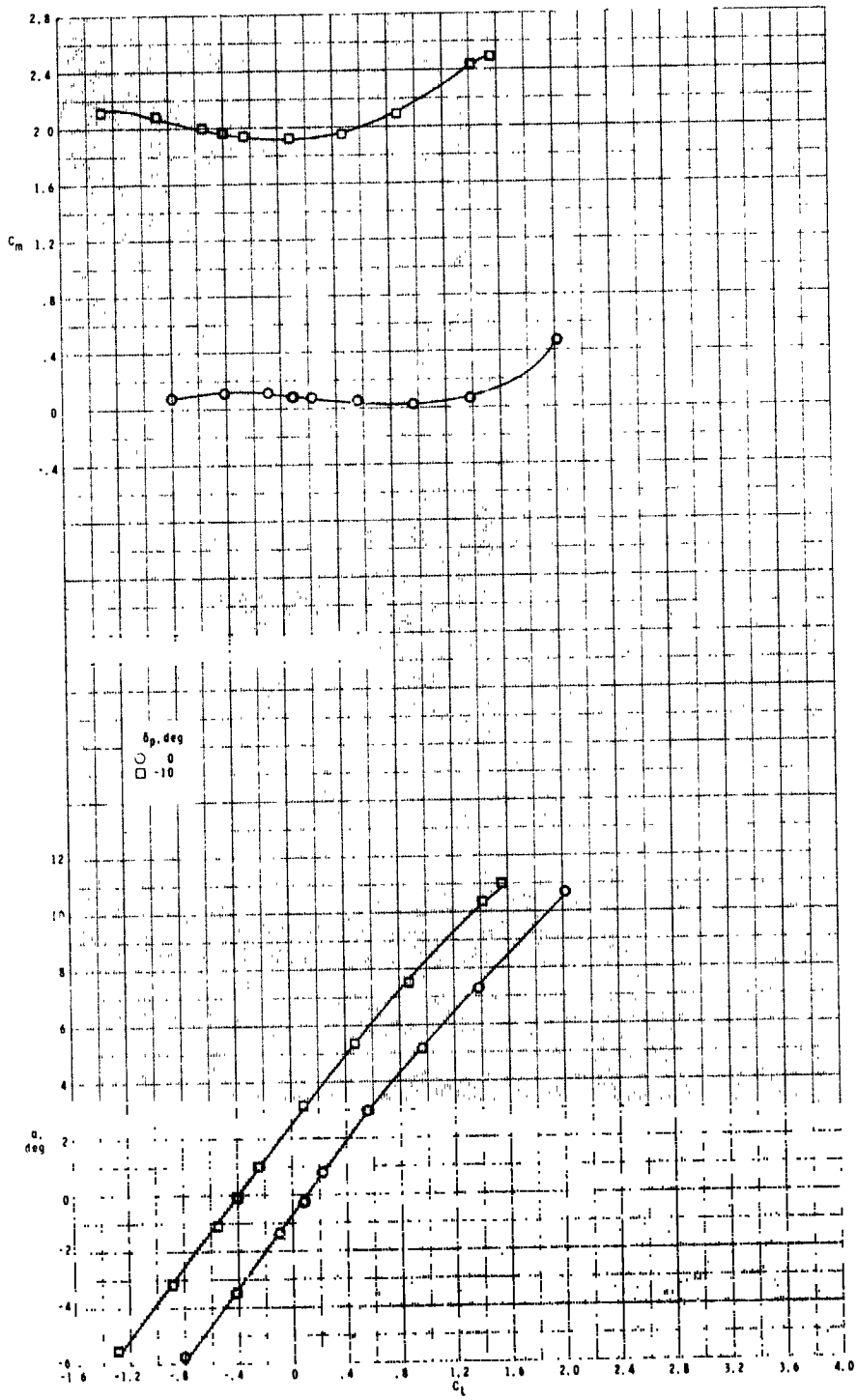

(c) Continued.

Figure 14.- Continued.

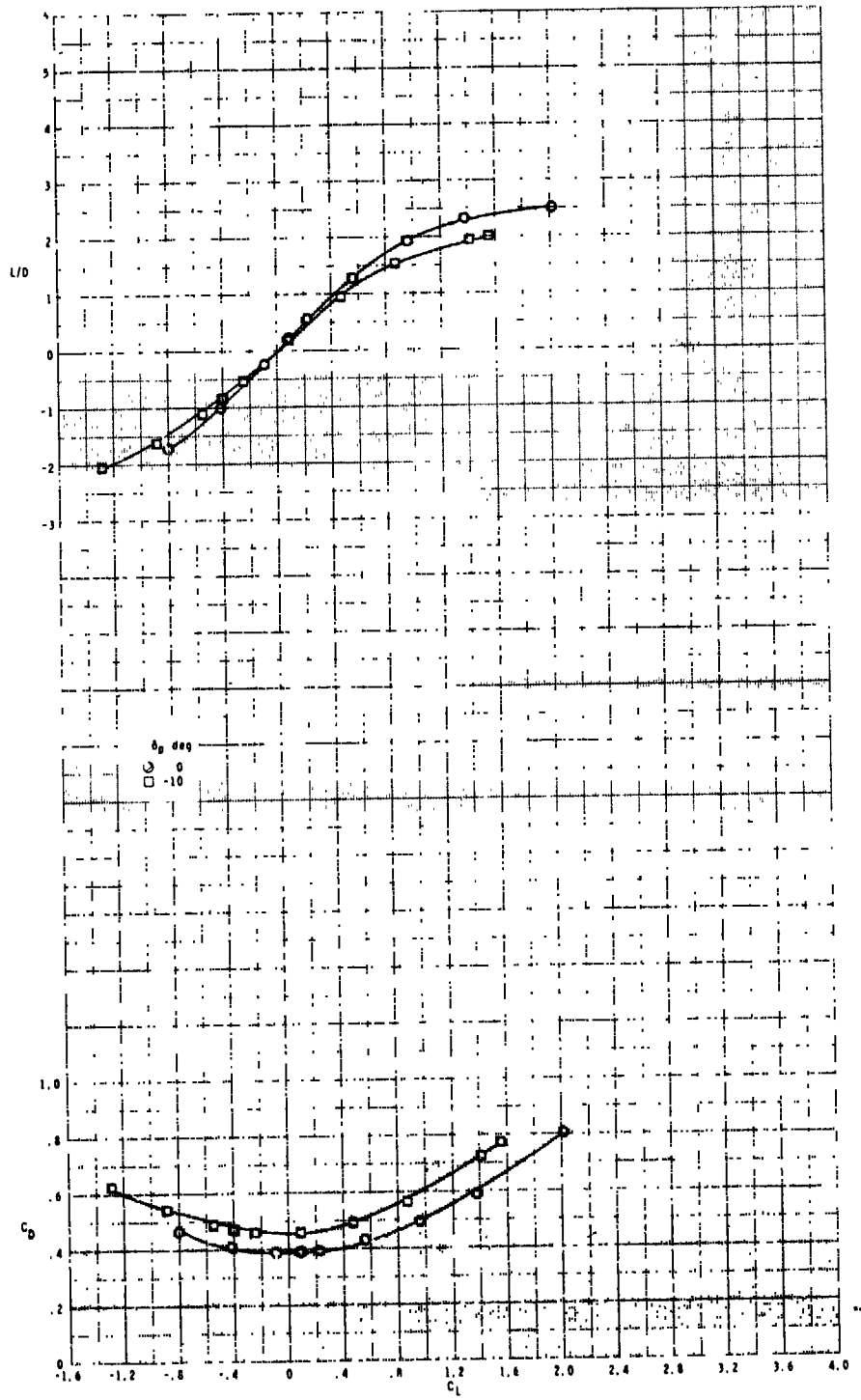

(c) Concluded.

Figure 14.- Concluded.

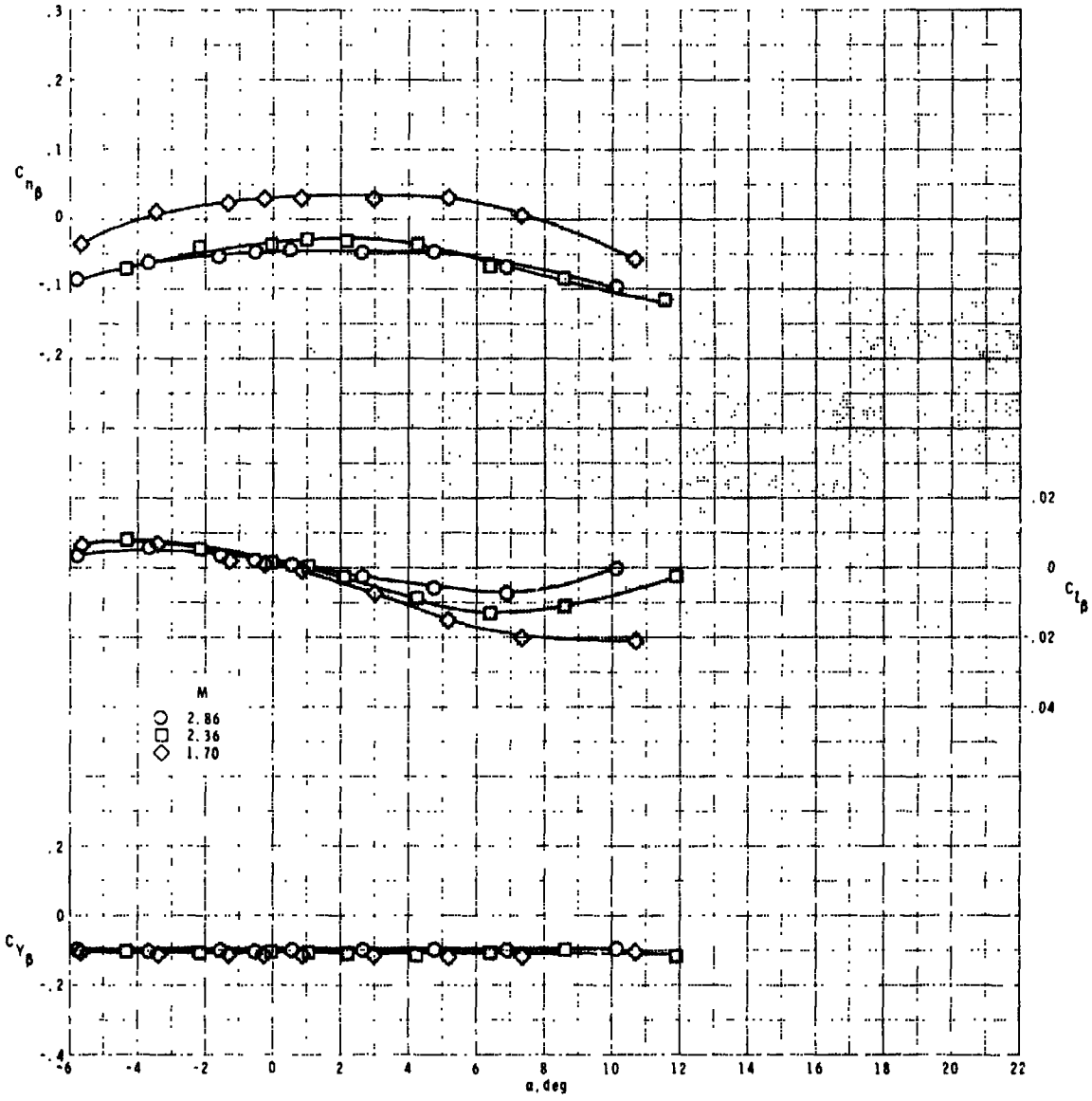

Figure 15.- Lateral-directional stability of body-tail, planar-wing, inlet-closed configuration.

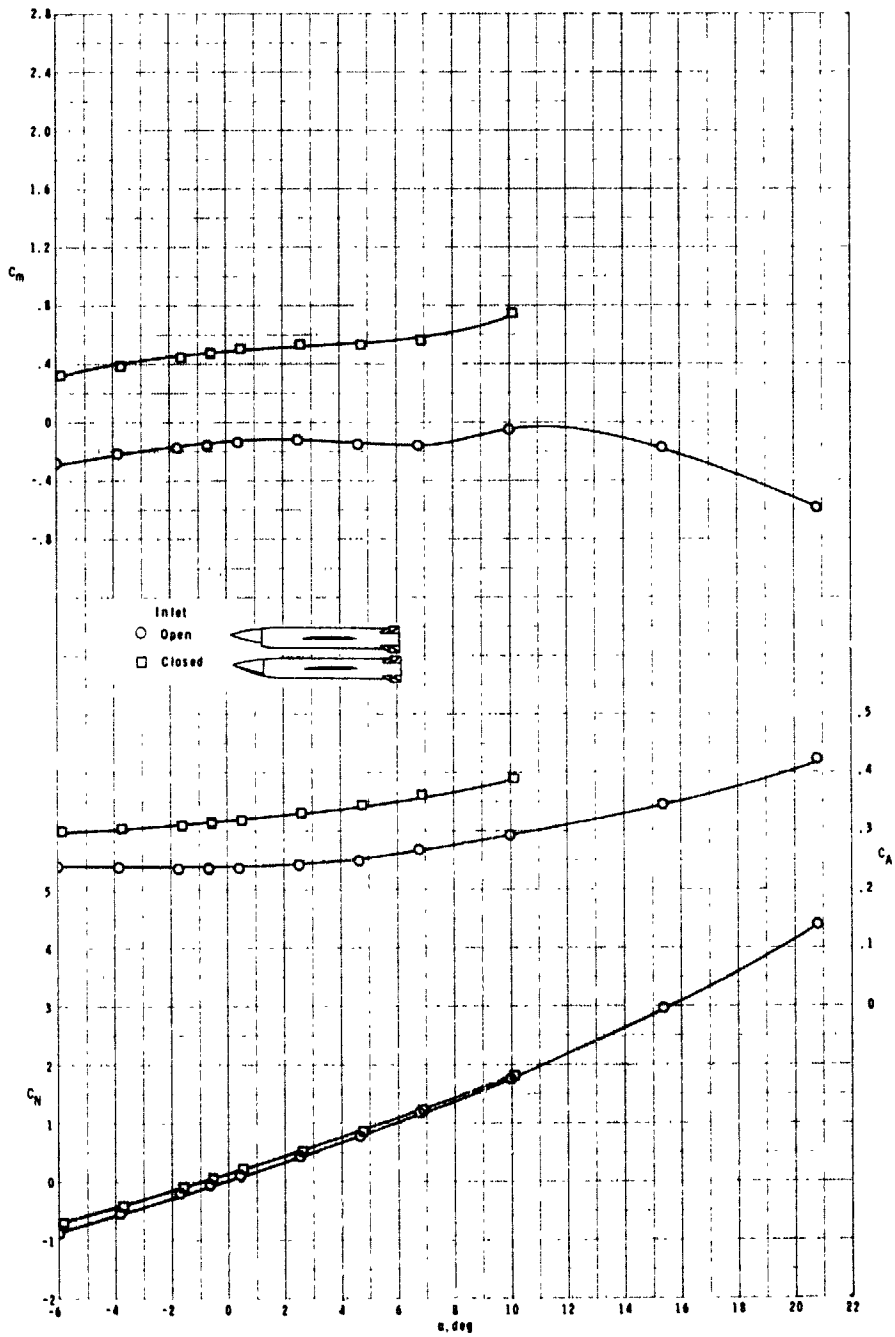

(a) Body axes.

Figure 16.- Comparison of longitudinal aerodynamic characteristics of body-tail, planar-wing configuration with inlet open and closed. M = 2.86.

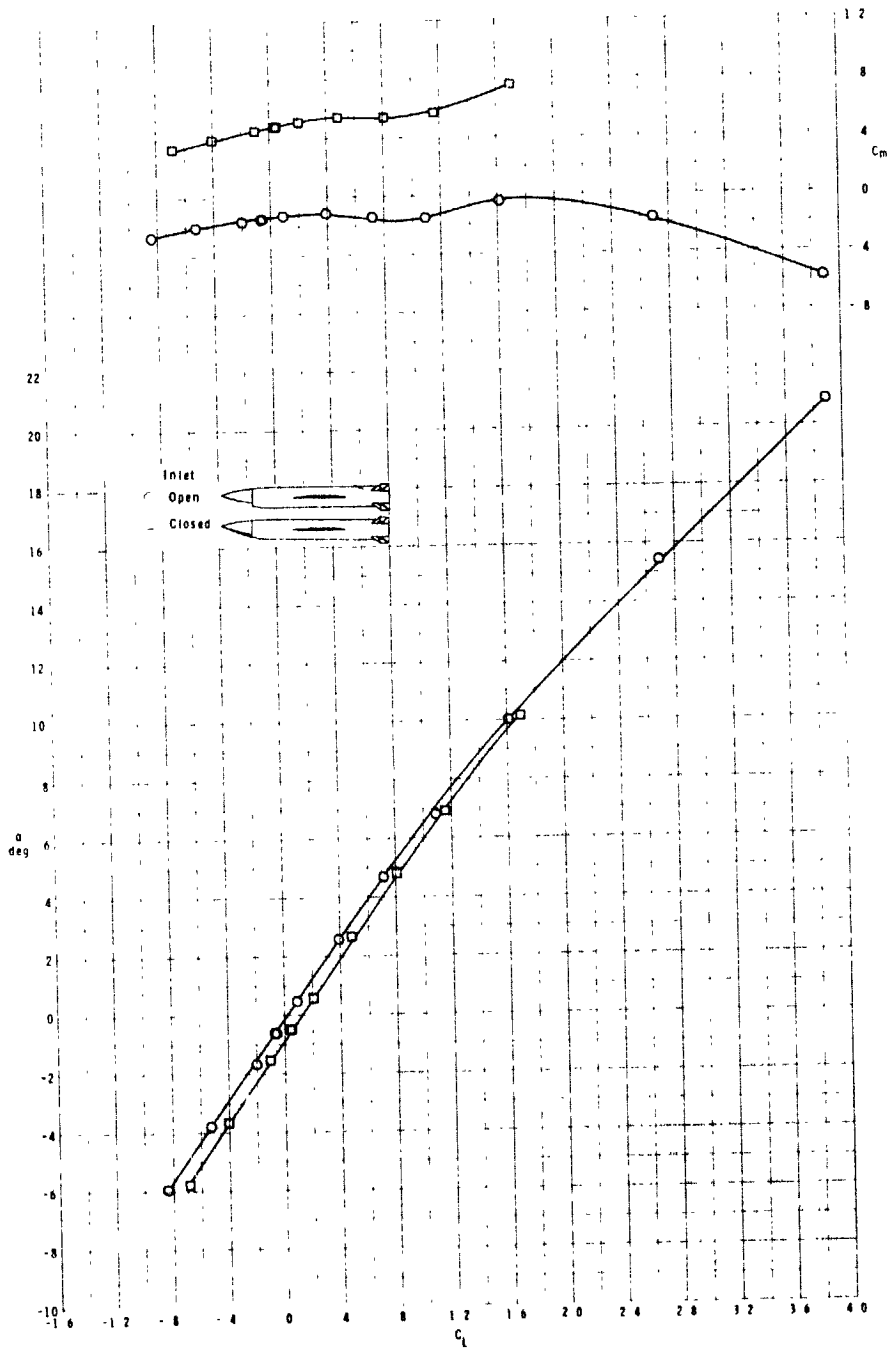

(b) Stability axes.

Figure 16.- Continued.

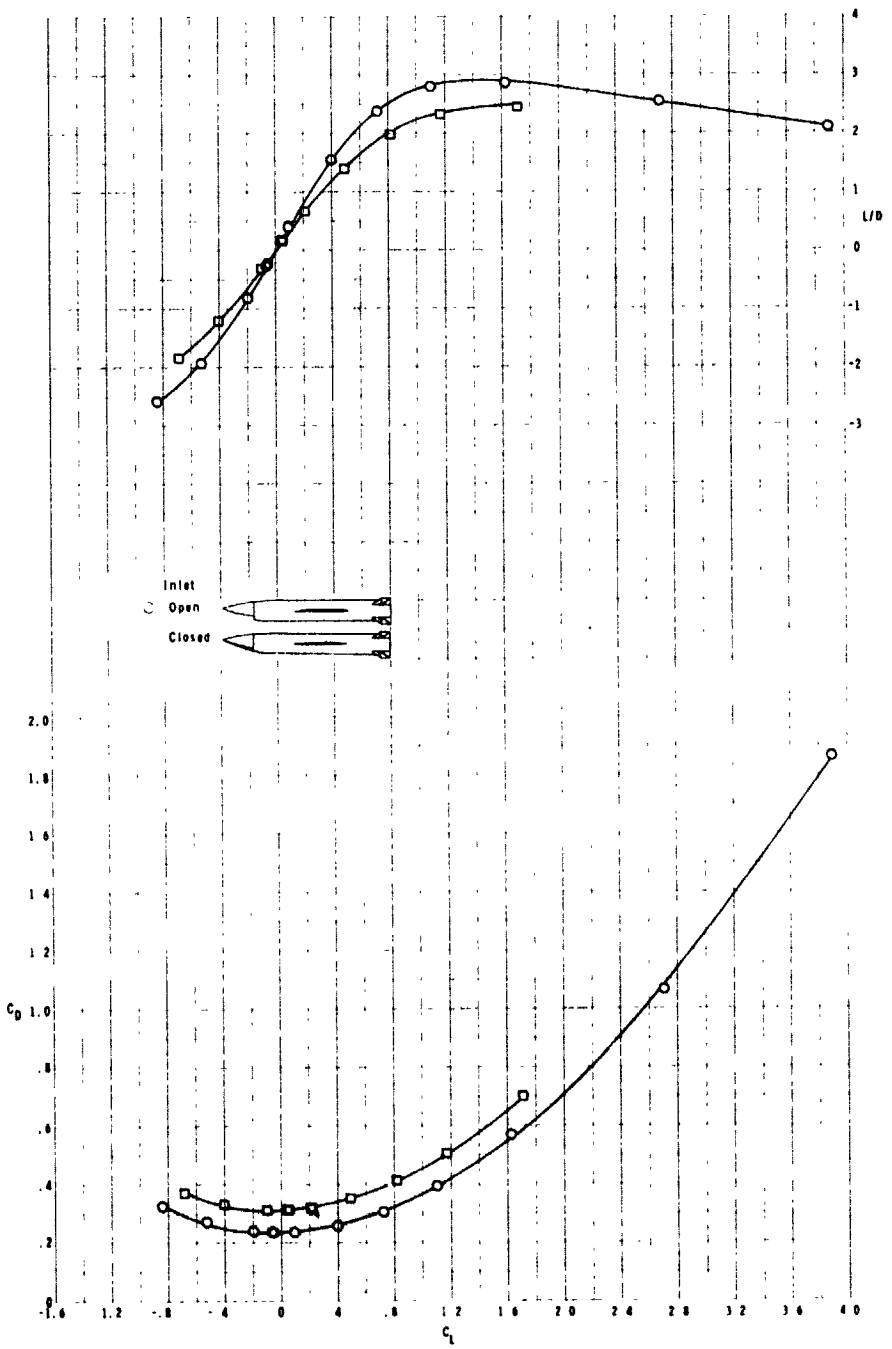

(b) Concluded.

Figure 16.- Concluded.

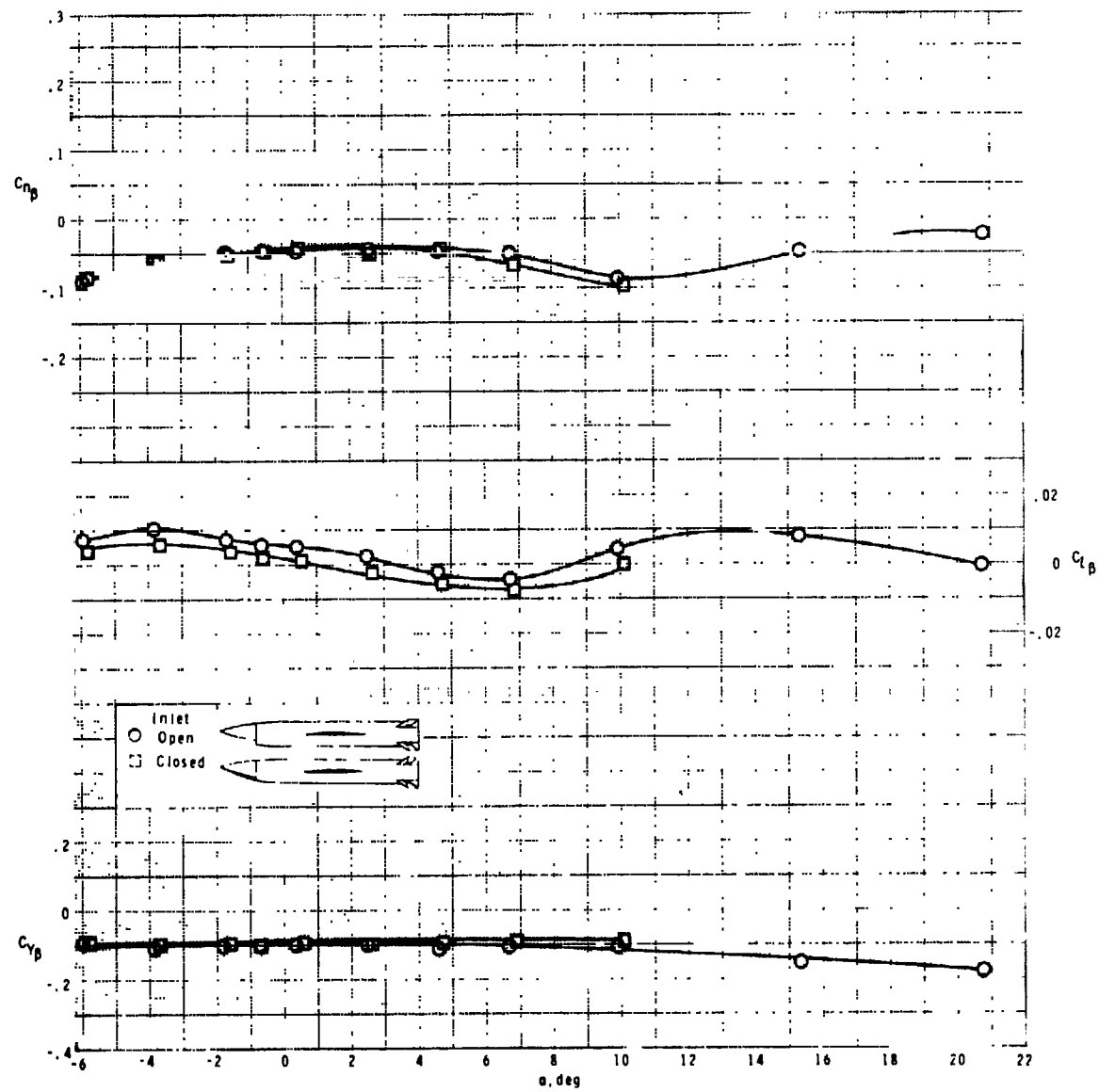

Figure 17.- Comparison of lateral-directional stability of body-tail, planar-wing configuration with inlet open and closed. M = 2.86.

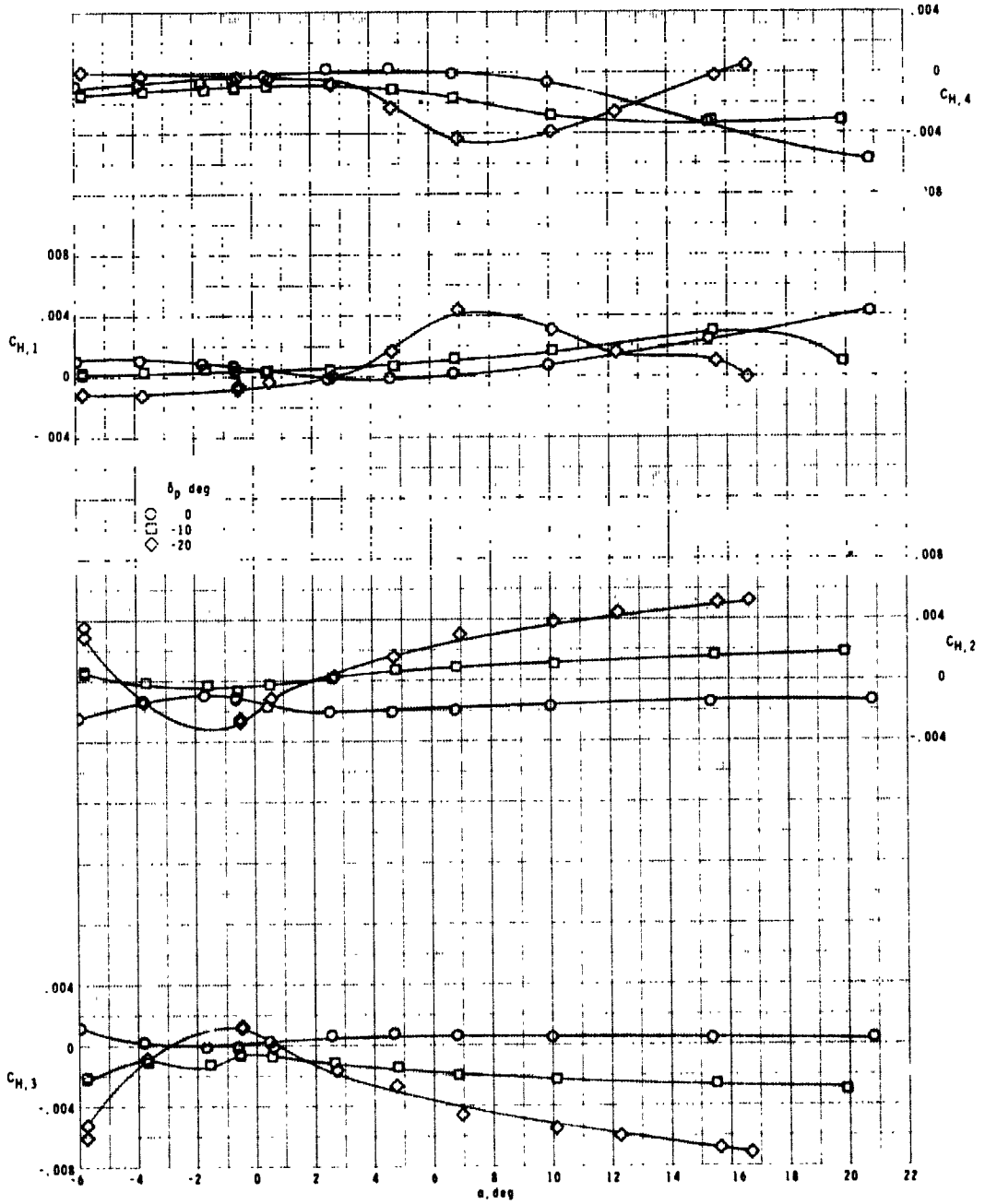

Figure 18.- Control-surface hinge-moment coefficients of body-tail, planar-wing, inlet-open configuration with pitch control. M = 2.60.

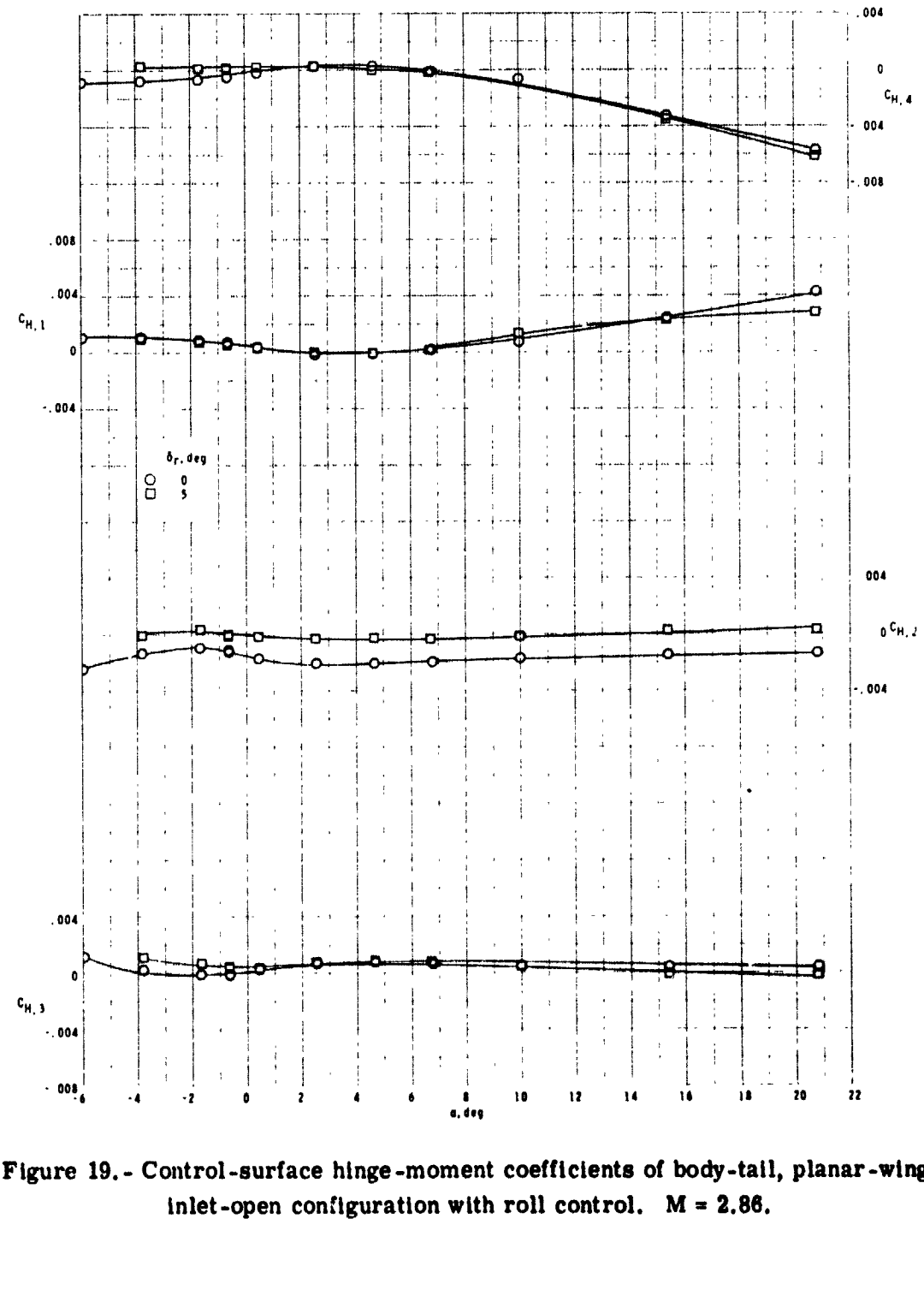

Figure 19.- Control-surface hinge-moment coefficients of body-tail, planar-wing, inlet-open configuration with roll control. M = 2.86.

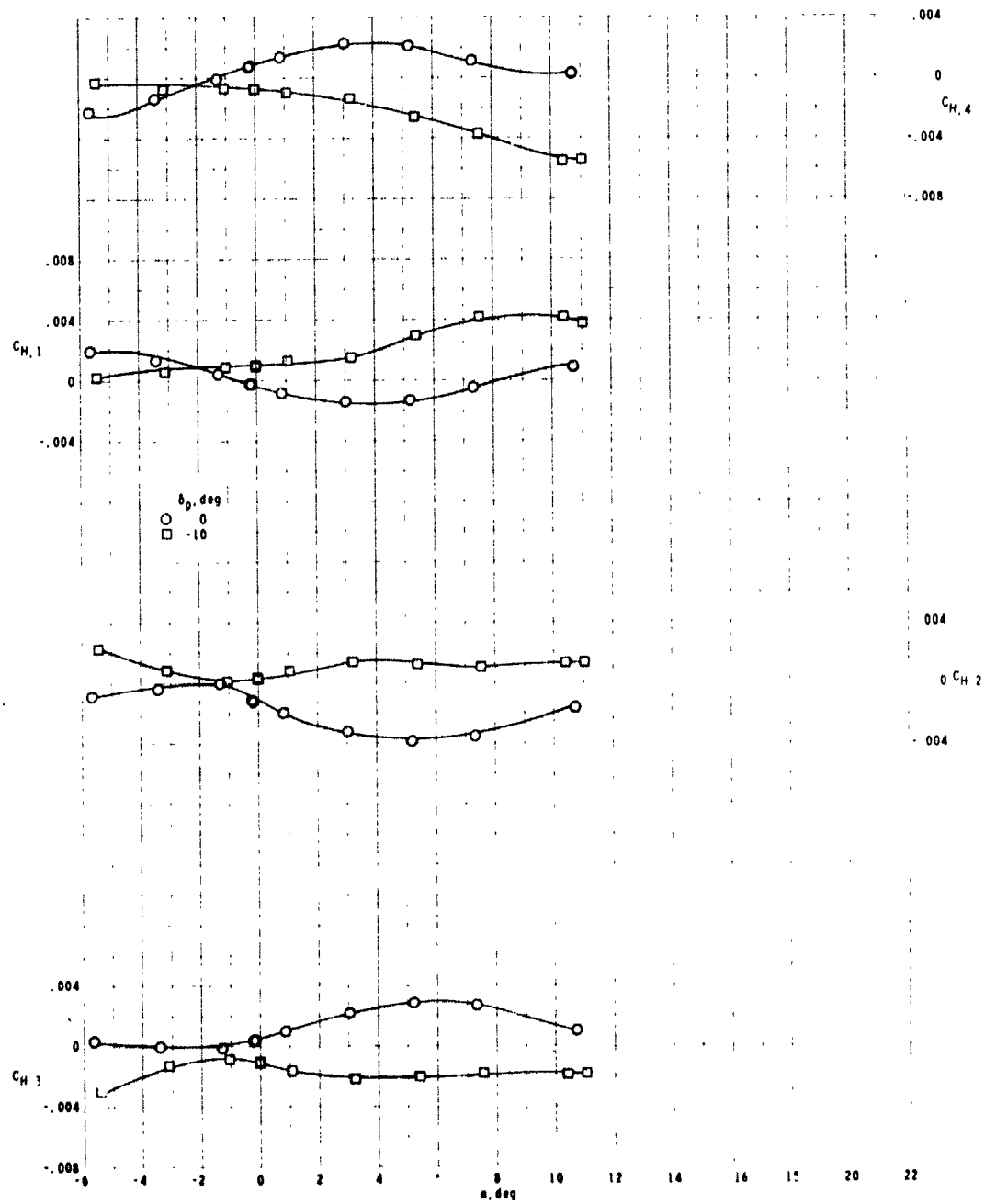

(a) M = 1.70.

Figure 20.- Control-surface hinge-moment coefficients of body-tail, planar-wing, inlet-closed configuration with pitch control.

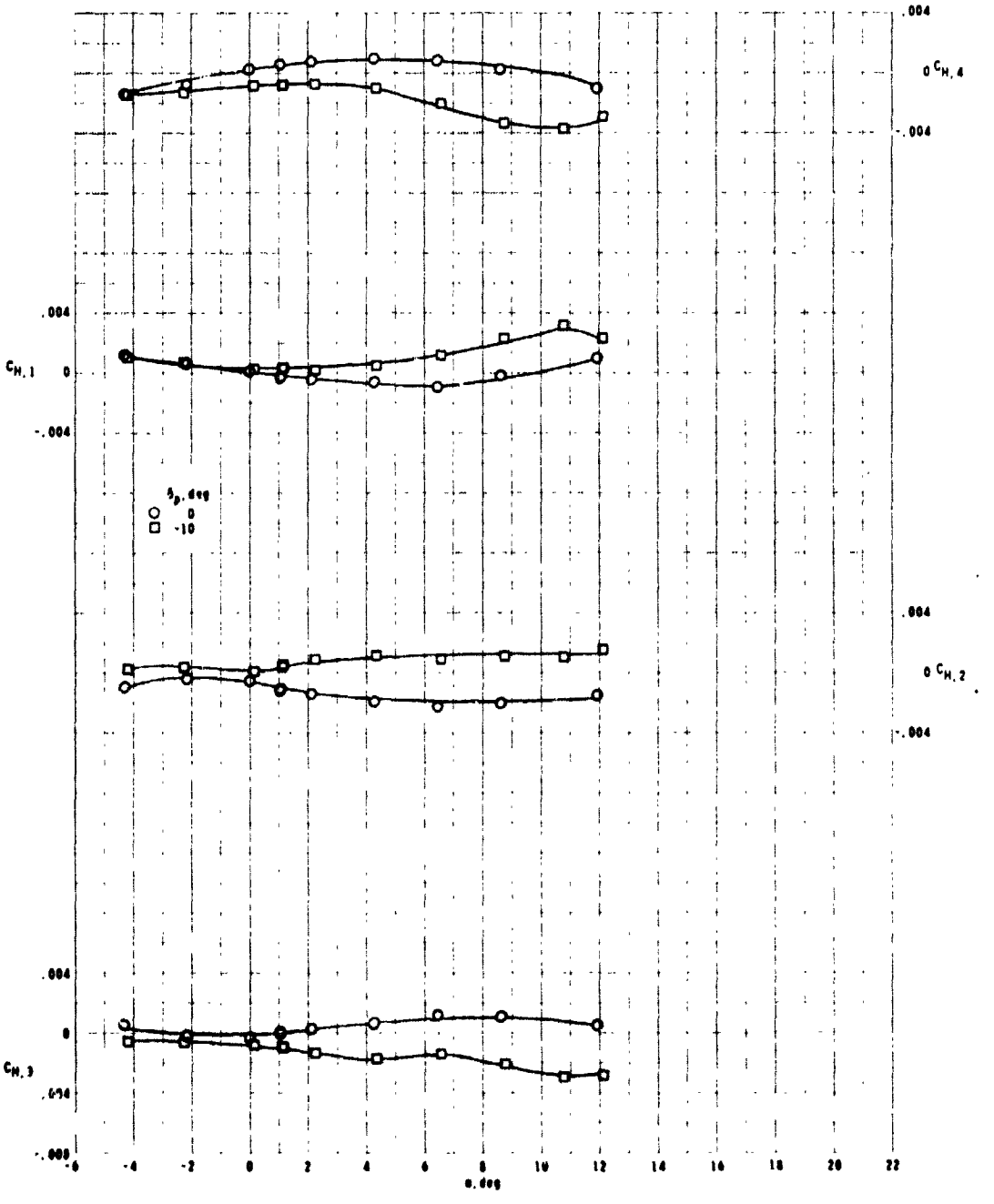

(b) M = 2.36.

Figure 20.- Continued.

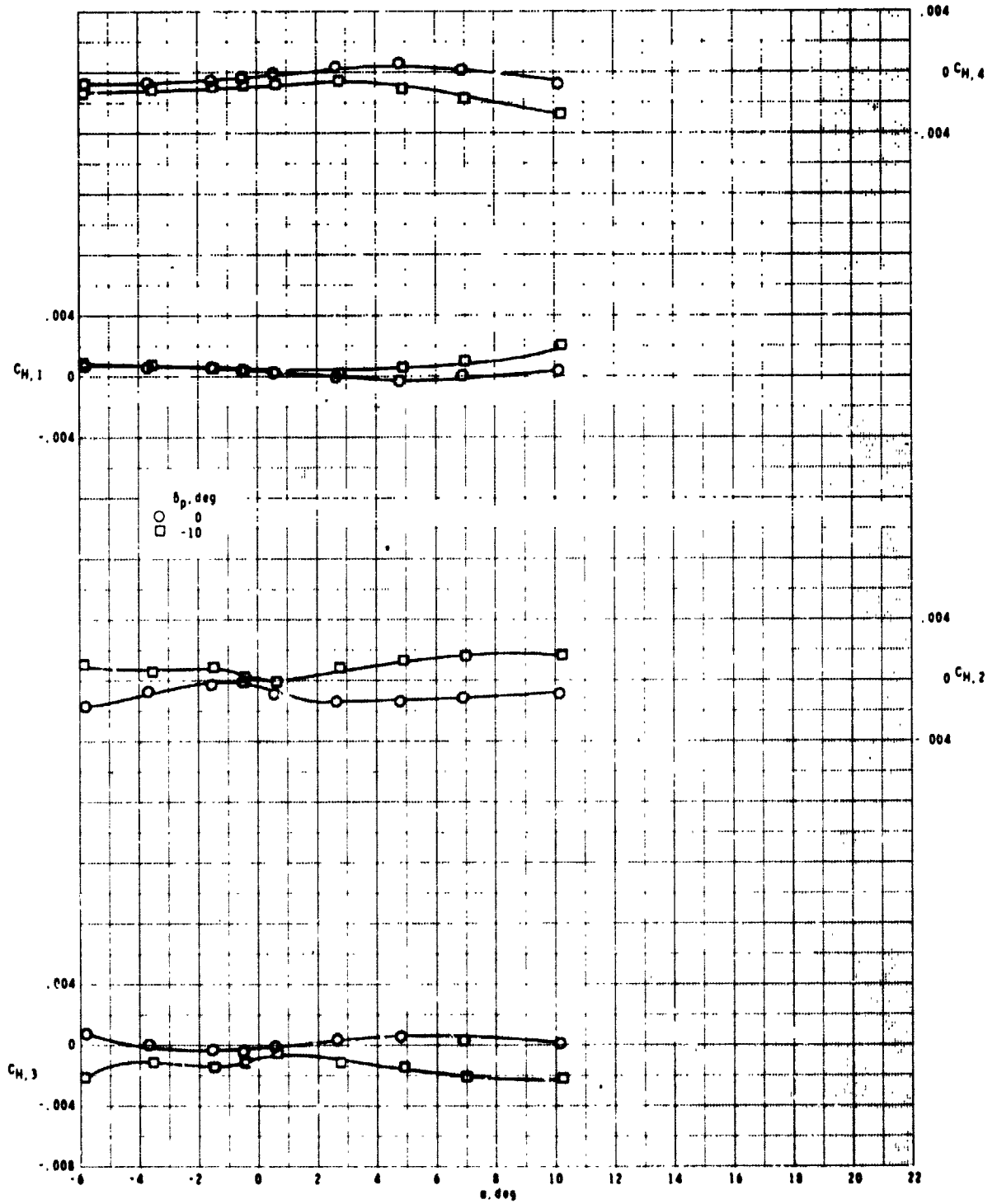

(c) M = 2.86.

Figure 20.- Concluded.